

CAPITAL UNIVERSITY OF SCIENCE AND
TECHNOLOGY, ISLAMABAD



**CONTROL ORIENTED
MODELING OF GASOLINE
ENGINES: A NEW PARADIGM**

by

Ahmed Yar

A thesis submitted in partial fulfillment for the
degree of Doctor of Philosophy

in the

Faculty of Engineering

Department of Electrical Engineering

October 2017

Copyright © 2017 by Ahmed Yar

All rights reserved. No part of this thesis may be reproduced, distributed, or transmitted in any form or by any means, including photocopying, recording, or other electronic or mechanical methods, by any information storage and retrieval system without the prior written permission of the author.

TO MISERY

An essential constituent of physical existence



**CAPITAL UNIVERSITY OF SCIENCE & TECHNOLOGY
ISLAMABAD**

Expressway, Kahuta Road, Zone-V, Islamabad
Phone: +92-51-111-555-666 Fax: +92-51-4486705
Email: info@cust.edu.pk Website: <https://www.cust.edu.pk>

CERTIFICATE OF APPROVAL

This is to certify that the research work presented in the thesis, entitled “**Control Oriented Modeling of Gasoline Engines: A New Paradigm**” was conducted under the supervision of **Dr. Aamir Iqbal Bhatti**. No part of this thesis has been submitted anywhere else for any other degree. This thesis is submitted to the **Department of Electrical Engineering, Capital University of Science and Technology** in partial fulfillment of the requirements for the degree of Doctor in Philosophy in the field of **Electrical Engineering**. The open defence of the thesis was conducted on **28 September, 2017**.

Student Name : Mr. Ahmed Yar
(PE-111001)

The Examining Committee unanimously agrees to award PhD degree in the mentioned field.

Examination Committee :

(a) External Examiner 1: Dr. Ghulam Mustafa
Associate Professor
PIEAS, Islamabad

(b) External Examiner 2: Dr. Adeel Mehmood
Assistant Professor
CIIT, Islamabad

(c) Internal Examiner : Dr. Fazal ur Rehman
Professor
CUST, Islamabad

Supervisor Name : Dr. Aamir Iqbal Bhatti
Professor
CUST, Islamabad

Name of HoD : Dr. Noor Muhammad Khan
Professor
CUST, Islamabad

Name of Dean : Dr. Imtiaz Ahmad Taj
Professor
CUST, Islamabad

AUTHOR'S DECLARATION

I, **Mr. Ahmed Yar (Registration No. PE-111001)**, hereby state that my PhD thesis entitled, '**Control Oriented Modeling of Gasoline Engines: A New Paradigm**' is my own work and has not been submitted previously by me for taking any degree from Capital University of Science and Technology, Islamabad or anywhere else in the country/ world.

At any time, if my statement is found to be incorrect even after my graduation, the University has the right to withdraw my PhD Degree.



(Mr. Ahmed Yar)

Dated:

September, 2017

Registration No : PE111001


PLAGIARISM UNDERTAKING

I solemnly declare that research work presented in the thesis titled “**Control Oriented Modeling of Gasoline Engines: A New Paradigm**” is solely my research work with no significant contribution from any other person. Small contribution/ help wherever taken has been duly acknowledged and that complete thesis has been written by me.

I understand the zero tolerance policy of the HEC and Capital University of Science and Technology towards plagiarism. Therefore, I as an author of the above titled thesis declare that no portion of my thesis has been plagiarized and any material used as reference is properly referred/ cited.

I undertake that if I am found guilty of any formal plagiarism in the above titled thesis even after award of PhD Degree, the University reserves the right to withdraw/ revoke my PhD degree and that HEC and the University have the right to publish my name on the HEC/ University Website on which names of students are placed who submitted plagiarized thesis.

Dated: September, 2017



(Mr. Ahmed Yar)
Registration No. PE111001

Acknowledgements

First and foremost, it is a matter of deepest pleasure to acknowledge the dedicated souls who developed such a beautiful framework called *Research*. A wonderful paradigm which, unlike other paradoxes, always strives for brilliance and remains impatient for identification of its own gray areas. It embraces its failures, incapacities and carries intrinsic design of rejecting the malcontents on the road of evolution. That is the way it moved in the history, gradually step by step and will carry on its endless journey to understanding the nature.

Following the legacy of this wonderful fraternity, I am highly obliged to my supervisor Aamer Iqbal Bhatti and co-supervisor Qadeer Ahmed. The persons who taught me the lessons of trying not to think outside the box, instead they led me on the way to break the box and enjoy having the intellectual independence.

I am also thankful to all the members of CASPR (Control And Signal Processing Research) Group. Special thanks to my seniors Dr. Yasir Awais Butt, Dr. Hameed Qaiser, Dr. Safdar Hussain, Dr. Mohammad Iqbal, Dr. Sohail Iqbal, Mr. Khobaib Ahmed, Mr. Armaghan Mohsin and Mr. Amin Akram. Also thanks to my colleagues, Mr. Ali Arshad, Mr. Ghulam Murtaza, Mr. Raheel Anjum, Mr. Muhammad Asghar, Mr. Syed Ussama Ali, Mr. Athar Hanif, Mr. Abdul Rehman Yasin, Mr. Zeeshan Babar, Mr. Rizwan Azam, Mr. Fahad Murad, Mr. Fahad Amin, Mr. Jamal Ahmed Bhatti, Mr. Farhan Hanif, Mr. Farooq Saleem and Mr. Farrukh Waheed.

It would be an ultimate pleasure to acknowledge my Father, who taught me the patience, devotion and commitment, and my mother who is a symbol of ultimate affection. I am thankful to a concomitant friend, my wife, and our kids Bahadur Yar and Nain Tara for understanding and accompanying me in difficult times.

It would be a matter of deep comfort to acknowledge Mr. Sikandar Zulqarnain, who is a true mentor and a selfless friend, Mr. Azam Khan and Mr. Mubeen Hanif. They provided me courage and motivation on every step.

List of Publications

Journal Publications

1. Yar, A., Bhatti, A. I., Ahmed, Q., 2017, “A First Principle based Control Oriented Gasoline Engine Model”, *Journal of Dynamic System Measurement, and Control*, 139(5), p.051002, DOI : 10.1115/1.4035174
2. Yar, A., Bhatti, A. I., Ahmed, Q., 2017, “First Principle based Control Oriented Model of Gasoline Engine including Multi-Cylinder Dynamics”, *Control Engineering Practice*, Accepted for Publication, Ms. Ref. No.: CONENGPRAC-D-16-00779.
3. Yar, A., Bhatti, A. I., Ahmed, Q., “First Principle based Gasoline Engine Model including Lumped Cylinder Dynamics”, *Journal of Dynamic Systems Measurement, and Control*, Under Review, Ref. No.: DS-17-1244.

Conference Publications

1. Yar, A., Bhatti, A. I., Ahmed, Q., High Fidelity Engine Model for A Unified Control, Diagnostic and Condition Monitoring Framework, In *American Control Conference (ACC), 2017*, (pp. 1629-1635). IEEE.
2. Yar, A., Bhatti, A. I., Control of Air-to-Fuel ratio of spark ignited engine using super twisting algorithm, In *International Conference on Emerging Technologies (ICET), 2012*, (pp. 1-5), DOI: 10.1109/ICET.2012.6375472, 2012.

Abstract

The advent of hybrid, flex fuel and smart vehicles has highlighted the need of an engine model suitable for a unified control and diagnostic framework. However, this may require a new engine modeling paradigm, deviating from traditional control oriented models and converging to first principle based models. These new developments have motivated the authors to bridge the prevailing gap between the existing control oriented engine models and the stringent requirements put up by new power-train architectures. In existing literature Mean Value Engine Models (MVEMs) are developed under a few assumptions and analogies. There exists a variety of approaches for evaluating the brake torque, however structure of engine speed dynamics remains the same. Though such a structure captures the mean value profile but builds an abstraction wall between model and the actual system. The said wall completely hides the aspects of crankshaft angular speed fluctuations, dynamics of multi-cylinders and others beneath its shadow. Among others, comprehensive control and diagnostic unification and derivation of the basis for model based cylinder-to-cylinder control are most prominent limitations.

To fill in the gap a new modeling strategy is presented in this thesis. The strategy takes into account the considerations of multi-cylinders and spatial orientation, without compromising the structural simplicity. The torque production subsystem is modeled by joining the model of torque producing mechanism and a simple closed form analytical gasoline engine cylinder pressure model. Model of the torque producing mechanism is derived using Constrained Lagrangian Equation of Motion, and is simplified to a suitable form to be integrated in overall engine model. An analytical gasoline engine cylinder pressure model is taken from literature and extended for a four cylinder engine, then integrated to the model of torque producing mechanism. Following such a modeling strategy unlike existing literature in control oriented gasoline engine models, torque production subsystem is not replaced by a continuously operating volumetric pump. As a result, the model vividly describes the crankshaft angular speed fluctuations and the dynamics introduced by multi-cylinders. The employed physical principles give the global envelope of validity to the model. Thus the model describes dynamics of the healthy system, as well as system under faulty conditions, comprehensively. The proposed model is tuned and successfully validated. Pattern of crankshaft angular speed fluctuation for misfire in one cylinder is simulated and found closely matching to an actual engine misfire data.

Contents

Author's Declaration	iii
Plagiarism Undertaking	iv
Acknowledgements	v
List of Publications	vi
Abstract	vii
Abbreviations	xiv
Symbols	xvi
1 INTRODUCTION	1
1.1 Background	1
1.2 Problem Statement	3
1.3 The Beginning	3
1.4 Proposed Strategy	5
1.5 Overview of the Thesis	6
2 CONTROL ORIENTED GASOLINE ENGINE MODELS: TRENDS AND FASHIONS	9
2.1 Gasoline Engines: An Overview	10
2.2 Gasoline Engines: Dynamic Modeling Facet	11
2.3 Research on Gasoline Engine Modeling	14
2.4 Technology Legislation and Research Trends	24
2.5 Constructing the Research Problem	28
2.6 Conclusions	32
3 LUMPED CYLINDER DYNAMICS	34

3.1	Model of the Mechanism	35
3.1.1	Model Derivation	36
3.1.2	Simplification of the Model	44
3.2	Cylinder Pressure Model	47
3.3	Model Realization	50
3.3.1	Existing Subsystems	50
3.3.2	Model Integration	52
3.3.3	Aspects of Realization	53
3.3.4	Tuning of the Model Parameters	56
3.4	Results and Discussion	57
3.4.1	Control Capabilities	62
3.4.2	Diagnostic Capabilities	63
3.4.3	Model Integrability with Other Systems	64
3.5	Conclusions	65
4	MULTI-CYLINDER DYNAMICS	66
4.1	Model of the Mechanism	67
4.1.1	Model Derivation	68
4.1.2	Model Simplification	75
4.2	Cylinder Pressure Model	78
4.2.1	Single Cylinder Pressure Model	79
4.2.2	Structure of a Multi-Cylinder Pressure Model	81
4.3	Model Realization	82
4.3.1	Model Integration	82
4.3.2	Tuning of the Model Parameters	83
4.4	Results and Discussion	84
4.4.1	Features of FPEM	86
4.4.2	FPEM Diagnostic Capabilities	89
4.4.3	FPEM Control Capabilities	91
4.4.4	Model Integrability with Other Systems	92
4.5	Conclusions	93
5	CONCLUSIONS AND FUTURE WORK	95
5.1	Featured Aspects	95
5.2	Future Direction	97
5.2.1	Utilization of the Model	97
5.2.2	Extension to Model	99

A	EXPERIMENTAL SETUP AND PARAMETER TUNING	100
A.1	Experimental Setup	100
A.1.1	Onboard Diagnostic Interface	100
A.1.2	High Speed DAQ Interface	103
A.2	Parameter Tuning	104
B	DETAILED MATHEMATICAL EXPRESSIONS IN LUMPED CYLINDER DYNAMICS	107
C	DETAILED MATHEMATICAL EXPRESSIONS IN MULTI- CYLINDER DYNAMICS	109
	Bibliography	111

List of Figures

1.1	Comparison of Harmonic and Reciprocating Motion	4
1.2	Organization of the Thesis	7
2.1	Gasoline Engine: An Overview	11
2.2	Gasoline Engine Cause and Effect Diagram [1]	13
2.3	Engine Subsystems and Interconnect [2] (*mean mass flow rate to intake manifold, **mean mass flow rate to engine cylinder)	16
2.4	Summary of Engine Evolution	26
2.5	Proposed Engine Control and Diagnostic Framework	31
3.1	Torque Producing Mechanism	35
3.2	Motion of Center of Mass of Crankshaft	37
3.3	Constraints on the Motion of Center of Mass of Crankshaft	38
3.4	Constraints for Motion of Connecting rod and Piston	40
3.5	Cylinder Pressure Model IOs	47
3.6	Piston Free Body Diagram	48
3.7	Subsystems from Existing Literature	52
3.8	A Complete Structure of Torque Production Subsystem	53
3.9	Realizations	54
3.10	Structure of First Realization (Figure 3.9(a))	55
3.11	Input Throttle Position	58
3.12	Intake Manifold Pressure	58
3.13	Crankshaft Angular Speed	58
3.14	Model Response for Second Data-set	59
3.15	Model Response for Third Data-set	59
3.16	Effects of Variation in Design Parameters of the Mechanism	60
3.17	Miscellaneous Model Outputs(A is SOC while B is TDC)	62
3.18	Piston Reciprocating Motion(a^* is crankoffset l_1)	63
3.19	Pattern of Crankshaft Angular Speed Fluctuation for Intermittent Misfire Condition	64

4.1	Torque Producing Mechanism in a Four Cylinder Engine (Model derivation is carried out in accordance with the generalized coordinated, spatial coordinated however are indicated only for geometric clarity)	67
4.2	Geometric Illustration of Cylinder Offset	72
4.3	Solution of the Model of Torque Producing Mechanism (shown in Figure 4.1). Initial Conditions for the Simulation are $\theta_c = 0\text{rad}$ and $\dot{\theta}_c = 117\text{rad/sec}$	78
4.4	Free Body Diagram of i^{th} Piston	79
4.5	A Multi-Cylinder Pressure Model	81
4.6	Integrated Model of the Mechanism and Combustion Model	83
4.7	Model Validation Results	85
4.8	Simulation Results for Staircase Input	86
4.9	Crankshaft Angular Speed Fluctuations	86
4.10	Capabilities of the Model	87
4.11	Simulation Results for Large Throttle Changes	88
4.12	Pattern of the Crankshaft Angular Speed Fluctuations	90
4.13	Pattern of Crankshaft Angular Speed Fluctuation for an Intermittent Misfire Condition (a) Single Intermittent Misfire (b) Two Consecutive Intermittent Misfires in one Cylinder	91
A.1	Engine Setup	101
A.2	OBD-II based Data Acquisition Scheme	102
A.3	Arrangement of Crankshaft Position Sensor	103
A.4	Intake Manifold Parameter Estimation	104
A.5	Parameter Estimation of Torque Production Subsystem	105
A.6	Estimate of Volumetric Efficiency	106

List of Tables

3.1	Description of the Generalized Variables	36
3.2	Description of the Generalized Efforts	40
3.3	Tuning Parameters of the Model	56
3.4	Optimized Parameters of Engine Model	57
3.5	Comparison of MVEMs and Proposed FPEM	64
4.1	Designation of the Generalized Coordinates	70
4.2	External Effort along Generalized Coordinates	73
4.3	Model Tuning Variables and Their Values	84
4.4	Comparison of MVEMs and Proposed FPEM	93
4.5	Comparison of Lumped Cylinder and Multi-Cylinder Approaches	94
A.1	Specifications of Engine Under Study	101
A.2	Parameters of Volumetric Efficiency	106

Abbreviations

MVEM	Mean Value Engine Model
DEM	Discrete Event Model
CCEM	Cylinder-to-Cylinder Engine Model
FPEM	First Principle based Engine Model
EGR	Exhaust Gas Recirculation
AFR	Air-to-Fuel Ratio
FAR	Fuel-to-Air Ratio
SA	Spark Advance
SI	Spark Ignition
CI	Compression Ignition
IC	Internal Combustion
GDI	Gasoline Direct Injection
HEV	Hybrid Electric Vehicle
VVL	Variable Valve Lift
VVT	Variable Valve Timing
EOM	Equation of Motion
DAE	Differential Algebraic Equation
ODE	Ordinary Differential Equation
PDE	Partial Differential Equation
MFB	Mass Fraction Burned
EOC	End of Combustion
SOC	Start of Combustion
IVO	Intake Valve Open
IVC	Intake Valve Close

EVO	Exhaust Valve Open
EVC	Exhaust Valve Close
TDC	Top Dead Center
BDC	Bottom Dead Center
OBD	On-board Diagnostics
ECU	Engine Control Unit
RPM	Revolution Per Minute
DAQ	Data Acquisition
TPU	Time Processing Unit
eTPU	Enhanced Time Processing Unit
ANN	Artificial Neural Network
FTC	Fault Tolerant Control
CTC	Cylinder-to-Cylinder

Symbols

Symbol	Description	Units
α	Throttle Angle	<i>rad</i>
C_D	Throttle Coefficient of Discharge	
\dot{m}_{ai}	Mass flow rate of air Past the Throttle	<i>Kg/sec</i>
\dot{m}_{aio}	Intake Manifold model fitting variable	<i>Kg/sec</i>
\dot{m}_{egr}	Mass flow rate in Exhaust Gas Recirculation	<i>Kg/sec</i>
P_{amb}	Ambient Pressure	<i>Pa</i>
T_{amb}	Ambient Temperature	<i>K</i>
D	Diameter of the Throttle	<i>m</i>
P_{man}	Intake Manifold Pressure	<i>Pa</i>
T_{man}	Intake Manifold Temperature	<i>k</i>
V_{man}	Intake Manifold Volume	<i>m³</i>
V_d	Engine Displacement Volume	<i>m³</i>
η_v	Volumetric Efficiency	%
\dot{m}_{ao}	Intake Port Mass Flow Rate of Air	<i>Kg/sec</i>
\dot{m}_{fi}	Input Mass Flow rate of Fuel	<i>Kg/sec</i>
\dot{m}_{fo}	Mass Flow Rate of Fuel to Cylinder	<i>Kg/sec</i>
τ	Fuel Film Evaporation Time Constant	<i>sec⁻¹</i>
ϵ	Fuel Separation Parameter	
R	Universal Gas Constant	<i>J.Kg⁻¹.K⁻¹</i>
N	Crankshaft Angular Speed	RPM
r_c	Compression Ratio	
P_{exh}	Exhaust Manifold Pressure	<i>Pa</i>

Symbol	Description	Units
γ	Ratio of Specific Heats	
τ_i	Indicated Torque	Nm
τ_f	Frictional Torque	Nm
τ_p	Pumping Torque	Nm
τ_L	Load Torque	Nm
τ_N	Net Torque	Nm
θ_o	Position at SOC	rad
$\delta\theta$	Combustion Duration	rad
T	Kinetic Energy	J
V	Potential Energy	J
L	Lagrangian of the System	
q_i	i^{th} Generalized Coordinate	
ϕ_i	i^{th} constraint of motion	
λ_i	i^{th} Lagrange Multiplier	
e_i^s	i^{th} Generalized Effort	
Γ	Set of the parameters of Torque Producing Mechanism	
T_{trans}	Translation Tension	
ω	Angular Velocity ¹	rad/sec
θ	Angular Position ¹	rad
x	X Component of Center of Mass of a rigid body ¹	m
y	Y Component of Center of Mass of a rigid body ¹	m
m	Mass ¹	Kg
J	Moment of Inertia ¹	$Kg.m^2$
l	Length ¹	m

¹Subscript (whereas applicable) will correspond to respective body

Chapter 1

INTRODUCTION

Two there are who are never satisfied – the lover of the world and the lover of knowledge.

Jalal Uddin Rumi

The chapter begins with the techno-historical background on Internal Combustion (IC) Engines in Section 1.1. Motives for the control oriented engine model are also addressed briefly. In order to avoid this introduction becoming a cut-and-dried material, an effort to summarize the initiating suppositions and motives of the research, contained in this thesis, are presented in Section 1.3 and Section 1.4. A complete overview of thesis is contained in Section 1.5.

1.1 Background

Energy, its reserves, utilization and the consequences, has ever been an on-going war of survival between human race and the nature. An optimal utilization of energy resource can buy the mankind more time for discovery of new energy resource. This can relax the time constraint on perpetual hunt of new reserves of energy. In this war, the mankind has enjoyed the victories and faced the defeats.

Till these times, IC engine has proven to be a favorable battle field for more than a century.

The efforts in development of IC engines had a long travel. It took the IC engines around hundred years to be able to run on a liquid fuel, efforts beginning by the work of Dutch physicist Christian Huygens in late 17th century to the work of Robert Street by end of 18th century. After a long trip, it was N. A. Otto [3], who established a first successful stable four stroke liquid fueled IC engine. Starting from those times, there were devoted efforts involved in turning this rumbling machine to a form, we are accustomed with. There came the revolution of 20th century flooded with technology, innovation and new concerns like environment. Concepts of fuel injection and electronic controls opened the gateway to concept of *Computer based Engine Controls*. The fact made the researchers to feel the need for development of dynamic engine models, [4]. Environmental legislation superimposed another factor in the evolution.

Attributes of simplicity, fidelity and diversity are the key features as well as conflicting constraints for mathematical modeling of non-linear dynamical systems. The indicated conflict is more worsening when mathematical modeling of engines is concerned. The said constraints mainly undergo two kinds of evolution:

1. *Technological Evolution*: such as development of more powerful embedded platforms relaxes simplicity and complexity trade-off for real-time performance,
2. *Forced Evolution*: for example more stringent environmental legislation and enhanced reliability requirements are significant ones. These also include introduction of new technologies, such as new power-trains, application of flex fuels and dynamic skip fire, [5].

Aforesaid progression process facilitates, and sometimes dictates, development of more powerful and complex control oriented models of internal combustion engines. Application specific embedded system architectures, such as Freescale Semiconductor's TPU and eTPU with PowerPC architecture, and upcoming generations are

ready to take more complex and more powerful control and diagnostic algorithm in automotive power-train applications. In addition, quest of new power-train architectures, flex fuel and autonomous vehicles require more flexible and detailed control oriented models to employ advanced control and diagnostic techniques for the purpose of respecting the new requirements.

1.2 Problem Statement

In light of the following:

1. The necessity of an engine model which supports the control and diagnostic unification and cylinder-to-cylinder control, and
2. The feasibility created by the recent powerful embedded systems

This thesis aims at extending the domain of control oriented gasoline engine models.

A methodology of developing the control oriented gasoline engine model is aimed which provides models with high fidelity and comprehensive capability of developing the control and diagnostics in a unified fashion. The model based description of multi-cylinder dynamics, description of system dynamics under fault conditions, wider region of validity and minimizing the usage of empirical relations are other attributes of interest.

1.3 The Beginning

It would be an appropriate time and place to begin with a fundamental discrimination. Among two types of the motion having close resemblance, but very different nature from behavioral point of view, that is the *Simple Harmonic Motion* and the *Reciprocating Motion*. Equation of motion for reciprocating motion of the piston is stated as follows, [6]:

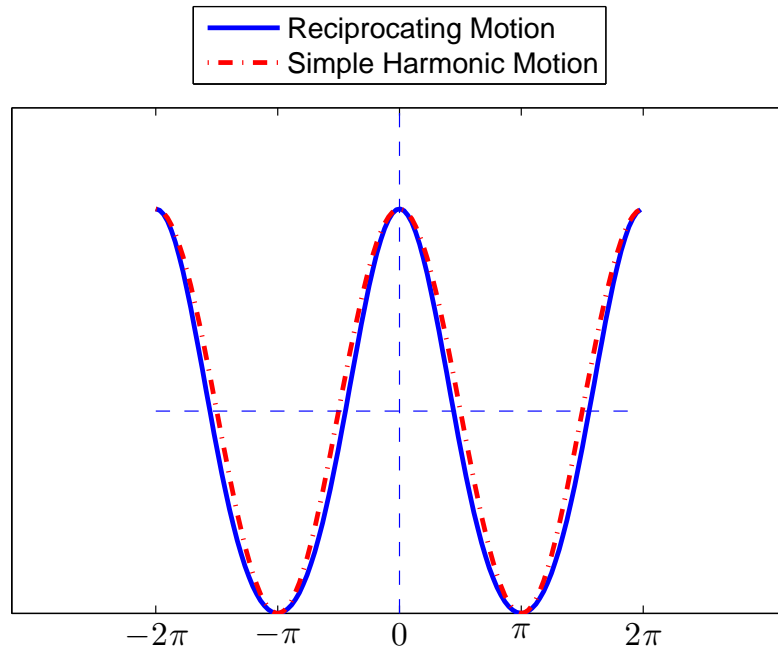


FIGURE 1.1: Comparison of Harmonic and Reciprocating Motion (offset subtracted and magnitude set to equal for visualization)

The Equation 1.1 clearly reflects two mathematical components forming the reciprocating motion. It should be noted that $f_1(\theta_c)$ impart a fundamental harmonic, similar to that of forming a simple harmonic motion. Whereas, there rides another component in Equation 1.1, $f_2(\theta_c)$. It should be noted that impact of second component reduces as the difference in l_c and l_i is reduced. Moreover, the reciprocating motion becomes simple harmonic motion as soon as difference among the two is brought to zero, that is $l_c = l_i$.

$$s = f_1(\theta_c) + f_2(\theta_c) \quad (1.1a)$$

$$f_1(\theta_c) = l_c \cos(\theta_c) \quad (1.1b)$$

$$f_2(\theta_c) = \sqrt{l_i^2 - l_c^2 \sin^2(\theta_c)} \quad (1.1c)$$

where s is distance of the piston from crankshaft axis of rotation, l_c is crank offset, l_i is length of connecting rod and θ_c is angular position of the crankshaft. In addition, simple harmonic motion is described by only one component, $f_1(\theta_c)$. This mechanism is discussed in detail in Chapter 2.

The fact triggered the thought to start modeling the reciprocating motion of the piston and to develop the engine model on this foundation. In order to investigate, if any benefits can be obtained by following derivation of the model on said directions.

1.4 Proposed Strategy

As discussed in previous section, in order to begin with modeling the reciprocating motion of the piston derivation of the detailed model of the mechanism is required. The other issue is development of model based means to determine the force acting on the piston, during different operational states of the engine and different phases of the four strokes. Initially, the assumption of lumped cylinder is taken, and it is perceived that methodology, tools and procedure will then be extended for multi-cylinder engines.

There is a variety of models for such mechanisms based on Newtonian Mechanics, following the conventional approach in engineering mechanics. However, it is foreseen that complexity of the model would increase with increase in number of cylinder. It is an important aspect, since evolving the model to multi-cylinder engines and putting basis for model based cylinder-to-cylinder control is one of the major objective of the research presented in this thesis.

It is concluded that devising an approach with Lagrangian Mechanics would give a better start. The way Lagrangian Mechanics looks at the modeling problem, together with proper simplification and solution strategy, would satisfy the constraints foreseen by the author.

Evaluation of the force acting on the piston needs model based description of pressure inside the cylinder of a gasoline engine. Cylinder pressure model together with cranks-case pressure, would give net external force acting on the piston. An analytical gasoline engine cylinder pressure model is taken from literature. It is

then utilized in study of Lumped Cylinder Dynamics. However, as explained later in details, the model is extended for multi-cylinder study.

Together with the model of the mechanism developed based on constrained equation of motion (EOM) in Lagrangian Mechanics and analytical gasoline engine cylinder pressure model, study of lumped cylinder dynamics is carried out earlier. Control oriented model of gasoline engine derived with such an approach, attained many interesting attributes.

Study on multi-cylinder dynamics is presented afterward. Investigation on novel applications of the model thus derived are analyzed against outlining features and attributes of the First Principle based Engine Model (FPEM).

1.5 Overview of the Thesis

Based on the foundation on engines and engine modeling laid by Chapter 1, Chapter 2 begins with an overview of gasoline engines and aspects of dynamical modeling in gasoline engines. Architectural considerations in gasoline engine control oriented models are explained with help of cause and effect diagram. Historical research trends and efforts in control oriented gasoline engine modeling are then made part of the Chapter 2. The author has made an effort to investigate the linkage between evolution of engine technology, environment legislation and research on engine models. The chapter, based on preceding discussion, identifies the research gap. Based on the research gap, the author proposes a unified control and diagnostic framework for gasoline engines. Moreover, thesis aims at development of a control oriented gasoline engine model, having sufficient flexibility and capability for the development of said unified framework.

The research problem posed in Chapter 2, is solved step-wise. Chapter 3 aims at summarizing the former step. Whereas, Chapter 4 extends the efforts presented in foregoing chapter.

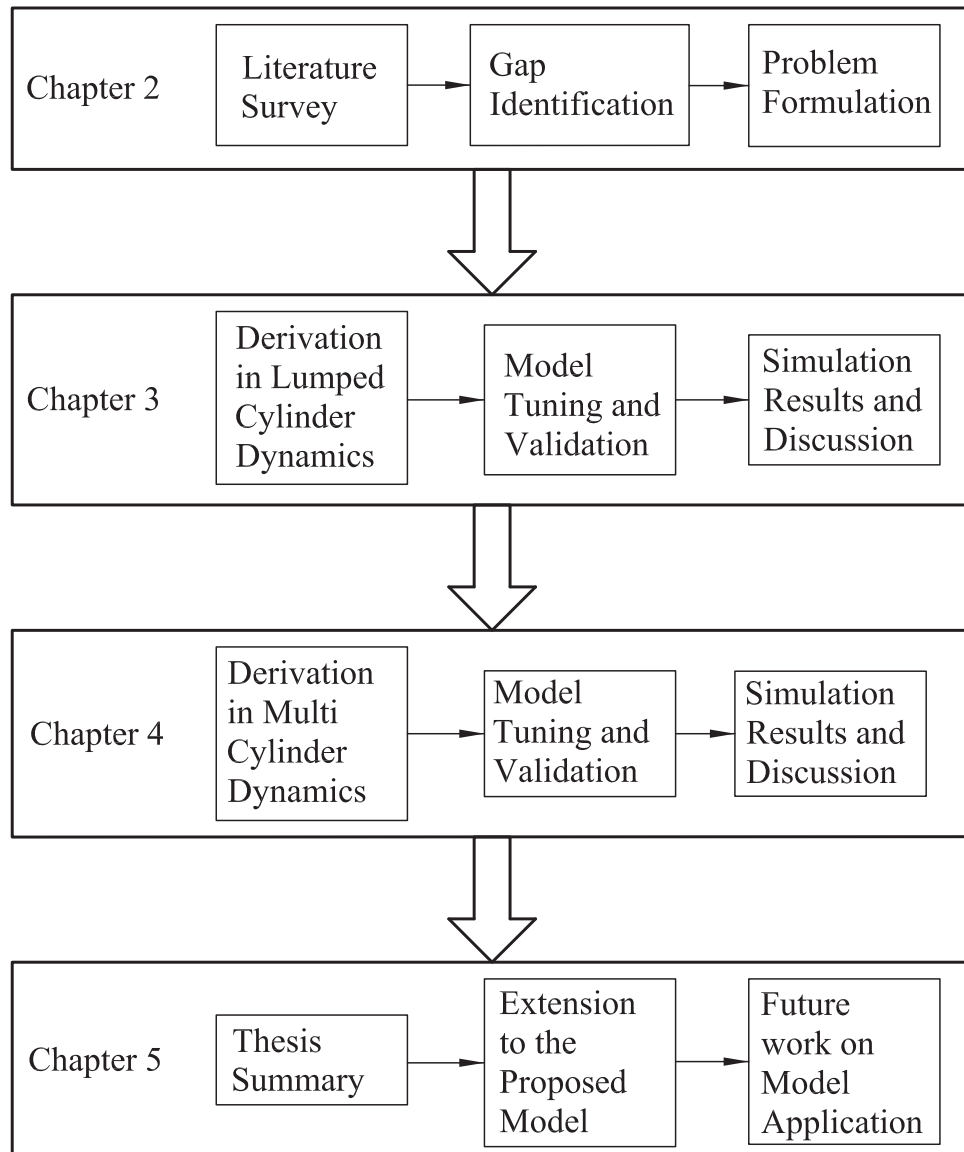


FIGURE 1.2: Organization of the Thesis

Further, Chapter 3 presents an effort to develop an FPEM, based on assumption of lumped cylinders. After derivation of the model of torque producing mechanism using constrained EOM in Lagrangian Mechanics, a suitable simplification strategy is explained. An analytical gasoline engine cylinder pressure model, used to evaluate the forces acting on the piston, is explained afterward. Aspects of sub-system integration, model realization, tuning and validation are addressed after simplification. The chapter ends with discussion on the main-stream attributes of the FPEM, derived earlier in the chapter.

Chapter 4 advances with an objective to waive-off the assumption of lumped cylinders. Derivation and suitable simplification strategy of torque producing mechanism corresponding to a multi-cylinder engine is presented. An analytical gasoline engine cylinder pressure model, presented in Chapter 3, is extended for a four cylinder engine. After discussion on the model integration and tuning, simulation results are presented. The capability of the model, to describe the dynamics of healthy as well as system under fault conditions, is elaborated by validation of crankshaft angular speed fluctuations pattern generated by the model for one cylinder misfire with the data acquired from the engine experimentally. The chapter ends with discussion on the attributes and extended capability of FPEM for control and diagnostic point of view.

Chapter 5 concludes the research presented in the thesis and summarizes the featured attributes of the FPEM. Possible utilization of the FPEM along-with potential extension to the FPEM itself ends the Chapter 5.

Appendix A explains the details of the experimental setup and detailed specifications of the engine under study are also included. Data acquisition interfaces applied to acquire the engine data for model tuning and subsequent validation are explained. Furthermore, the techniques and problem formulation of parameter estimation (applied in both Chapter 3 and 4) are explained. Tuning of the parameters of intake manifold and torque production subsystem are explained separately.

Appendix B and Appendix C present detailed mathematical expressions for lumped and multi-cylinder dynamics, respectively.

Chapter 2

CONTROL ORIENTED GASOLINE ENGINE MODELS: TRENDS AND FASHIONS

At the outset I wish to stress that the design of a superior and reliable control system for automotive engines is, in my opinion, a far more complex design problem than that required for most aerospace application.

Micheal Athans (1978).

With brief description on the background and summary of research presented in Chapter 1, this chapter begins with the introduction and modeling aspect of gasoline engines. The physical phenomena and underlying mechanism is described in Section 2.1. A panoramic overview of the modeling perspective of gasoline engine is presented in Section 2.2. Switching from steady state modeling to the dynamical modeling and efforts in dynamical control oriented models of gasoline engine are presented in Section 2.3. Section 2.4 aims at exploring the dynamics in engine research. The author has made an effort to investigate the link between the innovative engine technologies, relevant legislation and research on engine modeling. Based on the discussion included in previous sections, Section 2.5 precisely identify

the gaps in the relevant field and defines the objectives of the research presented in this thesis. The chapter is concluded in Section 2.6.

2.1 Gasoline Engines: An Overview

Gasoline engines are the machines which extract chemical energy from the gasoline fuels and convert it to mechanical form [7]. A gasoline engine consists of an arrangement of intake and exhaust valves together with a mechanism to convert the reciprocating motion of the piston to angular motion of the crankshaft, as shown in Figure 2.1. Piston cylinder mechanism inspires mixture of fuel and air during intake stroke and throws the combustion products out to the environment during exhaust stroke. There lies a combustion process, having the sole purpose to shift the expansion process away from the compression process in order to generate a working cycle[8].

The processes summarized above intake, compression, combustion, expansion and exhaust [3] have served the human race for more than hundred years. The reciprocating motion of the piston is then converted to rotational motion of crankshaft, by the mechanism jointly formed by piston, connecting rod and the crankshaft.

Looking at the picture from thermodynamic point of view, the cycle begins with constant pressure intake followed by an isentropic compression, constant volume heat addition, isentropic expansion and exhaust process. It is significant to note that gasoline, or generally speaking internal combustion engines are not precisely the heat engines. Since the boundary is not closed. They take the charge and exhaust it out to the environment.

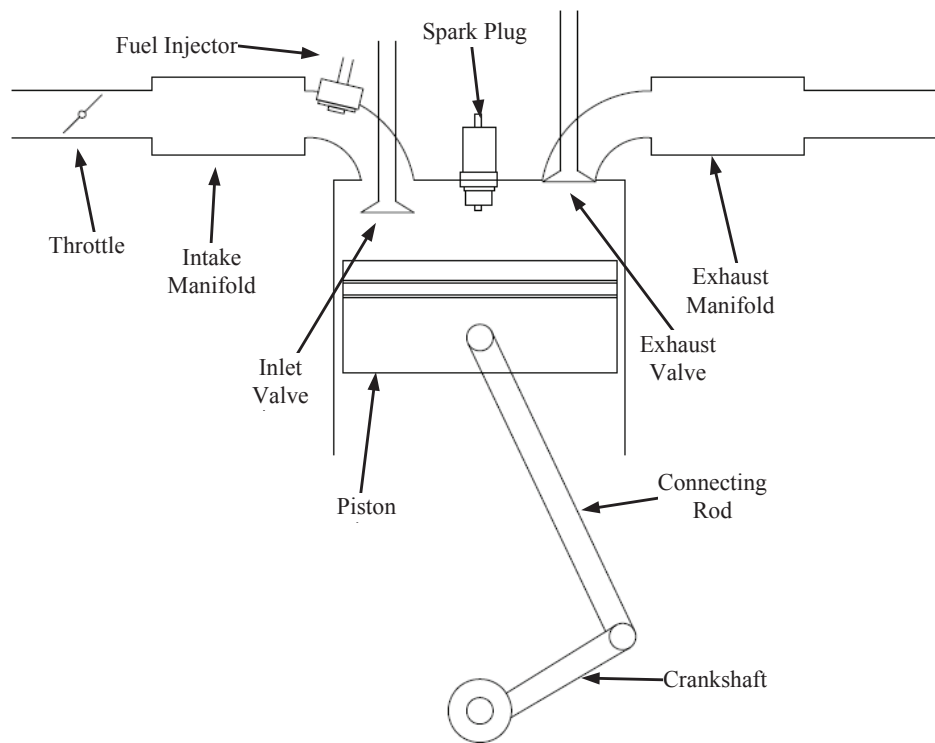


FIGURE 2.1: Gasoline Engine: An Overview

2.2 Gasoline Engines: Dynamic Modeling Facet

Control oriented modeling of IC Engines is not a trivial exercise in modeling paradigm. IC engines, being nexus of many disciplines, pose a difficult modeling problem. Capturing the nonlinear behavior, such as reciprocating motion of the piston, and discontinuous events, for instance opening/ closing of inlet or exhaust valves, proves not to be a straight forward task [1]. Therefore, taking assumptions and having journey with few analogies remains the only option for capturing the dynamics in theory. Development of the mathematical models on such a road, leads to application specific paradigms of IC engine modeling. As a result of taking assumptions and analogies, each specific class of model throw light on specific aspects of the physical system. These include Mean Value Engine Models (MVEMs) [9], Discrete Event Models (DEMs) [1], Cylinder-to-Cylinder Models (CCEMs) [10] and hybrid models [11].

As per overview of the gasoline engine described in Section 2.1, gasoline engine is

divided in subsystems from modeling point of view. Commonly found subsystems of a gasoline engine from control point of view are as follows [1]:

1. Air Intake
2. Fuel Supply
3. Intake Manifold
4. Torque Production

Physically, in a gasoline engine, these subsystems operate together. From aspect of modeling, by cause and effect analysis inputs and outputs of each subsystem are identified, a form of which is shown in Figure 2.2. Using this approach, model of individual subsystems are developed, which are then integrated to achieve the model based description of engine as a whole.

Air intake subsystem, consists of an air filter and throttle valve. The air filter traps down the dust particulates, throttle receives the driver demand and in result controls the amount of air entering the intake manifold. Objective of modeling of this part of the engine is to estimate the mass flow rate of air, being inspired and entering the intake manifold.

Fuel supply subsystem, sprays the fuel at intake port (in port fuel injection engines), which in turn evaporates and joins the air flowing from intake manifold to engine cylinder during intake process. Real challenge in developing the model of this part is to comprehend mathematically the fuel film formation, instantaneous evaporation of fuel, evaporation of the fuel back from the film and mathematical description of the mass flow rate of fuel entering the engine cylinder.

Intake manifold subsystem, is basically an air reservoir placed before induction stage. Purpose of modeling this subsystem is to estimate the intake manifold pressure and temperature. This in turn, together with other parameters, helps in estimating the mass flow rate of air entering the engine cylinders.

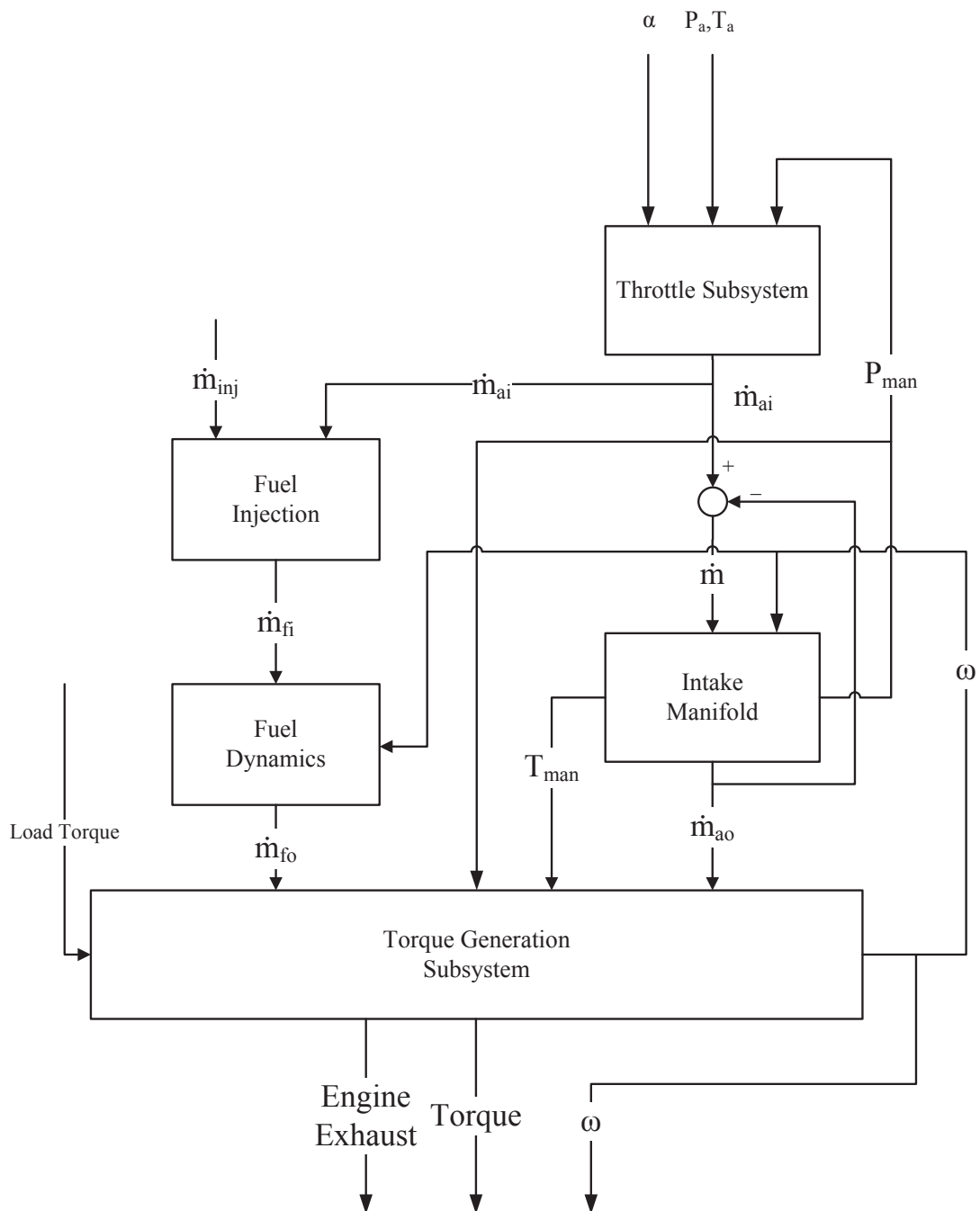


FIGURE 2.2: Gasoline Engine Cause and Effect Diagram [1]

Torque production subsystem, in principle spans the whole mechanism; engine cylinders to the crankshaft including inputs like spark timing. Objective of modeling this part of the engine is to capture the speed generation dynamics in the model. From modeling point of view incorporating the inputs like spark timing and air fuel ratio, and other aspects effecting the combustion and modeling the friction in the system form a widespread scope for this subsystem.

2.3 Research on Gasoline Engine Modeling

The literature in engine modeling was accustomed to algebraic or steady state engine models, until 1971 [12]. Though the engine emissions were main stream of the study, an abstract theme of a dynamical engine model was set to float on the research horizon. These were the times when control and modeling community was xenophobic against automotive engines. A pioneering work on necessity and probable structure of a control oriented model of an automotive engine was followed, it was Athans [4] who bite the bullet. The work brought to light the necessity and explained the role of a possible dynamical model of an automotive engine. It was further emphasized that in order to begin with the development of the dynamical model, it was necessary to identify the engine variables/ parameters and explore the cause and effects.

The work presented onwards in this chapter was carried out on different places, which mutually evolved to form a family of control oriented engine models. The family of models, based on its founding attributes, gained the name *Mean Value Engine Models (MVEMs)*.

The work of Athans [4] was followed by the foundation work carried out by B. K. Powell [13]. The work took the idea floated in [4], out of abstraction and provided mathematical shape to it. Mathematical formulation for engine acceleration was devised as follows:

$$J_e \ddot{\theta}_e(t) = \tau_e(t) - \tau_L(t)$$

where,

- J_e Engine moment of inertia
- τ_e Engine Torque
- θ_e Engine/ Crankshaft position
- τ_L Load torque

the engine torque was modeled as regression model. To consider the EGR, a ratio “ E ” was defined as follows:

$$E = \frac{\dot{m}_e}{\dot{m}_e + \dot{m}_a}$$

- \dot{m}_e Mass flow rate of air in EGR
- \dot{m}_a Fresh mass flow rate of air

Overall intake manifold pressure dynamics (the author termed it as “induction process dynamics”) were modeled as follows:

$$\dot{P} = K_p(\dot{m}_a + \dot{m}_e - \dot{M})$$

- P Intake Manifold Pressure
- M Mass flow rate of air to engine cylinder
- K_p Model constant

The author also presented an engine control policy, however the proposed model didn’t include the fuel dynamics. Moreover, instead of utilizing the engine parameters, the proposed model was regression based. For modeling of the engine torque, for instance, a regression model was tuned with port mass flow rate of air, AFR, SA and engine speed as inputs. As it is well known in modeling and control community, that regression based models suffer a limited envelope of validity.

This was the era of foundation work in dynamical engine modeling. Different approaches followed the base work of Athans [4] and B.K. Powell [13].

A significant effort was followed afterward by Dobner et al. [2, 14, 15]. The eminent aspects of the model presented in [2] were model of carburetor based fuel

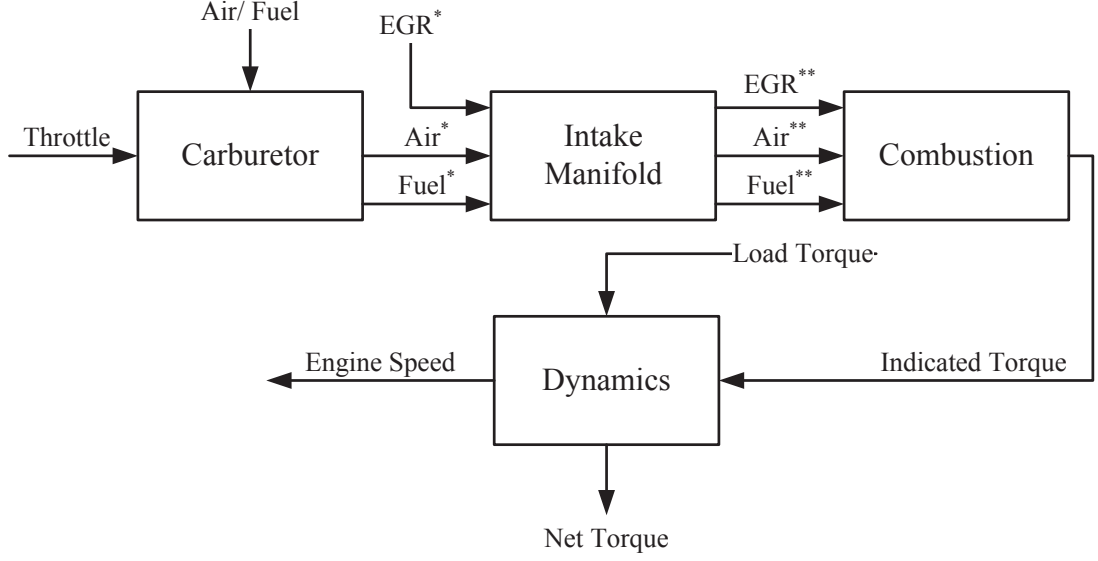


FIGURE 2.3: Engine Subsystems and Interconnect [2] (*mean mass flow rate to intake manifold, **mean mass flow rate to engine cylinder)

supply coupled with accelerator pump model, incremental evaluation of variables and last but the most significant was the modular approach presented in the study. Modularization of the engine system, from model point of view, presented in [2] is shown in Figure 2.3.

Air flow was taken as function of throttle angle and downstream pressure, that is P_{man} . Throttle characteristics were obtained experimentally. Following formulation was used for pressure ratios:

$$\sqrt{\left(\frac{P_{man}}{P_{amb}}\right)^{2/\gamma} - \left(\frac{P_{man}}{P_{amb}}\right)^{\gamma+1/\gamma}} \quad (2.1)$$

To accommodate the accelerator pump short, a model for accelerator pump was also devised. It was further explained that development of the intake manifold model was the most formidable part of the engine modeling, the reason behind the fact was availability of very little quantitative information for defining the physical process within the intake manifold.

As described about the discrete formulation, the engine mass flow variables were transformed to incremental masses, leaving or entering. The appropriate time

increment Δt was proposed as follows:

$$\Delta t = \frac{120}{n_{cyl}N}$$

where n_{cyl} is number of engine cylinders and N is engine speed. Following formulation was presented for incremental masses:

$$\Delta M_{AI} = \dot{M}_{AI}\Delta t$$

$$\Delta M_{EGR} = \dot{M}_{EGR}\Delta t$$

$$\Delta M_{FGI} = \dot{M}_{FGI}\Delta t$$

$$\Delta M_{FDI} = \dot{M}_{FDI}\Delta t$$

$$\Delta M_{FWI} = \dot{M}_{FWI}\Delta t$$

where AI, FGI, FDI and FWI are subscripts presenting input air flow, evaporated fuel flow, atomized fuel flow and wall fuel flow, respectively and Δ is change variable. Whereas, incremental mass leaving the intake manifold was modeled as:

$$\Delta M_{Go} = \dot{M}_{Go}(\eta_v V_d / V_{man})$$

$$M_G = M_A + M_{EGR} + M_{FG}$$

It was shown that combustion process generated torque in relation to the air ingested into the cylinder. The parameter/ variables influencing the torque were identified as air/ fuel, engine efficiency and spark timing. The torque constant K_T was used to relate the indicated torque to the air aspirated in the engine cylinder:

$$K_T = \frac{\tau_{NMX} + \tau_F}{\Delta M_{AC}}$$

where,

τ_{NMX}	maximum torque
τ_F	frictional torque
ΔM_{AC}	mass of air aspirated in the cylinder

Effects of other parameters affecting the indicated torque were investigated through static engine test data.

The model presented a beautiful modular approach. The foundation laid in the modules of engine for modeling purpose could be seen in modern control oriented engine models. Despite of this fact, there were a few shortcomings associated with the model.

1. The major shortcoming was the fuel supply system considered for the model development. The work was presented in the era when carburetors were rapidly being replaced by fuel injection/ electronic fuel injection.
2. Throttle characteristics were acquired experimentally and regression model was tuned.
3. Model didn't attained the form of ODEs (preferable for control oriented model).

After Dobner et al. [2], another groundbreaking work was carried out by C. F. Aquino [16]. The work emphasized on air and fuel dynamics, transient characteristics of gasoline engine were discussed. Indicated torque and speed dynamics of the engine were not included in the study. However, structure of the model of intake manifold was significantly improved. Instead of incremental masses, model based non-linear ODEs were derived. Many of the later studies followed the mathematical structure presented in this study.

For air dynamics, continuity equation for the manifold volume was stated as:

$$\frac{d}{dt}m = \dot{m}_{ai} - \dot{m}_{ao}$$

where m is residual mass of air in the intake manifold. Intake manifold pressure dynamics were obtained as follows:

$$\begin{aligned} m &= \frac{P_{man} V_{man}}{RT_{man}} \\ \dot{m}_{ao} &= P_{man} \frac{N \times V_d \times \eta_v}{2RT_m} \\ \frac{dP_{man}}{dt} + \frac{N \times V_d \times \eta_v}{2V_{man}} P_{man} &= \dot{m}_{ai} \frac{RT_{man}}{V_{man}} \end{aligned}$$

It could be seen that pressure dynamics are derived with an assumption of *Isothermal process*, as the T_{man} is taken as constant. Possibly, in the era when the study was carried out, almost all the engines were manufactured with a metallic intake manifold. With a metallic intake manifold (especially under low engine speeds when residual time of gases in intake manifold is larger) there is heat conduction from manifold to environment. This phenomenon makes it more like an isothermal process. Another prominent attribute of the description was structured expression for volumetric efficiency, with tuning variable. It was proposed as follows:

$$\eta_v = E \frac{\gamma - 1}{\gamma} + \frac{r_c - (P_{exh}/P_{man})}{\gamma(r_c - 1)}$$

Distinguishing feature of the model was a mathematical description of the throttle, expressed as:

$$\dot{m}_{ai} = \frac{C_d A P_a (2\gamma)}{R(\gamma - 1) \sqrt{T_a}} \left[\left(\frac{P_{man}}{P_{amb}} \right)^{2/\gamma} - \left(\frac{P_{man}}{P_{amb}} \right)^{\gamma+1/\gamma} \right]^{1/2}$$

where A is effective flow area at throttle. It should be noted that, same formulation for pressure ratio has been used in this work as that of presented in Equation 2.1 [2]. However, contrary to [2], model of fuel injection was proposed in this study.

The model of fuel flow proposed in [16] was a two state model.

$$\begin{aligned}\frac{d}{dt}M_f &= \dot{M}_{in} - \dot{M}_{out} \\ &= x\dot{M}_{fm} - \frac{1}{\tau_f}M_f \\ \frac{d}{dt}M_v &= \frac{1}{\tau_f}M_f - \dot{M}_{ao}\frac{M_v}{M}\end{aligned}$$

where

- M_{fm} metered fuel
- M_f mass of fuel in the film
- M_v mass of fuel vapors in the intake manifold
- x fuel separation parameter

As described earlier, though the formulation of torque generation and speed dynamics were not the objective of this study, fuel and air dynamics set the trend of research in the respective field.

Next link of the chain was formed by Moskwa et al. [17–20]. This part of the chain was greatly inspired by [16]. The work acquired modular approach from [2] and intake manifold dynamics from [16]. Mathematically refined manifold and fuel dynamics were integrated with torque production subsystem. The model was validated on a port fuel injected gasoline engine.

Model of the fuel dynamics proposed in [17], took its roots from [16]. However, in contrast to its root, a single state model was proposed to capture the dynamics of the fuel. Injected fuel flow rate was broken into the following parts:

1. Fuel injected after intake valve close event
2. Fuel injected before intake valve close event
 - (a) Fuel immediately converted to vapors
 - (b) Fuel imparted to the fuel puddle at intake port

Mathematically,

$$\begin{aligned}\ddot{m}_{fo} &= \dot{m}_{ff2} + \dot{m}_{ff3} + \dot{m}_{fsl} \\ \dot{m}_{ff2} &= \dot{m}_{fi}\epsilon(1 - \bar{\gamma}) \\ \dot{m}_{ff3} &= \dot{m}_{fi}\epsilon\bar{\gamma} \\ \ddot{m}_{fsl} &= (\dot{m}_{fi}(1 - \epsilon) - \dot{m}_{fsl})\frac{1}{\tau_f} \\ \bar{\gamma} &= \begin{cases} 1 & \text{if } \phi_{PW} \leq \phi_{IVC} - \phi_{SOI} \\ \frac{\phi_{IVC} - \phi_{SOI}}{\phi_{PW}} & \text{if } \phi_{PW} > \phi_{IVC} - \phi_{SOI} \end{cases}\end{aligned}$$

where,

- ϕ_{IVC} Crank Angle for Intake Valve Close
- ϕ_{SOI} Crank Angle for Start of Injection
- ϕ_{PW} Injection Pulse Width in Crank Angle

Dynamics of the fuel flow, from injection until the transport to engine cylinder are described by a single state model. The subsequent studies showed that single state model for fuel dynamics was sufficient rather than a two state model, derived in [16]. Intake manifold filling dynamics we modeled as:

$$\frac{d}{dt}P_{man} = \left[\frac{\dot{T}_{man}}{T_{man}} - \gamma\omega\eta_v \right] P_{man} + \frac{RT_{man}}{V_{man}}(\dot{m}_{ai} + \dot{m}_{egr})$$

Formulation described by above equation is definitely not an isothermal one, however as per author's knowledge formulation for \dot{T}_{man} was not included. Intake manifold filling components (\dot{m}_{ai} and \dot{m}_{egr}) and manifold emptying components (\dot{m}_{ao}) were also modeled as model based. Volumetric efficiency (η_v) was devised to have two components, one corresponding to steady state while the second component countered for dynamic correction. The said strategy to model the volumetric efficiency was somewhat different than that adopted in [16]. Engine speed dynamics were modeled as follows:

$$J_e \frac{d}{dt}\omega = \tau_i - \tau_f - \tau_p - \tau_L$$

In contrast to previous studies, though the speed dynamics were not exactly model based, but division into the components lowered the abstraction height.

The work presented in Hendricks et al. [9, 21, 22] put another link to the chain of engine modeling. The base work in this part of the chain [9] was greatly inspired by [2] and [17]. The work presented in [9] carried almost same modular approach towards engine modeling, as presented in [2]. A single state model of fuel dynamics was proposed in, however the model was somehow different than that in [17]. Along-with other mathematical aspects, it was the first work which precisely named the family as *Mean Value Engine Models*. Other than this, bases were also explained, that in an MVEM framework which model variables were to be modeled as algebraic and which ones required dynamical modeling. The basis as explained in [9], were as follows:

1. *Algebraic Modeling*: The variables which reach to the equilibrium value within one or two cycles of the engine, do not need a differential equation to be modeled mathematically,
2. *Dynamical Modeling*: The variables which take more than two engine cycles to evolve to the equilibrium state, do need a differential equation to describe the process.

There was yet another approach towards the objective of dynamical model a gasoline engine, presented in Crossley et al. [23]. The approach presented was mainly aimed at capturing the input output dynamics. Though the model seemed attractive and was included in mathematical packages, like Matlab[®]. However, the model failed to grow in the literature. Though the model captured the input output dynamics, however the model was like a black-box which hide the system behind the tuned regression models. Throttle characteristics were divided in two components, one responsible for throttle angle, while the other for incorporating

the pressure ratio, as follows:

$$\begin{aligned}\dot{m}_{ai} &= f(\alpha)g(P_{man}) \\ f(\alpha) &= 2.821 - 0.04121\alpha + 0.10299\alpha^2 - 0.0063\alpha^3\end{aligned}$$

and,

$$g(P_{man}) = \begin{cases} 1 & P_{man} \leq \frac{P_{amb}}{2} \\ \frac{2}{P_{amb}} \sqrt{P_{man}P_{amb} - P_{man}^2} & P_{man} > \frac{P_{amb}}{2} \end{cases}$$

Manifold emptying components, that is \dot{m}_{ao} , was also modeled as a function of engine speed and P_{man} as follows:

$$\dot{m}_{ao} = -0.366 + 0.08979NP_{man} - 0.0337NP_{man}^2 + 0.0001N^2P_{man}$$

Likewise, regression model was also tuned for engine torque in terms of \dot{m}_{ao} , AFR, engine speed, SA and EGR.

Other interesting approaches during initial ages of engine modeling also include Rizzoni et al. [24], Hedricks et al. [25] and Chaumerliac et al. [26]. An equivalent electrical circuit was devised in [24], where lumped component values like resistance, inductance and capacitance were linked to the physical parameters in engine system. A three state engine model, one for intake manifold (isothermal supposition), one for fuel dynamics and single state speed dynamics, was proposed in [25].

Many of survey efforts have been done in the field of IC engine modeling (for both SI and CI). Prominent survey studies include [27], [28] and [29]. In [28], the author compared his own and other literature in the field till the year of publication. Along-with other recommendations, the author emphasized the development of engine models which can track both time and crank angle domain.

A variant in torque production subsystem was devised in [30]. The kinematics of slider crank mechanism were utilized for the development of model. A combustion model was developed to formulate the forces acting on the piston. Full dynamic

model of slider crank mechanism was not included, however abstract model based on kinematic analysis was used to estimate the torques generated due to the forces acting on the piston

$$F(\theta) = p(\theta) \times A_p$$

where, $F(\theta)$, $p(\theta)$ and A_p represent forces acting on piston, in-cylinder pressure and area of piston respectively. Equation above, was employed to calculate the forces acting on the piston as a function of crank angular position [30]. The whole slider crank mechanism was modeled as two lumped masses i.e., mass in reciprocating motion and mass in rotating motion. As a result, in contrast to the conventional analogy of volumetric pump, model considered two masses. These masses were utilized to calculate the translational and rotational inertia. Moreover, component of force orthogonal to crank radius was transformed to torque with the help of trigonometric analysis. With such a modeling strategy, though the mathematical model included the design of slider crank mechanism. However, model was not capable of extension to multi-cylinder engines. Furthermore, the added complexity to the model did not provide other information in addition to angular speed of the crankshaft.

Artificial Neural Networks (ANNs) were applied for the modeling of spark ignition engine in [31]. Black-box neural network technique was utilized to develop the dynamic model of engine subsystems. Application of neural networks was shown advantageous for real-time applications. The work was further extended in [32]. However, the scope remained within the ANNs. ANN is one of the most suitable technique for block-box learning, but the dynamic system does not remain transparent. Other drawbacks of ANNs include undetermined degree of over-fitting.

2.4 Technology Legislation and Research Trends

The author has made an effort to throw light on the dynamics of the evolution, that is to investigate the cause, effect and outcome in fraternity of the engine modeling.

For the purpose, the author has considered the following three factors:

1. Engine Technology
2. Environmental Legislation
3. Research on Engine Model

The aforesaid contributors mutually form a kind of a three state dynamical model. Where, current value, conditions or circumstances in one state effect the other two. Resulting flow has been shown in Figure 2.4. The flow of evolution presented in Figure 2.4 is divided into three rows, as stated above. The top one contains the flow of engine technology like fuel injection, valve timing, valve lift, variable cylinder management and dynamic skip fire. The middle row is meant for the environmental legislation. For case study, environmental legislation from European Union Directives (EU) and Environment Protection Agency (USA) are taken. The bottom most, third row shows the trends of research on the subject of dynamical engine models.

The first row, along-with straight forward evolution like that of the fuel injection technology, shows some non-trivial patches of evolution. Such as reappearance of HEV, VVL or VVT. These can be well understood with an example of microprocessor development history. Intel introduced its 16-bit microprocessor in 1978, the well known 8086. The architecture *x86* became the Intel's most successful chain of the microprocessors. However, right after one year Intel's Laboratory at Israel, *Haiifa Laboratory*, released Intel 8088 an 8-bit microprocessor in 1979. The reason for going back from 16-bit to 8-bit was not enhancement of the architecture or any other. The 8088 was essentially equipped with the same architecture, internal 16-bit registers but external interface was designed as 8-bit. Such a variant decreased the throughput of the device by 50%. However, reason behind releasing such a variant were aspects like low availability and high cost of supporting hardware and peripherals. Back in those times, development of 8086 based systems faced the issues of more supporting hardware with complex and expensive designs. The issue was resolved by stepping back and introducing an 8-bit version. In a

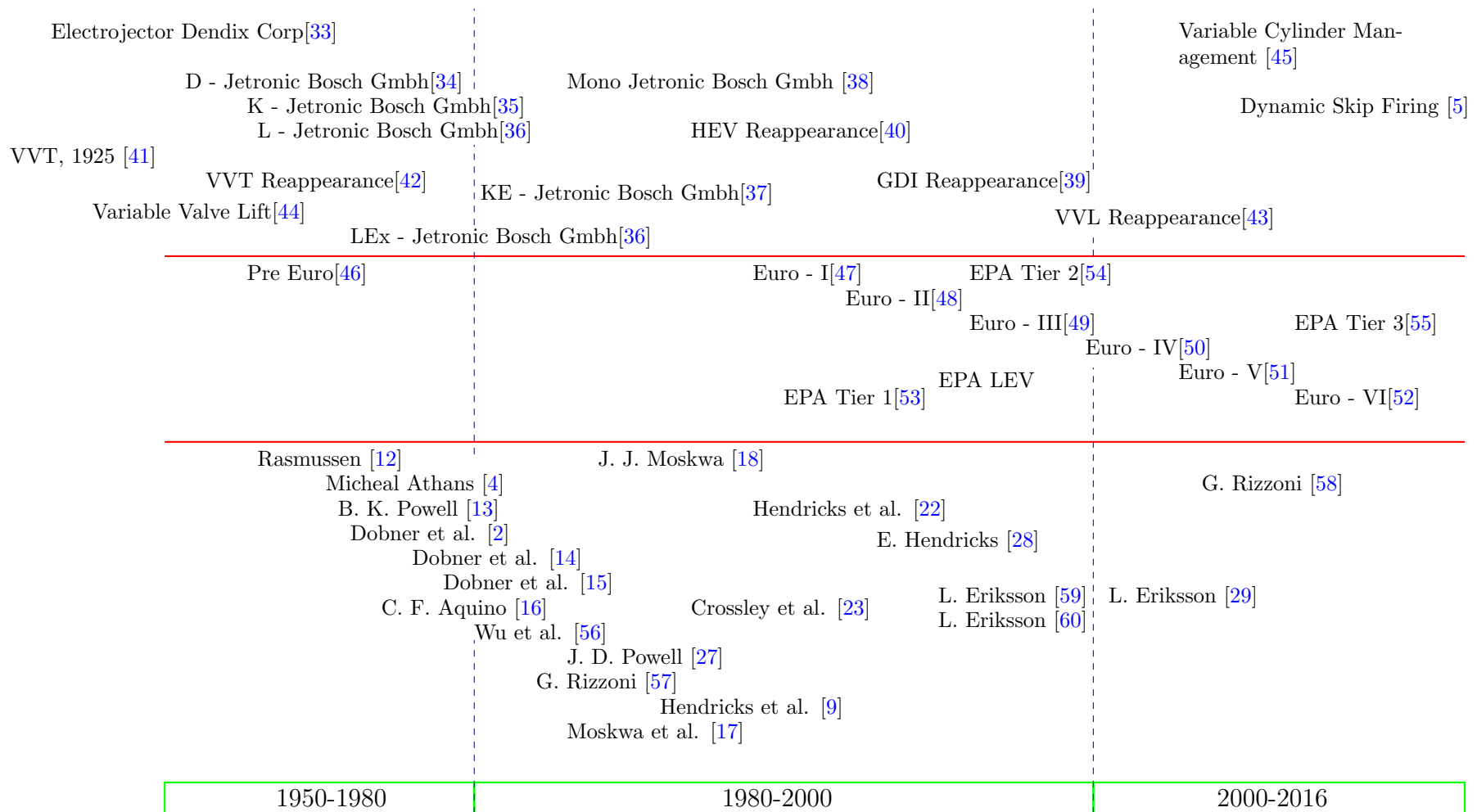


FIGURE 2.4: Summary of Engine Evolution

similar fashion, many technologies in engine systems and automotive power-train like HEV, VVT and VVL were developed years ago and remained suppressed or ignored due to the fact that other circumstances were not ready to digest the indicated innovative inventions. Subsequently, they re-appeared as soon as there became a feasible environment or being introduced by some forcing aspect.

The other aspect is legislation, among others there are two key governing aspects. The one is green house effect or pollutant emissions aspect while the other is fuel efficiency or economy. Aspect of fuel economy is further driven by the former aspect, the environment, and rising prices of fossil fuels. Overall, independent of engine/ power-train technology or research on the same field, legislation are going to keep the pace with most expectancy.

In author's view, as could be seen in the Figure 2.4, innovative technologies triggered the conditions. Introduction of fuel injection and parallel growth of embedded systems opened the horizon to electronic engine controls. Embedded systems in automotive power-train changed the possible view of the engine. As a result, engine modeling sorority started looking at the engine with a new point of view. Consequently, journey of engine modeling took turn from the long traveled route of steady state models to the highway of dynamical modeling.

Later times, last decade of 20th and beginning of 21st century, are rich with applications. The innovative engine technologies with control and diagnostic oriented models proved their necessary existence in order to respect the legislation and fulfill other requirements.

Evolution of the technology, blended with the research on engine models paved an easy way for respecting the legislation. Furthermore, as it could be seen in recent past, the re-appearance of technologies with an empty area in engine research. While as a matter of fact, legislation will keep the pace and will go on becoming more stringent and environment friendly. Based on history trend, it is foreseen that new engine technologies require new engine modeling frameworks. The said, engine technology together with new generation of engine models, will help in honoring the upcoming environment, reliability, efficiency and economy requirements. The

field of engine modeling is, once again, in need to enjoy the mercurial brilliant research, as it did during the second last decade of 20th century.

2.5 Constructing the Research Problem

As seen in Section 2.3 and 2.4, though modeling of torque production subsystem has variety of approaches. However, all of the techniques differ in a sense to evaluate the brake torque. As a result, basic mathematical structure being used in almost every patch of the literature is as follows:

$$\begin{aligned} J_e \omega_e &= \tau_b \\ &= \tau_i - \tau_L - \tau_p - \tau_f \end{aligned}$$

The underlying concept behind the equation above, is explained by [1]. Other inputs to the system either take the analogical or empirical formulation, [1, 61]. It is explained that while developing the model with such a strategy, whole mechanism formed by piston, connecting rod and crankshaft is replaced by an analogical volumetric pump. A pump which operates continuously, pumps air from intake to exhaust manifold, and produces torque in proportion to mean flow of air and fuel.

Following such a modeling approach, the control oriented model captures the approximate output profile. Subsequently, level of abstraction residing between physical system and the model is heightened. Along-with the transparency to the physical system, a few components of response are suppressed in the output generated by the model, commonly known as *crankshaft angular speed fluctuations*. Along-with other minor ones, there are two dominant factors generating the said speed fluctuations. They are as follows:

1. Dynamics of the mechanism generating the torque. That is, the mechanism formed by piston, connecting rod and crankshaft. Other than the dynamics of the mechanism, the reciprocating motion of the piston is converted to

angular motion of the crankshaft. Effective angle between the force acting on piston and the effective moment arm is always changing (crankshaft rotates continuously). Both aspects mutually give rise to fluctuating profile of crankshaft angular speed.

2. Different kinds of forces (accelerating or retarding) acting on the piston during different phases of four stroke, in other words rapidly changing in-cylinder conditions.

Crankshaft angular speed fluctuations carry useful information from control and diagnostic point of view. There exists a rich literature on significance (such as [62]) and utilization (for instance [63–65]) of crankshaft angular speed fluctuations. Devising a modeling strategy capable of capturing the complete crankshaft angular speed profile can enable the development of techniques, mentioned earlier in the paragraph as ones which are model based.

Besides the angular speed fluctuations, assumption of volumetric pump and invisibility of engine cylinder make the development of basis for model based cylinder-to-cylinder control an almost impossible task. Since individual cylinders are never visible to the model. On the other hand new engine technologies like [45] and [5] require the models suitable for developing the cylinder-to-cylinder control algorithms.

Alongside aforementioned aspects, invisibility of the core mechanism makes the model incapable of application of any estimation based techniques related to the mechanism.

Despite of the aspects explained above, since engine models are either time based (MVEMs) [9] or cranks angle based (DEMs) [1]. Both classes of models own their specific area of applications. In parallel to these classes, there are transformation technique [66], for switching between time and crank angle domain. Other than transformation, as indicated by [28], engine control framework requires the model which contain time and position information at the same time.

Another aspect, which is not addressed until now, is different control loops required for smooth engine operation. Which include idle speed control, AFR control, torque control, emission control, thermal management etc. A platform allowing integrated design of all engine control loops can add more flexibility, degree of freedom for control designer and enhanced system reliability.

In the last but not least, though the conventional MVEMs are employed to diagnostic techniques (such as, [64, 67, 68]). But the MVEMs stand incapable to describe the system dynamics under fault conditions comprehensively. That is, model could be used for detection of a misfire condition based on mean torque; however the model would not describe the system dynamics under misfire condition. Such a capability, if attained, blended with sensor/ actuator redundancy (which would come from the engine manufacturing technology) would enable the development of better fault-tolerant control frameworks for gasoline engines. Model based description of system dynamics under fault conditions is an important model attribute for development of fault tolerant control algorithms, as explained in [69].

Based on the discussion presented in this section, research trends and expected future trend as explained in Section 2.4 and to summarize the objective of the research presented in this thesis, author feel it an appropriate place to propose a unified engine control and diagnostic framework. The thesis will subsequently aim at developing a dynamical engine model capable of designing the framework presented here.

A unified framework, such as Fault Tolerant Control (FTC), for the purpose of control, fault diagnosis and condition monitoring is necessity for reliable and long-lasting dynamical systems, [69] and [70]. The unified framework for gasoline engines will make them more fuel efficient, reliable, compatible to safety [71] and greenhouse gas emission standards [72] both in transient and steady state operation. The situation becomes more challenging under fault conditions and limp-home operating modes.

Keeping these challenges in mind, a new unified framework is proposed as shown in Figure 2.5. Below are some of its key attributes.

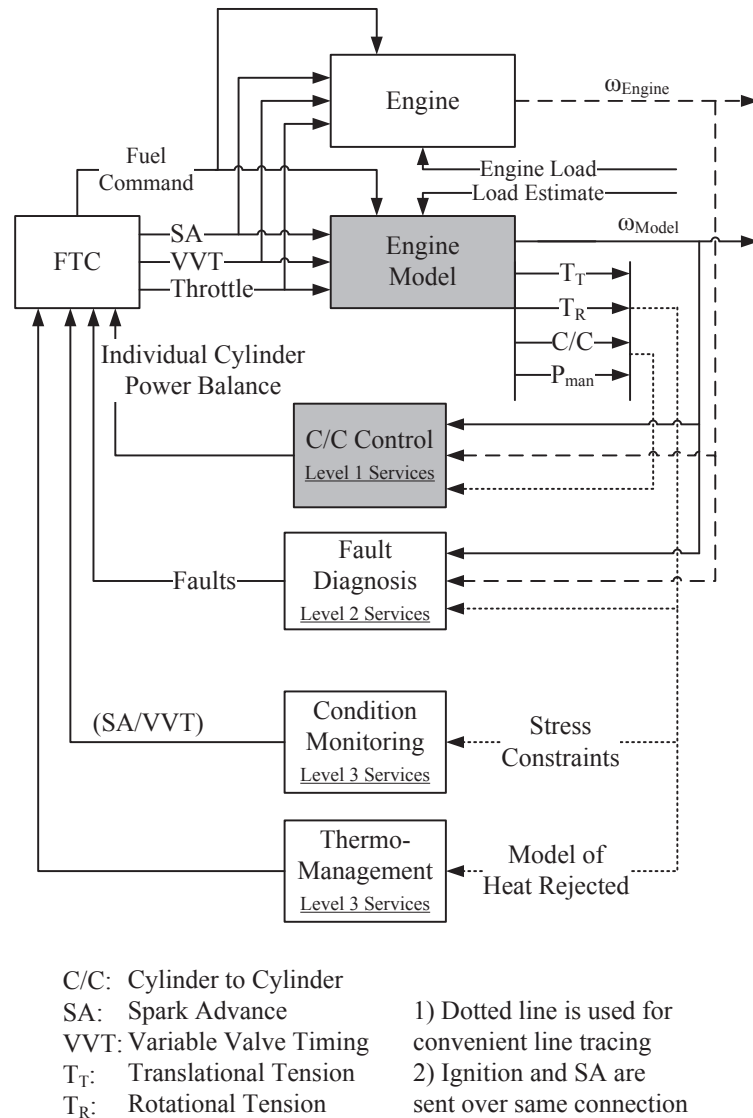


FIGURE 2.5: Proposed New Generation Unified Engine Control and Diagnostic Framework

Cylinder-to-Cylinder Control: This scheme can help for cylinder-to-cylinder control of fuel injection and spark ignition using multi-cylinder dynamics. That will lead to cylinder power balance and individual cylinder spark advance for flexible fuels. The scheme could also be helpful in deriving bases for dynamics skip firing, [73] and [5].

Fault Diagnosis: The scheme can offer extended diagnostic capabilities like misfire detection under idling and loaded operations and mechanical stresses and operational condition of rigid bodies in torque producing mechanism. These capabilities are brought to single framework by employing single high fidelity model.

Condition Monitoring: The framework requires monitoring of aging with the help of stresses in each engine component under different operating conditions to improve reliability and safety.

Thermo-Management: Integration of a gasoline combustion model with control oriented engine model can provide a means of integrating the thermo management with engine control framework. Integration of engine control and thermo management could be beneficial for limp-home modes and regions of extended engine operations, such as Otto-Atkinson engines [74].

Generally, control oriented gasoline engine models possess low fidelity, as seen earlier. As a result, abstraction between engine and its mathematical model increases. Hence, though MVEMs capture an approximate output profile but they prove to be incapable of supporting the analysis and development of proposed framework. Moreover, application specific models of gasoline engine put a major hindrance in development of a unified framework. In contrast to these facts, multi-dimensional, finite element or Cylinder-to-Cylinder Engine Models (CCEMs) show high levels of fidelity, but these are more likely analytical models. In addition they pose high levels of complexity issues, when implementation in an embedded system is concerned [10].

It can thus be concluded, that a framework shown in Figure 2.5 needs a high fidelity control oriented gasoline engine model, which keeps the essence of the engine mechanism preserved in mathematical model. It is clear that each subsystem shown in Figure 2.5 is a separate study. Despite the presence of rich literature on each sub-system indicated, the lack of a control oriented, unified, capable, real-time compatible and high fidelity gasoline engine model is creating a bottleneck.

2.6 Conclusions

Gasoline engines are not a straight forward trivial route of the control oriented models. The fact that engine runs on the junction of many disciplines, make the

ambiance hostile. Inclusion of innovative engine technologies require more capable control oriented engine models for development of advanced model based engine control algorithms. Enhanced engine control frameworks would rather be necessary to obey the upcoming, more stringent environmental constraints. Availability of advanced embedded platforms, as compared with those available when foundations for control oriented engine models were put, make the model enhancement a feasible idea. Based on the history trend of research on modeling, engine technology and legislation the author feel it an appropriate time for converging to the first principles and developing more capable engine models. Filling the gaps in the area of engine modeling, as indicated in the discussions included in this part of the thesis, could be an initiating milestone in approaching the foreseen objectives.

Chapter 3 presents first step in the endeavor in filling the indicated research gap by developing an FPEM describing the lumped cylinder dynamics.

Chapter 3

LUMPED CYLINDER DYNAMICS

Chapter 2 was an effort to highlight the research gap and bring in-line the foreseen motives of the proposed research methodology. This chapter is meant for inception of the development of a control oriented gasoline engine model, capable of establishing a framework presented in Section 2.5. Models of the subsystem are derived and then integrated to develop a First Principle based Engine Model (FPEM).

Derivation of the model of mechanism (with an assumption of lumped cylinders) and simplification strategy are addressed in Section 3.1. To evaluate the forces acting on piston at different operational conditions and different phases of four strokes, a cylinder pressure model is required. A closed form analytical gasoline engine cylinder pressure model is presented in Section 3.2. Realization aspects of the model are addressed in Section 3.3 along-with the parameter tuning strategy. The procedure for tuning the parameters described in Section 3.3 is presented in nexus to formulation presented in Appendix A. Simulation results of the tuned model, discussion on the results and outlining attributes of the model are presented by Section 3.4. Part of the work presented in this chapter is concluded by

Section 3.5, along-with a tabular comparison of underlining attributes of existing control oriented models and proposed FPEM.

3.1 Model of the Mechanism

This section presents derivation of the model of torque producing mechanism corresponding to a single cylinder engine, for investigation of lumped cylinder dynamics. Model simplification procedure is explained after the model development.

The mechanism shown in Figure 3.1, is considered for development of the model. The mechanism consists of a slider/ piston (body no. 3, having mass m_3) connected to a crankshaft (body no. 1, having crank-offset l_1) through connecting rod (body no. 2, having length l_2). This is the mechanism corresponding to that used in single cylinder engine. For investigation of lumped cylinder dynamics, this mechanism is modeled and resulting model is used in overall engine model after simplification. Study of multi-cylinder dynamics using the mechanism corresponding to a multi-cylinder engine is investigated later in this thesis.

Model of the mechanism, considered for deriving the formulation for the lumped cylinder dynamics, is derived using the constrained Equation of Motion (EOM) in

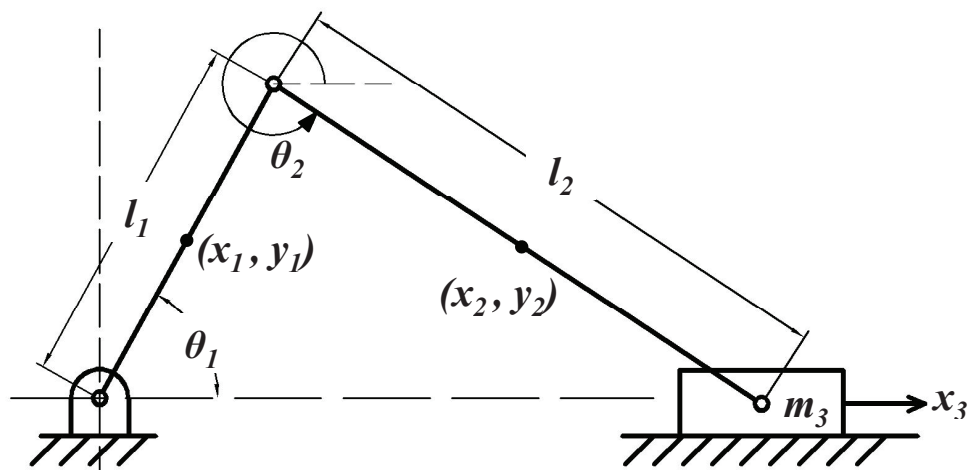


FIGURE 3.1: Torque Producing Mechanism

Lagrangian Mechanics, stated as below:

$$\frac{d}{dt} \frac{\partial T}{\partial \dot{q}_i} - \frac{\partial T}{\partial q_i} + \frac{\partial V}{\partial q_i} + \sum_{j=1}^k \lambda_j \frac{\partial \phi_j}{\partial q_i} = e_i^s \quad (3.1)$$

Subject to the constraints

$$\phi_j(q, t) = 0, \quad j = 1, 2, 3 \dots k \quad (3.2)$$

here j represent the j^{th} constraint, k represent the total number of constraints and i means the i^{th} generalized coordinate. Description of the generalized coordinates in Equation 3.1, in relation to physical variables in the system, is presented in Table 3.1.

TABLE 3.1: Description of the Generalized Variables

No.	Generalized Coordinate	Variable in Mechanism	Variable Description
1.	q_1	x_1	Center of Mass of Crankshaft
2.	q_2	y_1	
3.	q_3	θ_1	Crankshaft Angular Position
4.	q_4	x_2	Center of Mass of Connecting Rod
5.	q_5	y_2	
6.	q_6	θ_2	Connecting Rod Angular Position
7.	q_7	x_3	Piston Position

3.1.1 Model Derivation

Slider Crank Mechanism, shown in Figure 3.1, consists of a slider (called piston in engines), connecting rod and crankshaft. The following should be noted:

1. Body 1: Crankshaft (associated variables/parameters are $\theta_1, m_1, J_1, l_1, x_1, y_1$)
2. Body 2: Connecting Rod (associated variables/parameters are $\theta_2, m_2, J_2, l_2, x_2, y_2$)
3. Body 3: Piston (associated variables/parameters are m_3, x_3)

Total kinetic energy of the mechanism (shown in Figure 3.1) is stated as follows:

$$T = T_1 + T_2 + T_3 \quad (3.3a)$$

$$T_1 = \frac{1}{2}m_1(\dot{x}_1^2 + \dot{y}_1^2) + \frac{1}{2}J_1\dot{\theta}_1^2 \quad (3.3b)$$

$$T_2 = \frac{1}{2}m_2(\dot{x}_2^2 + \dot{y}_2^2) + \frac{1}{2}J_2\dot{\theta}_2^2 \quad (3.3c)$$

$$T_3 = \frac{1}{2}m_3\dot{x}_3^2 \quad (3.3d)$$

Potential energy of the system is assumed not to be changing significantly. Considering the Lagrangian EOM with constraints (stated in Equations 3.1 and 3.2) for the torque producing mechanism would yield the dynamical model for the system.

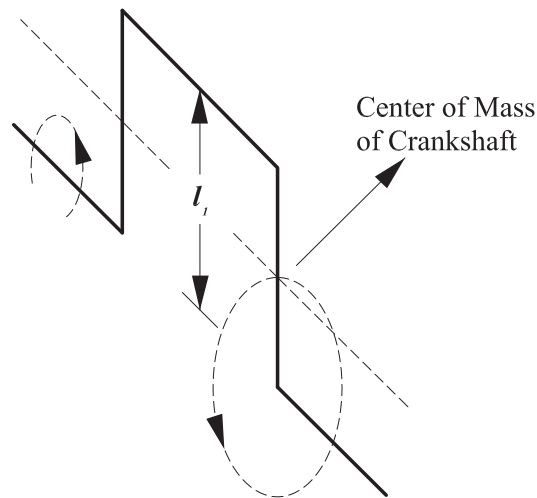


FIGURE 3.2: Motion of Center of Mass of Crankshaft

Before proceeding with the application of constrained EOM to the bodies in the mechanism, holonomic constraints involved in the motion of rigid bodies in the

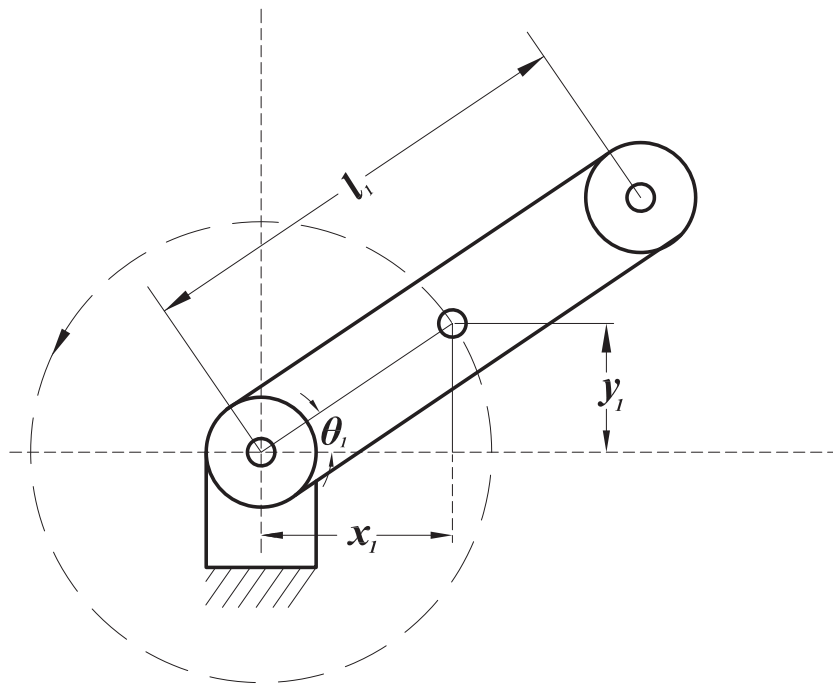


FIGURE 3.3: Geometric Interpretation for Constraints on the Motion of Center of Mass of Crankshaft

mechanism are to be identified. All six constraints are stated by Equation 3.6. Following enumeration explains the basis for derivation of the constraint equations:

1. Equations 3.6a and 3.6b represent the constraints, corresponding to those on the motion of center of mass of the crankshaft. It is geometrically explained by Figure 3.2, that center of mass of the crankshaft follows a circular trajectory as the crankshaft rotates. Resolving the horizontal and vertical components of the center of mass of crankshaft and determining the components for angle θ_1 provides the constraint of the motion, as graphically presented in Figure 3.3. Mathematically, horizontal and vertical components can be expressed as follows:

$$x_1 = \frac{l_1}{2} \cos(\theta_1) \quad (3.4a)$$

$$y_1 = \frac{l_1}{2} \sin(\theta_1) \quad (3.4b)$$

2. Equations 3.6c and 3.6d state the constraints of motion corresponding to the motion of center of mass of the connecting rod. As shown in Figure 3.4, position of center of mass of the connecting rod (along horizontal and vertical direction) is expressed as, respectively:

$$x_2 = l_1 \cos \theta_1 + \frac{l_2}{2} \cos \theta_2 \quad (3.5a)$$

$$y_2 = l_1 \sin \theta_1 + \frac{l_2}{2} \sin \theta_2 \quad (3.5b)$$

The equations formulated above, are brought to standard notation and shown as Equation 3.6c and Equation 3.6d.

3. Equations 3.6e and 3.6f are meant to describe the constraints on the motion of piston. Two aspects should be noted regarding motion of the piston while remaining part of the mechanism. Piston can only perform motion along one axis. Piston is constrained to obey the horizontal distance constraint (shown in the Figure 3.4), while performing the motion.

Based on the discussion presented above and Figures 3.2, 3.3 and 3.4 total constraints involved in motion of bodies in the mechanism are stated as follows:

$$\phi_1 = x_1 - \frac{l_1}{2} \cos \theta_1 = 0 \quad (3.6a)$$

$$\phi_2 = y_1 - \frac{l_1}{2} \sin \theta_1 = 0 \quad (3.6b)$$

$$\phi_3 = x_2 - (l_1 \cos \theta_1 + \frac{l_2}{2} \cos \theta_2) = 0 \quad (3.6c)$$

$$\phi_4 = y_2 - (l_1 \sin \theta_1 + \frac{l_2}{2} \sin \theta_2) = 0 \quad (3.6d)$$

$$\phi_5 = l_1 \cos \theta_1 + l_2 \cos \theta_2 - x_3 = 0 \quad (3.6e)$$

$$\phi_6 = l_1 \sin \theta_1 + l_2 \sin \theta_2 = 0 \quad (3.6f)$$

¹In connection to Figure 3.4, please note that $\cos(2\pi - \theta) = \cos \theta$ and $\sin(2\pi - \theta) = -\sin \theta$

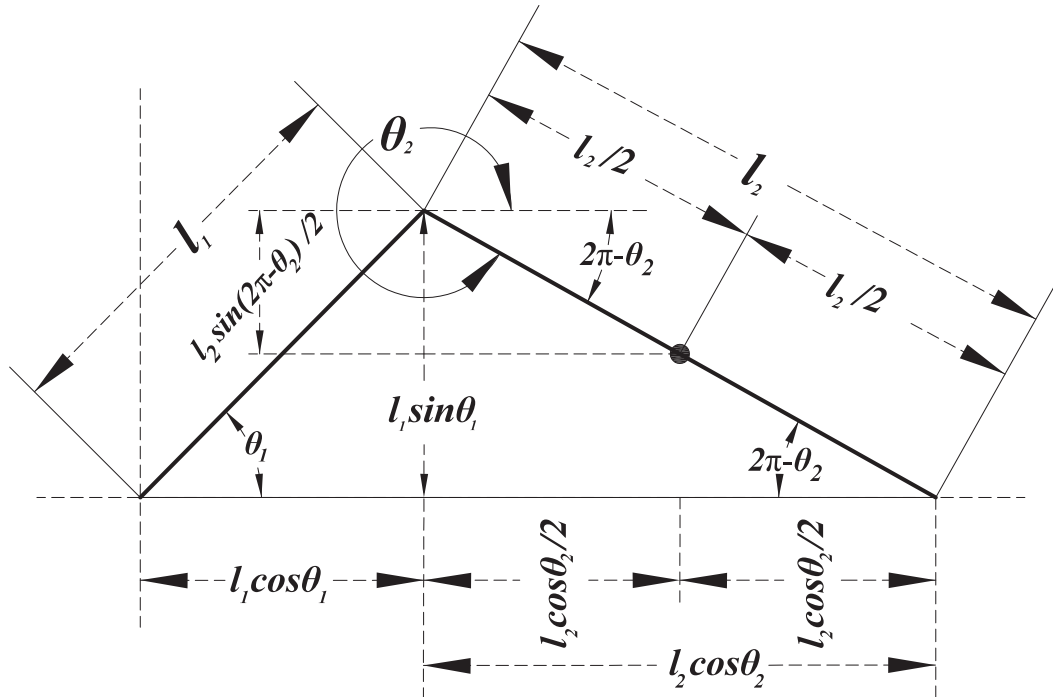


FIGURE 3.4: Developing the Constraints for Motion of Connecting rod and Piston Equations 3.6c through 3.6f ¹

TABLE 3.2: Description of the Generalized Efforts

No.	Generalized Coordinate	External Effort	Description
1.	x_1	0	No External Input
2.	y_1	0	No External Input
3.	θ_1	τ_N	Net torque acting on crankshaft
4.	x_2	0	No External Input
5.	y_2	0	No External Input
6.	θ_2	0	No External Input
7.	x_3	F	Force acting on Piston

In order to begin with the derivation, the term $\frac{d}{dt} \frac{\partial T}{\partial \dot{q}_i}$ is solved for each q_i , (before the derivation, for sake of simplification). Results are obtained as follows:

$$\begin{aligned}
 \text{Crankshaft} &\Rightarrow \frac{d}{dt} \frac{\partial T}{\partial \dot{x}_1} = m_1 \ddot{x}_1 & \frac{d}{dt} \frac{\partial T}{\partial \dot{y}_1} = m_1 \ddot{y}_1 & \frac{d}{dt} \frac{\partial T}{\partial \dot{\theta}_1} = J_1 \ddot{\theta}_1 \\
 \text{Connecting Rod} &\Rightarrow \frac{d}{dt} \frac{\partial T}{\partial \dot{x}_2} = m_2 \ddot{x}_2 & \frac{d}{dt} \frac{\partial T}{\partial \dot{y}_2} = m_2 \ddot{y}_2 & \frac{d}{dt} \frac{\partial T}{\partial \dot{\theta}_2} = J_2 \ddot{\theta}_2 \\
 \text{Piston} &\Rightarrow \frac{d}{dt} \frac{\partial T}{\partial \dot{x}_3} = m_3 \ddot{x}_3
 \end{aligned}$$

To begin with, $i = 1$ that is $q_i = q_1 = x_1$. Furthermore, in reference to Table 3.2, there is no external input to this generalized coordinate. By application of constrained EOM the following is obtained:

$$\frac{d}{dt} \frac{\partial T}{\partial \dot{x}_1} - \frac{\partial T}{\partial x_1} + \sum_{j=1}^6 \lambda_j \frac{\partial \phi_j}{\partial x_1} = 0 \quad (3.8a)$$

$$m_1 \ddot{x}_1 + \lambda_1 \frac{\partial}{\partial x_1} \left[x_1 - \frac{l_1 \cos \theta_1}{2} \right] = 0 \quad (3.8b)$$

$$m_1 \ddot{x}_1 + \lambda_1 = 0 \quad (3.8c)$$

Proceeding with the derivation further for $i = 2$, $q_i = q_2 = y_1$. Moreover, as enlisted in Table 3.2, this generalized coordinate has the same scenario, that is no external input is acting as input along it. Application of constrained EOM yields following:

$$\frac{d}{dt} \frac{\partial T}{\partial \dot{y}_1} - \frac{\partial T}{\partial y_1} + \sum_{j=1}^6 \lambda_j \frac{\partial \phi_j}{\partial y_1} = 0 \quad (3.9a)$$

$$m_1 \ddot{y}_1 + \lambda_2 \frac{\partial}{\partial y_1} \left[y_1 - \frac{l_1 \sin \theta_1}{2} \right] = 0 \quad (3.9b)$$

$$m_1 \ddot{y}_1 + \lambda_2 = 0 \quad (3.9c)$$

Moving on, for $i = 3$ with reference to Table 3.1 $q_i = q_3 = \theta_1$. Moreover, as evident from Table 3.2, net torque τ_N acting on the crankshaft acts as external input to this generalized coordinate. Application of constrained EOM to angular motion of the center of mass of the crankshaft θ_1 , results in the following equation:

$$\frac{d}{dt} \frac{\partial T}{\partial \dot{\theta}_1} - \frac{\partial T}{\partial \theta_1} + \sum_{j=1}^6 \lambda_j \frac{\partial \phi_j}{\partial \theta_1} = \tau_N \quad (3.10a)$$

$$\begin{aligned} J_1 \ddot{\theta}_1 + \lambda_1 \frac{\partial}{\partial \theta_1} \left[x_1 - \frac{l_1 \cos \theta_1}{2} \right] + \lambda_2 \frac{\partial}{\partial \theta_1} \left[y_1 - \frac{l_1 \sin \theta_1}{2} \right] + \\ \lambda_3 \frac{\partial}{\partial \theta_1} \left[x_2 - \left(l_1 \cos \theta_1 + \frac{l_2 \cos \theta_2}{2} \right) \right] + \\ \lambda_4 \frac{\partial}{\partial \theta_1} \left[y_2 - \left(l_1 \sin \theta_1 + \frac{l_2 \sin \theta_2}{2} \right) \right] + \end{aligned} \quad (3.10b)$$

$$\begin{aligned}
& \lambda_5 \frac{\partial}{\partial \theta_1} [l_1 \cos \theta_1 + l_2 \cos \theta_2 - x_3] + \lambda_6 \frac{\partial}{\partial \theta_1} [l_1 \sin \theta_1 + l_2 \sin \theta_2] = \tau_N \\
& J_1 \ddot{\theta}_1 + \lambda_1 \left[\frac{l_1}{2} \sin \theta_1 \right] - \lambda_2 \left[\frac{l_1}{2} \cos \theta_1 \right] + \lambda_3 l_1 \sin \theta_1 \\
& - \lambda_4 l_1 \cos \theta_1 - \lambda_5 l_1 \sin \theta_1 + \lambda_6 l_1 \cos \theta_1 = \tau_N
\end{aligned} \tag{3.10c}$$

For $i = 4$, in reference to Table 3.1 $q_i = q_4 = x_2$. Application of constrained EOM to said coordinate results the following (no external effort along coordinate under consideration, as shown in Table 3.2):

$$\frac{d}{dt} \frac{\partial T}{\partial \dot{x}_2} - \frac{\partial T}{\partial x_2} + \sum_{j=1}^6 \lambda_j \frac{\partial \phi_j}{\partial x_2} = 0 \tag{3.11a}$$

$$m_2 \ddot{x}_2 + \lambda_3 \frac{\partial}{\partial x_2} \left[x_2 - \left[l_1 \cos \theta_1 + \frac{l_2 \cos \theta_2}{2} \right] \right] = 0 \tag{3.11b}$$

$$m_2 \ddot{x}_2 + \lambda_3 = 0 \tag{3.11c}$$

Moving on for $i = 5$ according to Table 3.1, $q_i = q_4 = x_2$. Application of constrained EOM to said coordinate results the following (coordinate under discussion bears no external input, as enlisted in Table 3.2):

$$\frac{d}{dt} \frac{\partial T}{\partial \dot{y}_2} - \frac{\partial T}{\partial y_2} + \sum_{j=1}^6 \lambda_j \frac{\partial \phi_j}{\partial y_2} = 0 \tag{3.12a}$$

$$m_2 \ddot{y}_2 + \lambda_4 \frac{\partial}{\partial y_2} \left[y_2 - \left[l_1 \sin \theta_1 + \frac{l_2 \sin \theta_2}{2} \right] \right] = 0 \tag{3.12b}$$

$$m_2 \ddot{y}_2 + \lambda_4 = 0 \tag{3.12c}$$

For angular rotation of center of mass of connecting rod, it is $i = 6$ and $q_i = q_6 = \theta_2$. Furthermore, there is no external effort as shown in Table 3.2. For such a condition, following is obtained:

$$\frac{d}{dt} \frac{\partial T}{\partial \dot{\theta}_2} - \frac{\partial T}{\partial \theta_2} + \sum_{j=1}^6 \lambda_j \frac{\partial \phi_j}{\partial \theta_2} = 0 \tag{3.13a}$$

$$J_2 \ddot{\theta}_2 + \lambda_3 \frac{\partial}{\partial \theta_2} \left[x_2 - \left[l_1 \cos(\theta_1) + \frac{l_2 \cos(\theta_2)}{2} \right] \right] +$$

$$\lambda_4 \frac{\partial}{\partial \theta_2} \left[y_2 - \left[l_1 \sin \theta_1 + \frac{l_2 \sin \theta_2}{2} \right] \right] +$$

$$\lambda_5 \frac{\partial}{\partial \theta_2} (l_1 \cos(\theta_1) + l_2 \cos(\theta_2) - x_3) + \quad (3.13b)$$

$$\lambda_6 \frac{\partial}{\partial \theta_2} (l_1 \sin(\theta_1) + l_2 \sin(\theta_2)) = 0$$

$$J_2 \ddot{\theta}_2 + \lambda_3 \frac{l_2}{2} \sin \theta_2 - \lambda_4 \frac{l_2}{2} \cos \theta_2 - \lambda_5 l_2 \sin \theta_2 + \lambda_6 l_2 \cos \theta_2 = 0 \quad (3.13c)$$

Eventually, for $i = 7$ the scenario is $q_i = q_7 = x_3$. It could be seen that, there is an external input to the system along this generalized coordinate, that is *force acting on the piston*. Application of constrained EOM to said coordinate, the following is obtained:

$$\frac{d}{dt} \frac{\partial T}{\partial \dot{x}_3} - \frac{\partial T}{\partial x_3} + \sum_{j=1}^6 \lambda_j \frac{\partial \phi_j}{\partial x_3} = F \quad (3.14a)$$

$$m_3 \ddot{x}_3 + \lambda_5 \frac{\partial}{\partial x_3} (l_1 \cos \theta_1 + l_2 \cos \theta_2 - x_3) = F \quad (3.14b)$$

$$m_3 \ddot{x}_3 - \lambda_5 = F \quad (3.14c)$$

In order to put the scattered things together, Equations 3.8c, 3.9c, 3.10c, 3.11c, 3.12c, 3.13c and 3.14c are re-written at one place. The equation for each generalized coordinate, q_1 through q_7 , are sorted order-wise as follows:

$$m_1 \ddot{x}_1 + \lambda_1 = 0 \quad (3.15a)$$

$$m_1 \ddot{y}_1 + \lambda_2 = 0 \quad (3.15b)$$

$$J_1 \ddot{\theta}_1 + \lambda_1 \left[\frac{l_1}{2} \sin \theta_1 \right] - \lambda_2 \left[\frac{l_1}{2} \cos \theta_1 \right] + \lambda_3 l_1 \sin \theta_1 - \lambda_4 l_1 \cos \theta_1 - \lambda_5 l_1 \sin \theta_1 + \lambda_6 l_1 \cos \theta_1 = \tau_N \quad (3.15c)$$

$$m_2 \ddot{x}_2 + \lambda_3 = 0 \quad (3.15d)$$

$$m_2 \ddot{y}_2 + \lambda_4 = 0 \quad (3.15e)$$

$$J_2 \ddot{\theta}_2 + \lambda_3 \frac{l_2}{2} \sin \theta_2 - \lambda_4 \frac{l_2}{2} \cos \theta_2 - \lambda_5 l_2 \sin \theta_2 + \lambda_6 l_2 \cos \theta_2 = 0 \quad (3.15f)$$

$$m_3 \ddot{x}_3 - \lambda_5 = F \quad (3.15g)$$

Model of the mechanism is described by the algebraic equations (constraints described by Equation 3.6) and differential equations (described by Equation 3.15). It should be noted that there are seven generalized variables, while there are six

constraints of motion. Mechanism in result, described by the DAEs presented above, attains one degree of freedom. Through proper model simplification, the system is simplified to an appropriate form which can be integrated with the models of other subsystems of the engine model.

3.1.2 Simplification of the Model

There are different strategies for solution of DAEs formed by the constrained EOM in Lagrangian Mechanics, such as Kane's Method [75, 76]. However, since efforts in this study are made to develop a control oriented model. The form attained by developing the matrices for the system of DAEs under study, would rather be problematic in integrating with models of other subsystems. Moreover, resultant model would not be of the form, accustomed in the control community. For a control oriented model, finally model of the following form would be preferable (since there are two inputs, τ_N and F):

$$\dot{\theta} = \omega \tag{3.16a}$$

$$\dot{\omega} = f(\Gamma, \theta, \omega) + g_1(\Gamma, \theta, \omega)\tau_N + g_2(\Gamma, \theta, \omega)F \tag{3.16b}$$

In order to obtain the required form, a different model simplification strategy is adopted. Relation among the generalized coordinates described by the Lagrange Multipliers (λ_i 's) is utilized to simplify the system of DAEs. That is, each holonomic constraint is used to reduce one degree of freedom. As a result for a system with seven ODEs and six holonomic constraints, one 2^{nd} order ODE is achieved for θ_1 . The procedure described above is explained in [77], for a system of rolling disc on an inclined plane.

Following is notable in steps 1 to 8:

$$x_i(\Gamma, \theta_1, \dot{\theta}_1, \ddot{\theta}_1) = f_a(\Gamma, \theta_1, \dot{\theta}_1, \ddot{\theta}_1) \quad (3.17a)$$

$$\dot{x}_i(\Gamma, \theta_1, \dot{\theta}_1, \ddot{\theta}_1) = f_b(\Gamma, \theta_1, \dot{\theta}_1, \ddot{\theta}_1) \quad (3.17b)$$

$$\ddot{x}_i(\Gamma, \theta_1, \dot{\theta}_1, \ddot{\theta}_1) = f_c(\Gamma, \theta_1, \dot{\theta}_1, \ddot{\theta}_1) \quad (3.17c)$$

$$\lambda_i = f_d(\Gamma, \theta_1, \dot{\theta}_1, \ddot{\theta}_1) \quad (3.17d)$$

Mathematical expression in Equations 3.17a to 3.17c means that x_i , \dot{x}_i and \ddot{x}_i are expressed as function of Γ , θ_1 , $\dot{\theta}_1$ and $\ddot{\theta}_1$. Whereas, mathematical expression in Equation 3.17d means λ_i is obtained as function of Γ , θ_1 , $\dot{\theta}_1$ and $\ddot{\theta}_1$. The following procedure precisely describes the simplification steps carried out:

1. Constraint defined by Equations 3.6a is used to determine x_1 and its higher time derivatives as function of θ_1 and its derivatives. Value of \ddot{x}_1 obtained is put in Equation 3.15a, and λ_1 is expressed as function of θ_1 and its derivatives.

$$(x_1(\Gamma, \theta_1, \dot{\theta}_1, \ddot{\theta}_1), \dot{x}_1(\Gamma, \theta_1, \dot{\theta}_1, \ddot{\theta}_1), \ddot{x}_1(\Gamma, \theta_1, \dot{\theta}_1, \ddot{\theta}_1)) \quad \text{using Equation 3.6a}$$

$$\lambda_1 = f_1(\Gamma, \theta_1, \dot{\theta}_1, \ddot{\theta}_1) \quad \text{using Equation 3.15a}$$

2. In a similar fashion, Equations 3.6b and 3.15b are used to express λ_2 as a function of θ_1 and its derivatives.

$$(y_1(\Gamma, \theta_1, \dot{\theta}_1, \ddot{\theta}_1), \dot{y}_1(\Gamma, \theta_1, \dot{\theta}_1, \ddot{\theta}_1), \ddot{y}_1(\Gamma, \theta_1, \dot{\theta}_1, \ddot{\theta}_1)) \quad \text{using Equation 3.6b}$$

$$\lambda_2 = f_2(\Gamma, \theta_1, \dot{\theta}_1, \ddot{\theta}_1) \quad \text{using Equation 3.15b}$$

3. Constraint defined by Equation 3.6f is utilized to express θ_2 and its derivatives as function of θ_1 and its derivatives.

$$(\theta_2(\Gamma, \theta_1, \dot{\theta}_1, \ddot{\theta}_1), \dot{\theta}_2(\Gamma, \theta_1, \dot{\theta}_1, \ddot{\theta}_1), \ddot{\theta}_2(\Gamma, \theta_1, \dot{\theta}_1, \ddot{\theta}_1)) \quad \text{using Equation 3.6f}$$

4. To express x_2 and its derivatives as function of θ_1 and its derivatives, constraint defined by Equation 3.6c is used. Furthermore, using Equation 3.15d λ_3 is expressed as θ_1 and its derivatives.

$$\begin{aligned} (x_2(\Gamma, \theta_1, \dot{\theta}_1, \ddot{\theta}_1), \dot{x}_2(\Gamma, \theta_1, \dot{\theta}_1, \ddot{\theta}_1), \ddot{x}_2(\Gamma, \theta_1, \dot{\theta}_1, \ddot{\theta}_1)) & \text{ using Equation 3.6c} \\ \lambda_3 = f_4(\Gamma, \theta_1, \dot{\theta}_1, \ddot{\theta}_1) & \text{ using Equation 3.15d} \end{aligned}$$

5. Procedure explained in above step is carried out for Equations 3.6d and 3.15e to obtain expression for λ_4 as function of θ_1 .

$$\begin{aligned} (y_2(\Gamma, \theta_1, \dot{\theta}_1, \ddot{\theta}_1), \dot{y}_2(\Gamma, \theta_1, \dot{\theta}_1, \ddot{\theta}_1), \ddot{y}_2(\Gamma, \theta_1, \dot{\theta}_1, \ddot{\theta}_1)) & \text{ using Equation 3.6d} \\ \lambda_4 = f_5(\Gamma, \theta_1, \dot{\theta}_1, \ddot{\theta}_1) & \text{ using Equation 3.15e} \end{aligned}$$

6. Constraint defined by Equation 3.6e is used to express x_3 and its derivatives as function of θ_1 and its derivatives. State Equation 3.15g is further used to express λ_5 as function of θ_1 and its derivatives.

$$\begin{aligned} (x_3(\Gamma, \theta_1, \dot{\theta}_1, \ddot{\theta}_1), \dot{x}_3(\Gamma, \theta_1, \dot{\theta}_1, \ddot{\theta}_1), \ddot{x}_3(\Gamma, \theta_1, \dot{\theta}_1, \ddot{\theta}_1)) & \text{ using Equation 3.6e} \\ \lambda_5 = f_6(\Gamma, \theta_1, \dot{\theta}_1, \ddot{\theta}_1) - F & \text{ using Equation 3.15g} \end{aligned}$$

7. Expressions for λ_1 through λ_5 obtained in steps 1, 2, 4, 5, and 6 and expressions for θ_2 and its time derivatives expressed as function of θ_1 and its derivatives obtained in step 3 are used to obtain expression for λ_6 as function of θ_1 and its derivatives, using Equation 3.15f.

$$\lambda_6 = f_7(\Gamma, \theta_1, \dot{\theta}_1, \ddot{\theta}_1) \quad \text{using Equation 3.15f}$$

8. Expressions for λ_1 through λ_6 obtained in steps 1, 2, 4, 5, 6 and 7 are put back in Equation 3.15c.

9. A 2^{nd} order ODE for θ_1 is finally obtained, by separating $\ddot{\theta}_1$ in step 8 as follows:

$$\ddot{\theta}_1 = f(\Gamma, \theta_1, \dot{\theta}_1) + g_1(\Gamma, \theta_1, \dot{\theta}_1)\tau_N + g_2(\Gamma, \theta_1, \dot{\theta}_1)F$$

All of the steps described above are carried out in Mathematica[®], and results of the form shown in Equation 3.16 are obtained. Detailed mathematical expressions obtained after simplification, are presented in Appendix B.

3.2 Cylinder Pressure Model

An analytic cylinder pressure model together with piston area and crankcase pressure (assumed as constant), provides the net force acting on the piston. In such a way, force produced by the combustion, power stroke and losses like pumping losses are incorporated by this part of the model.

The fact, that commonly found combustion or cylinder pressure models are complex as explained in [78], renders them infeasible for a control oriented framework. Moreover, for a control oriented framework model based definition of parameters, variables and inputs is usually preferred, so as the model attains an attribute of global validity. If cylinder pressure model is taken as black box, it can be viewed as shown in Figure 3.5.

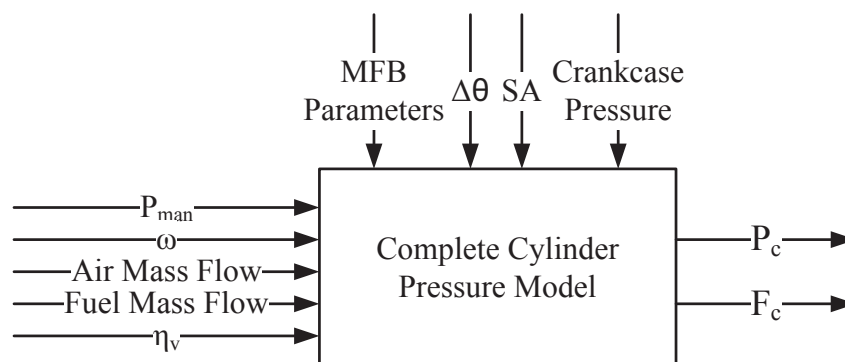


FIGURE 3.5: Cylinder Pressure Model IOs

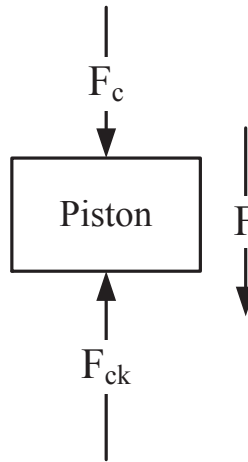


FIGURE 3.6: Piston Free Body Diagram (F_{cyl} is force acting on the piston from cylinder side and F_{ck} is the force acting on piston from crank-case)

Free body diagram of the piston is shown in Figure 3.6, following formulation is used for evaluating the net force acting on the piston:

$$F_c = P_{cyl}A_p$$

$$F_{ck} = P_{ck}A_p$$

$$F = F_c - F_{ck}$$

where, F_c is force acting on piston at cylinder side, F_{ck} is force acting on piston at crank-case side, F is net force acting on the piston, P_{cyl} is cylinder pressure, P_{ck} is crank-case pressure and A_p is piston area

An analytical parametric model for cylinder pressure in a four stroke gasoline engine is presented in [78]. The model is simple, parametric and of the closed form. Model of the cylinder pressure in all four phases of the four strokes is described by joining the asymptotes of intake, compression, ignition, power and exhaust strokes.

Each phase of four strokes is portrayed by its own physical principle. For intake stroke, intake manifold pressure and volumetric efficiency are utilized to estimate the in-cylinder pressure. Likewise, for the exhaust stroke.

Compression Phase: compression asymptote is modeled by a polytropic process, with polytropic exponent γ_c . Starting conditions for polytropic compression are taken by the end of intake process. In such a way, intake and compression asymptotes are automatically joined. Mathematical description of cylinder pressure (P_c) and temperature (T_c) (subscript c , denotes compression phase) as a function of crank angle (θ_1) are as follows:

$$P_c(\theta_1) = P_{ivc} \left[\frac{V_{ivc}}{V(\theta_1)} \right]^{\gamma_c} \quad (3.19a)$$

$$T_c(\theta_1) = T_{ivc} \left[\frac{V_{ivc}}{V(\theta_1)} \right]^{\gamma_c-1} \quad (3.19b)$$

Combustion Phase: The combustion phase is assumed to begin with the Start of Combustion (SOC) event (physically triggered by the spark plug) and remain until the End of Combustion (EOC). The fuel burn profile between SOC and EOC is called *Combustion Phasing*. The well known Wiebe Function is used to model the combustion phasing, explained in [79], [80]. Values of the parameters for pure gasoline are tabulated in [79].

Expansion Phase: Expansion asymptote is modeled by polytropic process with polytropic exponent γ_e . Starting conditions for expansion phase are taken as in-cylinder conditions at EOC. Mathematically, polytropic expansion is described as:

$$P_e(\theta_1) = P_{EOC} \left[\frac{V_{EOC}}{V(\theta_1)} \right]^{\gamma_e} \quad (3.20a)$$

$$T_e(\theta_1) = T_{EOC} \left[\frac{V_{EOC}}{V(\theta_1)} \right]^{\gamma_e-1} \quad (3.20b)$$

The overall closed form expression for in-cylinder pressure could be attained by joining the asymptote corresponding to each phase as presented in, [78].

3.3 Model Realization

Aspects of the model realization are addressed in this section. These include integration of the models of proposed torque production subsystem and intake manifold. Different possible formulations, which the net torque acting on the crankshaft can attain, are discussed. Moreover, tuning parameters of the model for each class of possible realization are identified. An enumeration is presented below to enlist the entities required to be integrated:

1. Model of Subsystem from existing literature
 - (a) Air intake subsystem
 - (b) Intake manifold subsystem
 - (c) Fuel subsystem
2. Torque Production Subsystem
 - (a) Model of the mechanism, derived in Section [3.1](#)
 - (b) Analytical cylinder pressure model, presented in Section [3.2](#)

3.3.1 Existing Subsystems

The model of air intake, intake manifold and fuel subsystems are taken from the existing literature. Model of each of these subsystems is discussed in this section.

There exist a variety of air intake system models, from very complex to the simple ones. It is even claimed that diameter of the shaft causing the throttle plate to rotate affects the mass flow rate of air, [\[7\]](#). However, to achieve the accuracy while keeping the simplicity, model of air intake subsystem devised by [\[9\]](#) is adopted.

Mass flow rate of air (\dot{m}_{ai}) is formulated as follows:

$$\dot{m}_{ai} = C_D \frac{P_{amb} \sqrt{\gamma'}}{\sqrt{RT_{amb}}} \times \beta_1(\alpha) \beta_2(P_{man}) + \dot{m}_{aio} \quad (3.21a)$$

$$\beta_1(\alpha) = \frac{\pi}{4} D^2 \times (1 - \cos(\alpha)) \quad (3.21b)$$

$$\beta_2(P_{man}) = \begin{cases} \sqrt{P_r^{\frac{2}{\gamma}} - P_r^{\frac{\gamma+1}{\gamma}}} & \text{if } P_r \geq \left[\frac{2}{\gamma+1}\right]^{\frac{\gamma}{\gamma-1}} \\ \sqrt{\left[\frac{1}{\gamma'}\right] \left[\frac{2}{\gamma+1}\right]^{\frac{\gamma+1}{\gamma-1}}} & \text{, otherwise} \end{cases} \quad (3.21c)$$

Equations 3.21a, 3.21b and 3.21c describe the mass flow rate of air past the throttle, where, P_r is P_{man}/P_{amb} , $\gamma' = 2\gamma/\gamma - 1$, α is throttle angle and \dot{m}_{aio} is model fitting variable. The term \dot{m}_{aio} is used in describing the mathematical model of the intake manifold in [9]. As explained in [9], the term physically quantifies the Idle Air Control (IAC) Valve and any possible manifold leakages. It is further discussed, that the parameter in the work [9] was used as model tuning variable. Discontinuity presented by Equation 3.21c is the result of a phenomena called *choked flow* [81].

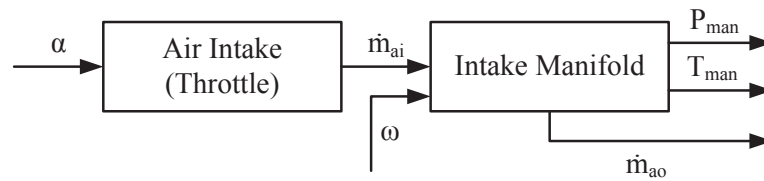
The model of the intake manifold subsystem has been adopted from [1], based on emptying and filling concept under the assumption of isothermal process. The mass flow rate of air into the intake manifold (\dot{m}_{ai}) fills the intake manifold, while mass flow rate of air entering the engine cylinders (\dot{m}_{ao}) empties the intake manifold. Equations describing the mathematical model of for said process under isothermal conditions are as follows:

$$\frac{d}{dt} P_{man} = \frac{T_{amb} \gamma R}{V_{man}} \{\dot{m}_{ai} - \dot{m}_{ao}\} \quad (3.22a)$$

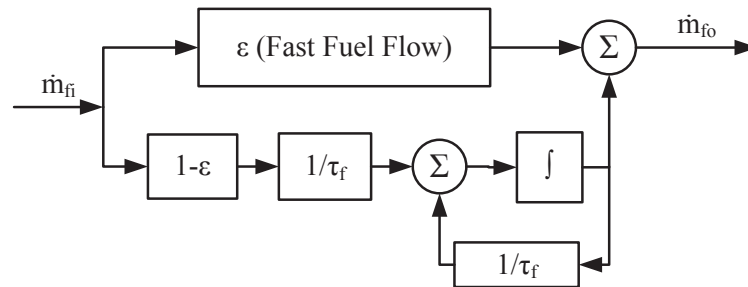
$$T_{man} = T_{amb} \quad (3.22b)$$

where (\dot{m}_{ao}), is defined as follows:

$$\dot{m}_{ao} = \eta_v \times \frac{V_d \omega_1 P_{man}}{RT_{man} \times 4\pi} \quad (3.23)$$



(a) Air Intake and Intake Manifold



(b) Fuel

FIGURE 3.7: Subsystems from Existing Literature

Model of port injected fuel subsystems has been taken from [9]. The fuel flow is modeled by dividing the injected fuel flow (\dot{m}_{fi}) in two components, slow fuel flow and fast fuel flow. The fast component reach the cylinder in immediate upcoming induction cycle, while slow component reach the cylinder but there is a time constant τ_f in-between the path, and mass flow rate of fuel entering the engine cylinder is shown as \dot{m}_{fo}

Structures of air subsystems (air intake and intake manifold) and fuel supply system are shown in Figures 3.7(a) and 3.7(b) respectively.

3.3.2 Model Integration

To put the things together, model of the torque producing mechanism derived in Section 3.1 and model of the intake manifold, explained in Section 3.3.1 are put together to form a complete gasoline engine model. Model attains the following

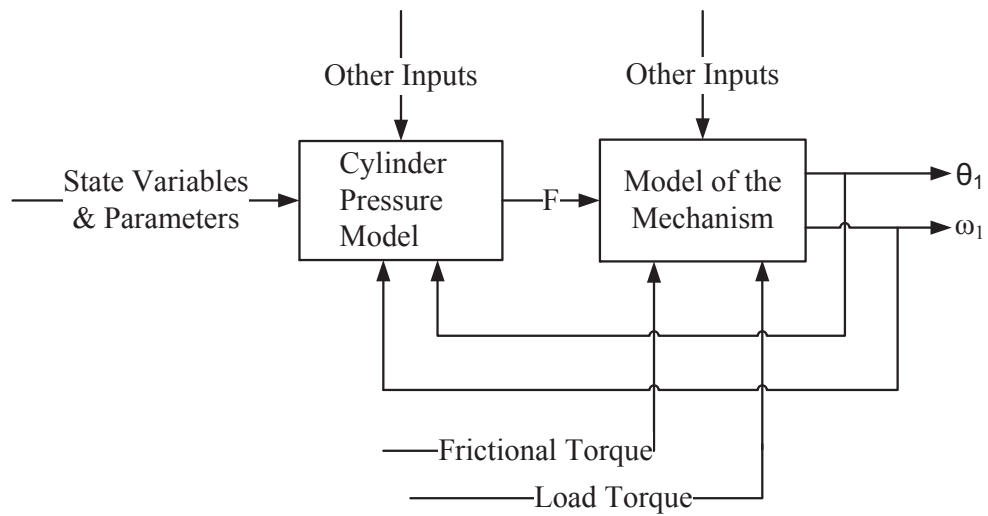


FIGURE 3.8: A Complete Structure of Torque Production Subsystem

form:

$$\dot{P}_{man} = \frac{RT_{man}}{man}(\dot{m}_{ai} - \dot{m}_{ao}) \quad (3.24a)$$

$$\dot{\theta}_1 = \omega_1 \quad (3.24b)$$

$$\dot{\omega}_1 = f(\theta_1, \omega_1, \Gamma) + g_1(\theta_1, \omega_1, \Gamma)\tau_N + g_2(\theta_1, \omega_1, \Gamma)F \quad (3.24c)$$

Torque production subsystem further consist of two parts, they are as follows:

1. Model of the mechanism
2. Analytical closed form cylinder pressure model

Integration of the said constituents of torque production subsystem is shown in Figure 3.8.

3.3.3 Aspects of Realization

As discussed earlier, and evident from the final from Equation 3.24c there are two inputs to the equation for speed dynamics. They are as follows:

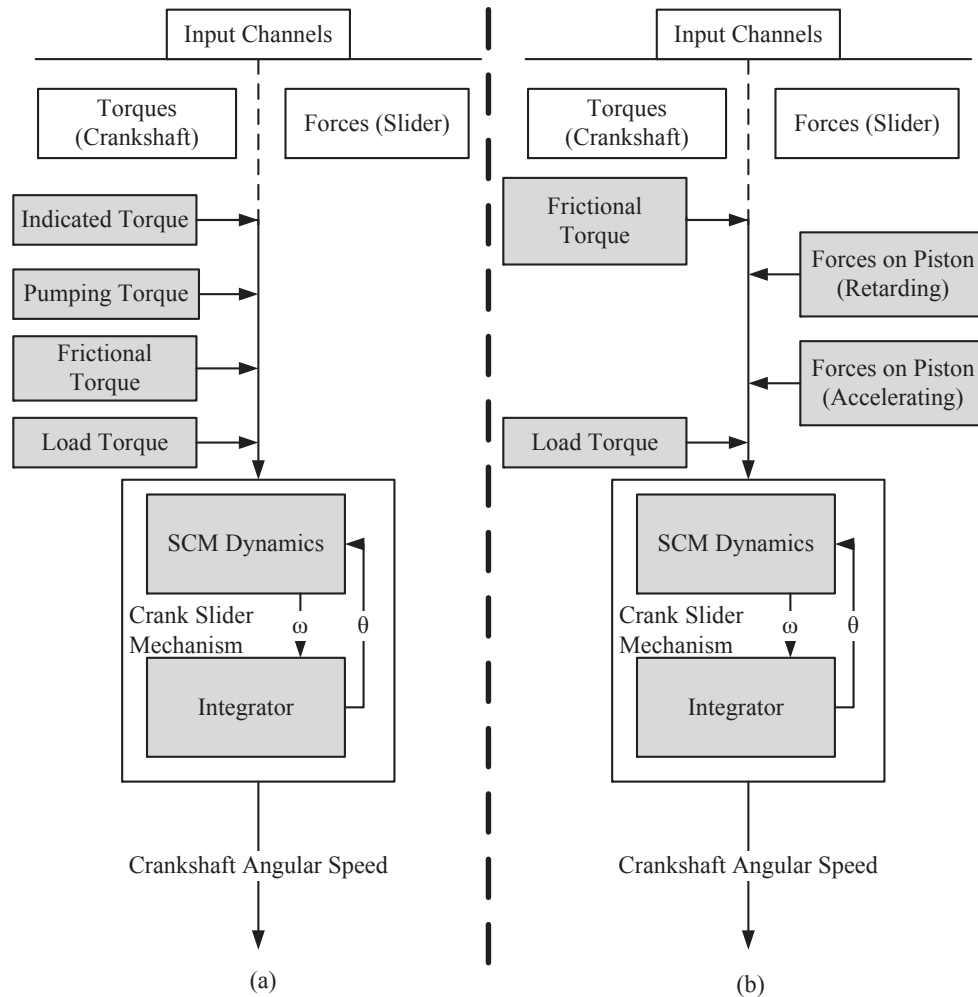


FIGURE 3.9: Realizations

1. Torque acting on the crankshaft (τ_N)
2. Force acting on the piston (F)

As mechanism producing the torque is of one degree of freedom, an easy manipulation with the inputs can be carried out. Two possible realizations of the model are shown in Figure 3.9. Each realization is discussed separately here, followed by discussion on pros and cons of each one.

1. *First Realization* (Figure 3.9(a)): All inputs are considered as torques acting on the crankshaft. That is, input channel defined by the force acting on the piston is not considered. However, to let the model surround the full boundary of the system, an equivalent torque is considered on the crankshaft.

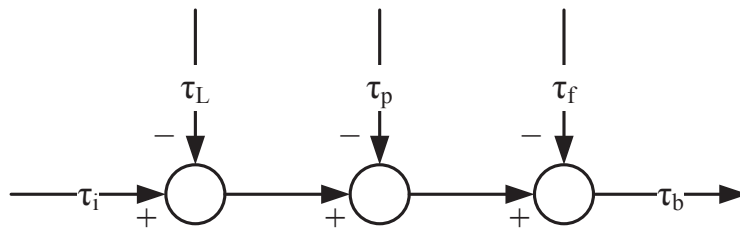


FIGURE 3.10: Structure of First Realization (Figure 3.9(a))

For example, a resisting force acting on the piston during suction or intake is modeled as pumping torque. In such a case, net torque acting on the crankshaft (τ_N) takes the form as: $\tau_N = \tau_i - \tau_p - \tau_f - \tau_L$. Structure of estimating the brake or the net torque acting on crankshaft accordingly is shown in Figure 3.10 [82].

2. *Second Realization* (Figure 3.9(b)): There are two types of inputs to the mechanism, 1) forces acting on the piston and 2) torques acting on the crankshaft. In such a case, two types of the torques (assumed to be acting on crankshaft in realization shown by Figure 3.9(a)) vanish away, instead they are incorporated by the force acting on the piston. For such a scenario, the net torque acting on the crankshaft takes the form as follows: $\tau_N = -\tau_f - \tau_L$. While aspects of pumping and indicated torques are incorporated by the cylinder pressure model. Aspects of work done by the system (intake, exhaust and compression) and work done on the system (combustion phase and power stroke) are covered by the force acting on the piston. Force acting on the piston is evaluated on the base of difference of pressure on both sides of the piston, as derived in Section 3.2.

There are two main factors responsible for crankshaft angular speed fluctuations, as stated in Section 2.5:

1. Dynamics of the mechanism
2. Rapidly changing in-cylinder conditions

Realization of the model shown by Figure 3.9(a), make the model capable of capturing the first aspect of the two factors enlisted above. Whereas, the realization presented by Figure 3.9(b), renders the model capable of describing the effects of both factors in the output.

3.3.4 Tuning of the Model Parameters

Subsystems described above are integrated to form an FPEM. As discussed earlier in respective section, each subsystem of the model contains parameters to be tuned to the actual engine system. Tuning variables belonging to each subsystem are enlisted Table 3.3.

Tuning variables corresponding to the intake manifold, belongs to the model developed by [9]. While for the torque production subsystem, coefficients of the polynomial forming the frictional mean effective pressure are to be determined, as presented in Equation 3.25a.

TABLE 3.3: Tuning Parameters of the Model

Parameter Scope	Parameter
Intake Manifold	Coefficient of Discharge (C_D)
	Volumetric Efficiency (η_v)
	Model Fit Variable (\dot{n}_{aio})
Frictional Torque	Polynomial Parameters of f_{mep}

Frictional torque is obtained by estimating the frictional mean effective pressure (f_{mep}). Following formulation is used:

$$f_{mep} = a_o + \sum_{i=1}^4 a_i \omega_1^i \quad (3.25a)$$

$$\tau_f = \frac{V_d}{4\pi} f_{mep} \quad (3.25b)$$

Tuning of the parameters is carried out step-wise, as described in Appendix A. Tuned values of the parameters of intake manifold and torque production subsystem, tuned by application of optimization technique presented in Appendix A, are enlisted in Table 3.4.

TABLE 3.4: Optimized Parameters of Engine Model

Parameter	Value
C_D	0.35
\dot{m}_{aio}	0.1g/sec
η_v	Curve fit Appendix A
a_o	4×10^4
a_1	64.4×10^{-2}
a_2	8.4×10^{-4}
a_3	6.4×10^{-9}
a_4	4×10^{-6}

3.4 Results and Discussion

Integrated model of the gasoline engine presented in Section 3.3, is tuned to the engine under study (explained in Appendix A), according to the tuning procedure described in Section 3.3.4. As described in Appendix A, separate data-sets are acquired for tuning and subsequent model validation. For tuning and validation of the model in lumped cylinder dynamics, engine data is used which is acquired through OBD-II interface only while data acquired through high speed acquisition interface is used for tuning and validation of engine model with multi-cylinder dynamics.

The tuned model is simulated against the throttle signal shown in Figure 3.11. The response of the model is shown for the states of intake manifold pressure and crankshaft angular speed. Figure 3.12 shows the P_{man} acquired from engine and constructed by proposed FPEM for the said throttle input. Figure 3.13 shows the angular speed of the crankshaft against same throttle input for FPEM. The validation percent errors (model and those acquired from the engine) for P_{man} and ω are presented in Table 3.5.

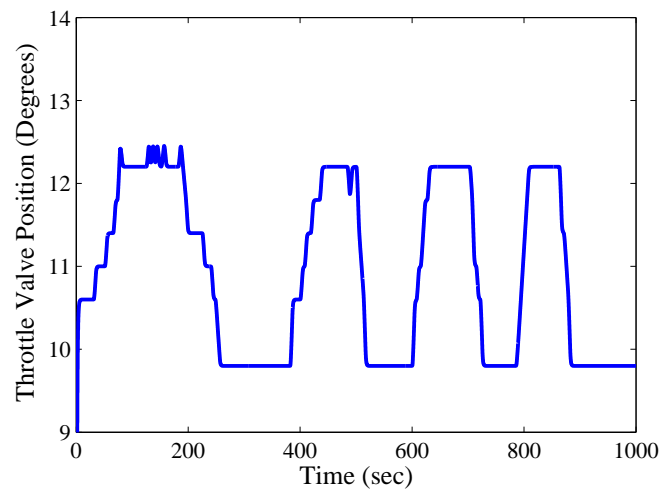


FIGURE 3.11: Input Throttle Position

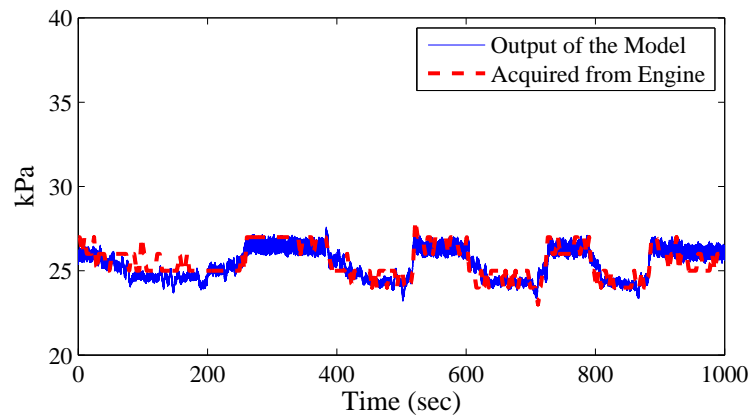


FIGURE 3.12: Intake Manifold Pressure

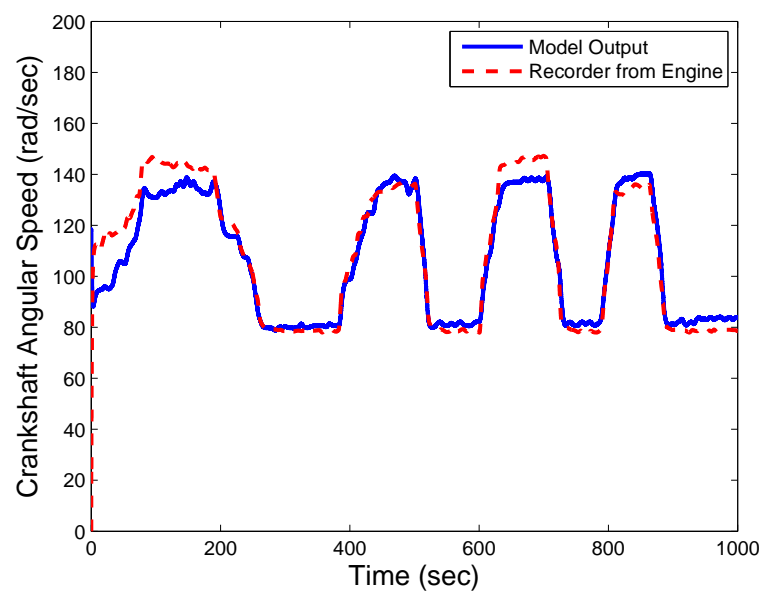


FIGURE 3.13: Crankshaft Angular Speed

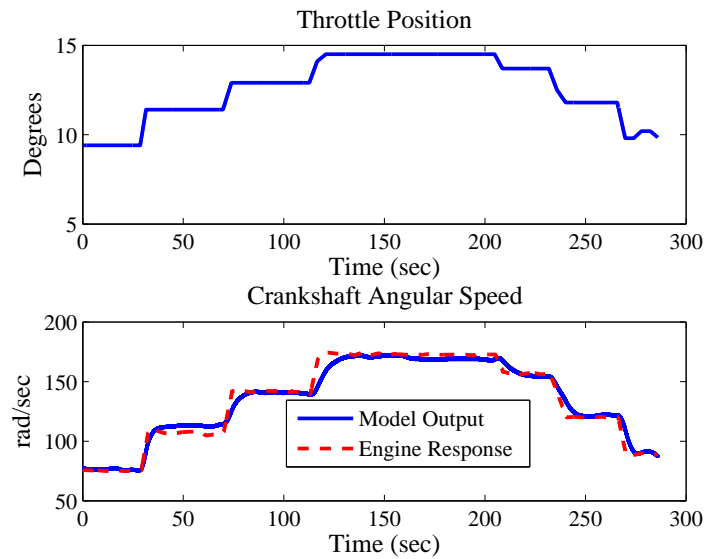


FIGURE 3.14: Model Response for Second Data-set

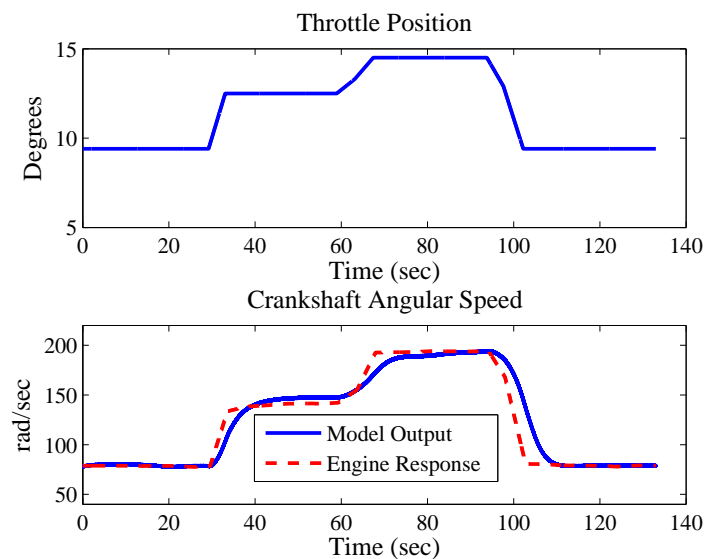


FIGURE 3.15: Model Response for Third Data-set

To further validate the efficacy of the model, response of the model against more data-sets is obtained. In one data set a stair case throttle is applied to the engine first in up direction and then downwards. The stair case is applied to investigate the response for different operational states. Input throttle and crankshaft angular speed response is shown in Figure 3.14. In second data set, relatively large step size input is applied, similarly first upwards then downwards. Input throttle and crankshaft angular speed response is shown in Figure 3.15.

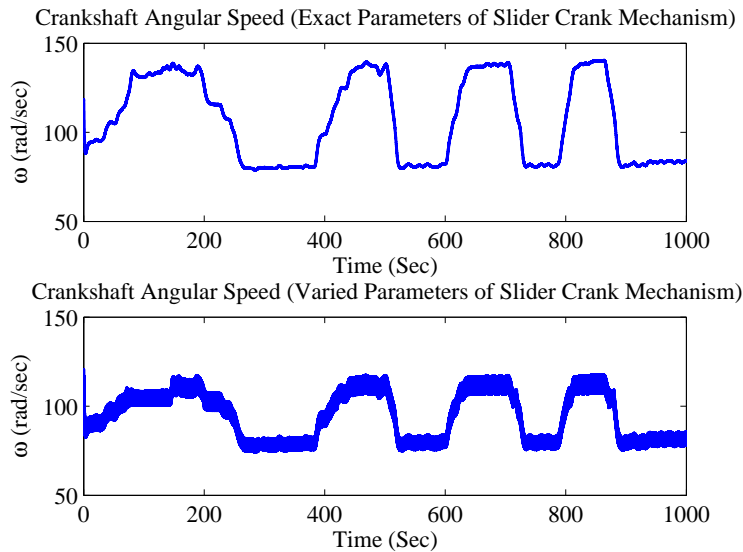


FIGURE 3.16: Effects of Variation in Design Parameters of the Mechanism

The proposed model is more parametric in nature, utilizing design parameters of torque producing mechanism which was not the case in existing MVEMs [1], where mechanism was replaced by a continuously operating volumetric pump. As a consequence, the effects of variation in engine design parameters (length of connecting rod or crank offset etc.) could readily be seen in the FPEM. A comparison is shown in Figure 3.16. The angular speed profile of crankshaft is compared for two systems, where everything is kept same and design parameters of slider crank mechanism are varied. The difference in the output clearly reflects role of the design parameters of torque producing mechanism in engine output.

Incorporating the model of the torque producing mechanism in FPEM enhances the capabilities of the model. Six Lagrange multipliers λ_1 to λ_6 correspond to physical quantities in the system. For the purpose of getting insight into the system, Equation 3.26 is stated (which is of the form of equations modeled for connecting rod in Equations 3.15d and 3.15e). If we consider $F = 0$ and visualize the motion of mass m , $-\lambda$ in Equation 3.26 clearly reflects force acting on mass m .

$$m\ddot{x} + \lambda = F \quad (3.26)$$

$F = 0$ is considered to make this equation compatible to the form of Equations 3.15d and 3.15e. The consideration of $F = 0$ physically signifies the situation when no external force is being exerted on the mass m . In such a case λ will correspond to force/ tension on the body applied by interacting bodies of the mechanism, connecting rod for example.

For a vivid view, connecting rod for example, associated Lagrange multipliers represent tension in connecting rod in respective direction. The evaluation of these Lagrange multipliers needs evaluation of algebraic expressions once speed dynamics are solved. Modeling approach thus carries the provision to analyze tension in connecting rod against variations in spark advance etc. Or the subject could be the tuning of variable valve timing map. Consequently, study of the effects on mechanism against spark advance and variable valve timing can be formulated as a model based problem. Formulation for translational tension in connecting rod is as follows:

$$T_{trans} = \sqrt{\lambda_3^2 + \lambda_4^2} \quad (3.27)$$

Likewise, for piston position Equation 3.6e could be utilized. Accordingly:

$$\begin{aligned} x_3 &= l_1 \cos(\theta_1) + l_2 \cos(\theta_2) \\ &= l_1 \cos(\theta_1) + l_2 \sqrt{l_2^2 - l_1^2 \sin^2(\theta_1)} / l_2 \\ &= l_1 \cos(\theta_1) + \sqrt{l_2^2 - l_1^2 \sin^2(\theta_1)} \end{aligned} \quad (3.28)$$

Simulation results for the formulations presented in Equations 3.27 and 3.28 are shown in Figure 3.17(d) and Figure 3.17(c), respectively. A magnified view of fluctuations in crankshaft angular speed is also shown in Figure 3.17(b).

The piston reciprocates about a mean position that lies above the rotational axis of the crankshaft. Additionally, the reciprocating motion is around the mean point with magnitudes (up and down) equal to that of the crank offset (l_1), the same is graphically presented in Figure 3.18. Position of the piston (x_3) evaluated from the model solution is shown in Figure 3.17(c), which is in agreement with the physical

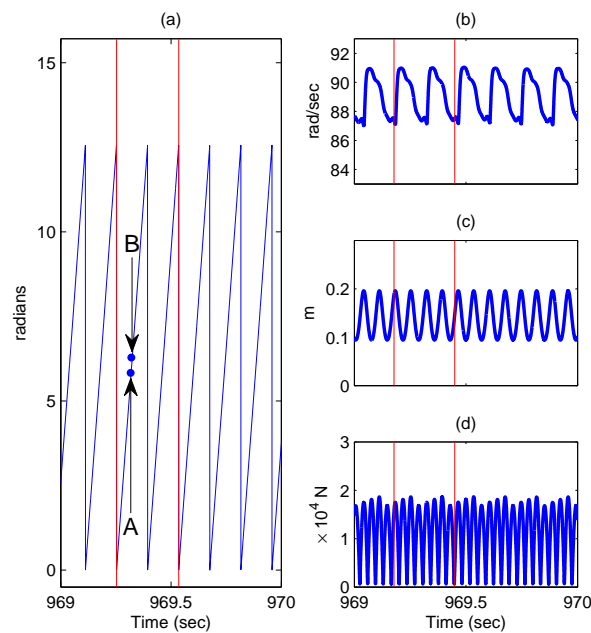


FIGURE 3.17: Miscellaneous Model Outputs(A is SOC while B is TDC)

description stated above. This further verifies the derivation, simplification and simulation procedure.

Following subsections summarize the possible utilization of different attributes of FPEM.

3.4.1 Control Capabilities

As shown in Figures 3.5, 3.8 and the model description, the proposed model presents the spark timing as a model based input to the torque production mechanism. In addition, as described earlier, tension in connecting rod is evaluated along-with solution of the rotational dynamics of the crankshaft. The model can thus play role in online tuning of spark advance against tension in connecting rod (especially in operations under fault conditions).

In conventional control oriented models, spark advance is introduced as model based input using empirical formulations. However, in proposed FPEM spark advance is not defined empirically. Empirical definitions remain valid until the system is healthy. Whereas, application of first principle bestows the model with

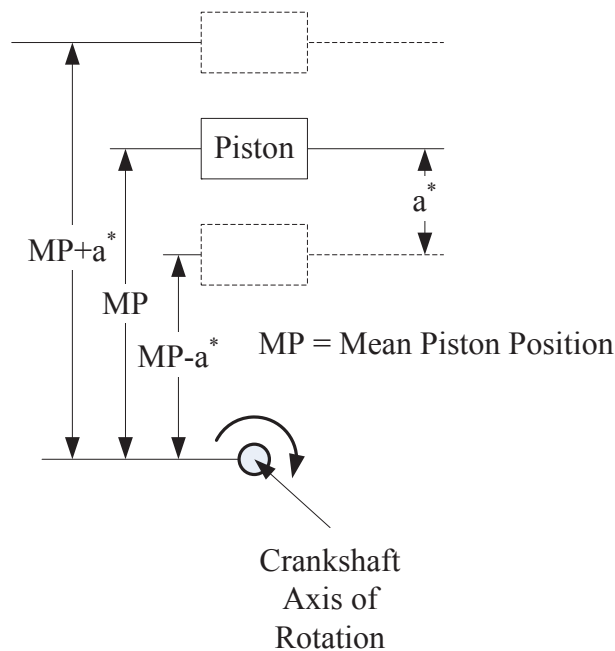


FIGURE 3.18: Piston Reciprocating Motion(a^* is crankoffset l_1)

capability to describe the healthy as well as system dynamics under fault conditions.

3.4.2 Diagnostic Capabilities

Ignition timing and spark health contributes to cylinder pressure. Which in turn is a contributing factor towards fluctuations in angular speed of the crankshaft. The fact is shown in [62], it was shown that in-cylinder conditions correspond to fluctuations in crankshaft angular speed. As a result, conventional diagnostic observer based techniques could be applied for estimation of spark health in spark ignition engines. The said feature can even serve as basis for prognosis for misfire conditions.

To further validate the model capacity to describe the system dynamics under fault conditions, a simulated intermittent misfire condition is used. An intermittent misfire condition is generated using the cylinder pressure model. Crankshaft angular speed fluctuation pattern for intermittent misfire condition is found consistent with those present in the literature, [83].

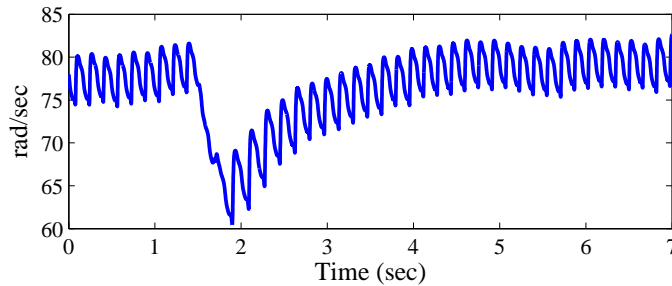


FIGURE 3.19: Pattern of Crankshaft Angular Speed Fluctuation for Intermittent Misfire Condition

TABLE 3.5: Comparison of MVEMs and Proposed FPEM

Attribute	Existing MVEMs	Proposed FPEM
Speed Equation	$\dot{\omega} = \frac{1}{J}\tau_b$	$\dot{\omega} = f(\theta, \omega, \Gamma)$ $+g_a(\theta, \omega, \Gamma)F(t)$ $+g_b(\theta, \omega, \Gamma)\tau_N$
Rotational Dynamics	Modeled based on approximation	Modeled based on first principle
Crankshaft Speed Fluctuations	Since Mechanism is replaced, fluctuations are not modeled	Fluctuations are modeled
Tension in Individual Bodies of Mechanism (Connecting Rod, Crankshaft)	Not Capable	Evaluated along-with rotational Dynamics
SA and VVT	Modeled indirectly (in a few cases)	Can directly be modeled with F
Description of system dynamics under fault conditions	Very limited capability	Model describes the dynamics (Section 3.4.2)
Extension Capability to Multi Cylinder Engines	Model cannot show multi-cylinder dynamics	Extended model can show the multi-cylinder dynamics

3.4.3 Model Integrability with Other Systems

The model utilizes an analytical cylinder pressure model, [78] and [84]. It is explained that heat rejected during different phases could mathematically be described. In the work presented in this thesis, cylinder pressure model is used only to calculate the force acting on the piston. Model based evaluation of rejected heat can lead to integration of control framework and engine thermo-management. Thus based on this capability, integration of control and engine cooling framework can be achieved.

3.5 Conclusions

Model of a gasoline engine, developed under the assumption of lumped cylinder dynamics is presented in this part of the thesis. Derivation of the model is presented followed by the simplification strategy. Simplification strategy is chosen based on the required final form of the model. Different realization aspects of the derived model are addressed. An analytical closed form cylinder pressure model is used to evaluate the force acting on the piston, forming one input channel to model of the mechanism. In such a way, model based formulation for inputs like valve and spark timing are derived, instead of empirical ones.

Simulation results of the proposed model are presented by end of the chapter along-with discussion on novel and outstanding model attributes.

Convergence to the first principle has shown the benefits of high fidelity, enhanced envelope of validity, lowered level of abstraction and comprehensive description of state variables. A comparison of different model attributes among conventional MVEMs and proposed FPEM is presented in Table 3.5.

Chapter 4 of the thesis presents an effort to include the aspects of multi-cylinders and spatial orientation into the mathematical model. That is, to depart from the lumped cylinder dynamics and develop the modeling methodology, which is capable of describing the multi-cylinder dynamics. Efforts are put to attain results of the following form:

$$\dot{\theta}_c = \omega_c \tag{3.29a}$$

$$\dot{\omega}_c = f(\theta_c, \omega_c, \Gamma) + \mathbf{g}_1(\theta_c, \omega_c, \Gamma)\tau_N + \sum_{b=1}^N g_b(\theta_c, \omega_c, \Gamma)f_{inb} \tag{3.29b}$$

where N is total number of cylinders.

Chapter 4

MULTI-CYLINDER DYNAMICS

Chapter 3 described derivation and benefits of an FPEM under assumption of lumped cylinders. Despite of the benefits presented earlier, presented modeling approach like MVEMs made the individual cylinders invisible. However, in author's view visibility of individual cylinders in a control oriented model is an outlining attribute to pave the way for cylinder-to-cylinder control. This part of the thesis aims at explaining the derivation, tuning, validation and possible benefits of a multi-cylinder control oriented model of gasoline engine. That is, to complete the FPEM picture. For the derivations purpose, foundation of Chapter 3 is kept in view and mathematical steps are executed straight forward.

The chapter takes the first step by developing and simplifying model of the mechanism corresponding to a four cylinder engine in Section 4.1. To evaluate the force acting on each of four pistons at different operational conditions and different phases of four strokes an extension to cylinder pressure model, presented in Chapter 3 would be required. A gasoline engine cylinder pressure model, presented in Chapter 3 is extended to a four cylinder engine in Section 4.2. Integration of analytical cylinder pressure model and dynamical model of the mechanism is carried out, to form a complete torque production subsystem in Section 4.3. Integration

of the said torque production subsystem with model of other subsystems (taken from the literature), is also addressed in the same section. Model validation and main-stream attributes of the FPEM are presented in Section 4.4. The chapter is summarized by Section 4.5.

4.1 Model of the Mechanism

The model of torque producing mechanism of an I-type, four cylinder gasoline engine with firing sequence of 1-3-4-2, is derived in this section. After derivation of the model equations (governing ODEs and constraints), based on Constrained Lagrangian EOM, the model is simplified. Simplification methodology is selected while keeping in view the required final form of the model. That is, the form as required by other subsystems of the gasoline engine model. Factors of multi-cylinders and spatial orientation (firing order and cylinder layout) have been considered while model derivation. Mechanism corresponding to said firing order and

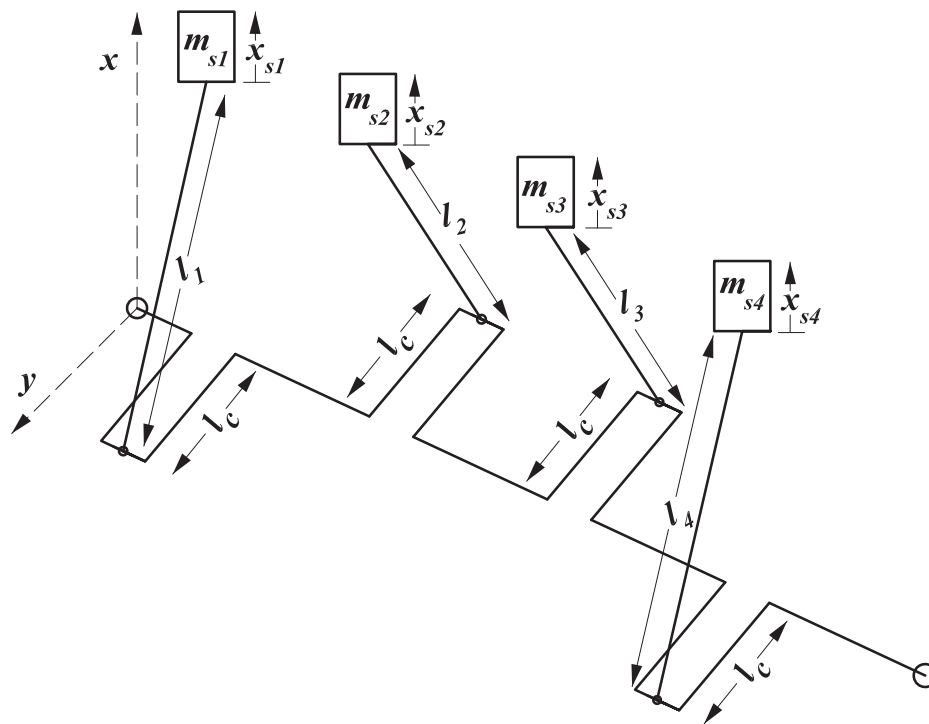


FIGURE 4.1: Torque Producing Mechanism in a Four Cylinder Engine (Model derivation is carried out in accordance with the generalized coordinated, spatial coordinated however are indicated only for geometric clarity)

number of cylinders is shown in Figure 4.1. Model of the indicated mechanism is derived in the following section.

4.1.1 Model Derivation

Model derivation is considered with the generic torque producing mechanism corresponding to a four cylinder engine, that is, single crankshaft connected to four pistons with four connecting rods. Arrangement of rigid bodies in the mechanism corresponding to engine discussed above is shown in Figure 4.1, along with parameter description.

Throughout this derivation, subscript c presents the parameter/ variable corresponding to crankshaft. A numeric subscript i shows parameter/ variable of i^{th} connecting rod. Whereas, a numeric subscript i with s (that is subscript si) symbolize the parameter/ variable corresponding to i^{th} piston.

The constrained EOM in Lagrangian Mechanics can be stated as:

$$\frac{d}{dt} \frac{\partial L}{\partial \dot{q}_m} - \frac{\partial L}{\partial q_m} + \sum_{j=1}^k \lambda_j \frac{\partial \phi_j}{\partial q_m} = e_m^s \quad (4.1)$$

subject to the constraints:

$$\phi_j(q, t) = 0 \quad j = 1, 2, 3, \dots, k \quad (4.2)$$

where m correspond to the m^{th} generalized coordinate of the mechanism, subscript j denotes the j^{th} constraint. Additionally, k represent the total number of constraints. The term e denotes the generalized effort and L is Lagrangian of the mechanism defined as follows:

$$L = T - V$$

where T is total kinetic energy of the mechanism and V is the total potential energy of the mechanism. Model is derived with the following assumptions:

1. Bodies in the mechanism are assumed to be rigid/ inflexible

2. Change in potential energy of the mechanism is assumed to be negligible ($\partial V/\partial q_m, \partial V/\partial \dot{q}_m \approx 0 \quad \forall \quad q_m$)
3. Friction is modeled with a lumped approach and all friction components are taken as frictional torque (acting on the crankshaft), incorporated in Section 4.3.2 while carrying out the model integration

Total kinetic energy of the mechanism has the following form:

$$T = T_c + \sum_{i=1}^4 T_i + \sum_{i=1}^4 T_{si} \quad (4.3)$$

It should be noted that crank offset of two cylinders (1, 4) lies exactly opposite to that of the other two cylinders (2, 3), as shown in Figure 4.1. As a result, mass of the crankshaft is symmetrically distributed around its own axis of rotation. Consequently, center of mass of such a distribution exhibits only rotational motion. It could thus be concluded that only one generalized coordinate is required to model the motion of the crankshaft. Moreover, center of mass of each connecting rod exhibits three motions namely Rotational, horizontal component of translational motion and vertical component of translational motion. Therefore, modeling the motion of each connecting rod require three generalized coordinates. As far as, four pistons are concerned, each exhibits translational motion only in one direction. So, one generalized coordinate is required to model the motion of each piston. Hence, total of seventeen generalized coordinates are involved in modeling the motion of the mechanism, shown in Figure 4.1. These 17 generalized coordinates q_1 to q_{17} are defined in Table 4.1.

Based on the description stated above, kinetic energy of the crankshaft can be stated as follows:

$$T_c = \frac{1}{2} J_c \dot{\theta}_c^2 \quad (4.4)$$

TABLE 4.1: Designation of the Generalized Coordinates

Generalized Variable	Variable Designation	Generalized Variable	Variable Designation
q_1	θ_c	q_{10}	θ_3
q_2	x_1	q_{11}	x_4
q_3	y_1	q_{12}	y_4
q_4	θ_1	q_{13}	θ_4
q_5	x_2	q_{14}	x_{s1}
q_6	y_2	q_{15}	x_{s2}
q_7	θ_2	q_{16}	x_{s3}
q_8	x_3	q_{17}	x_{s4}
q_9	y_3		

while for the four connecting rods, kinetic energy takes the following form:

$$T_1 = \frac{1}{2}m_1(\dot{x}_1^2 + \dot{y}_1^2) + \frac{1}{2}J_1\dot{\theta}_1^2 \quad (4.5a)$$

$$T_2 = \frac{1}{2}m_2(\dot{x}_2^2 + \dot{y}_2^2) + \frac{1}{2}J_2\dot{\theta}_2^2 \quad (4.5b)$$

$$T_3 = \frac{1}{2}m_3(\dot{x}_3^2 + \dot{y}_3^2) + \frac{1}{2}J_3\dot{\theta}_3^2 \quad (4.5c)$$

$$T_4 = \frac{1}{2}m_4(\dot{x}_4^2 + \dot{y}_4^2) + \frac{1}{2}J_4\dot{\theta}_4^2 \quad (4.5d)$$

As per discussion presented above, kinetic energy for each connecting rod contains the terms, corresponding to each associated generalized coordinate. For four pistons, kinetic energy could be formulated as:

$$T_{s1} = \frac{1}{2}m_{s1}\dot{x}_{s1}^2 \quad (4.6a)$$

$$T_{s2} = \frac{1}{2}m_{s2}\dot{x}_{s2}^2 \quad (4.6b)$$

$$T_{s3} = \frac{1}{2}m_{s3}\dot{x}_{s3}^2 \quad (4.6c)$$

$$T_{s4} = \frac{1}{2}m_{s4}\dot{x}_{s4}^2 \quad (4.6d)$$

Formulation of kinetic energy of each rigid body and holonomic constraints governing the motion of bodies of the mechanism are required for application of constrained Lagrangian EOM. For the formulation of constraints, first cylinder is taken as reference while all other angles are taken with respect to the reference. The connecting rod and the slider belonging to first cylinder bear the following

constraints:

$$\phi_1 = x_1 - (l_c \cos(\theta_c) + \frac{l_1}{2} \cos(\theta_1)) \quad (4.7a)$$

$$\phi_2 = y_1 - (l_c \sin(\theta_c) + \frac{l_1}{2} \sin(\theta_1)) \quad (4.7b)$$

$$\phi_3 = l_c \cos(\theta_c) + l_1 \cos(\theta_1) - x_{s1} \quad (4.7c)$$

$$\phi_4 = l_c \sin(\theta_c) + l_1 \sin(\theta_1) \quad (4.7d)$$

It should be noted that, Equations 4.7a and 4.7b correspond to the constraint on the motion of center of mass of first connecting rod. Moreover, Equations 4.7c and 4.7d present constraints on the motion of piston corresponding to first cylinder (constraint equations for other three cylinders are also arranged in the same order). The constraint equations are formulated, based on the detailed discussion presented in Chapter 3.

As indicated by the Figure 4.1, angle of the crank offset for cylinder two is $(\theta_c + \pi)$ with respect to reference cylinder, that is cylinder one. The same is shown graphically in Figure 4.2. This spatial geometry of the mechanism is considered and represented by the constraints for connecting rod and piston belonging to cylinder two and three. So, for second and third cylinders, the constraint equations will take the similar form. For second cylinder the constraints are as follows:

$$\phi_5 = x_2 - (l_c \cos(\theta_c + \pi) + \frac{l_2}{2} \cos(\theta_2)) \quad (4.8a)$$

$$\phi_6 = y_2 - (l_c \sin(\theta_c + \pi) + \frac{l_2}{2} \sin(\theta_2)) \quad (4.8b)$$

$$\phi_7 = l_c \cos(\theta_c + \pi) + l_2 \cos(\theta_2) - x_{s2} \quad (4.8c)$$

$$\phi_8 = l_c \sin(\theta_c + \pi) + l_2 \sin(\theta_2) \quad (4.8d)$$

while for the third one, these are stated as below:

$$\phi_9 = x_3 - (l_c \cos(\theta_c + \pi) + \frac{l_3}{2} \cos(\theta_3)) \quad (4.9a)$$

$$\phi_{10} = y_3 - (l_c \sin(\theta_c + \pi) + \frac{l_3}{2} \sin(\theta_3)) \quad (4.9b)$$

$$\phi_{11} = l_c \cos(\theta_c + \pi) + l_3 \cos(\theta_3) - x_{s3} \quad (4.9c)$$

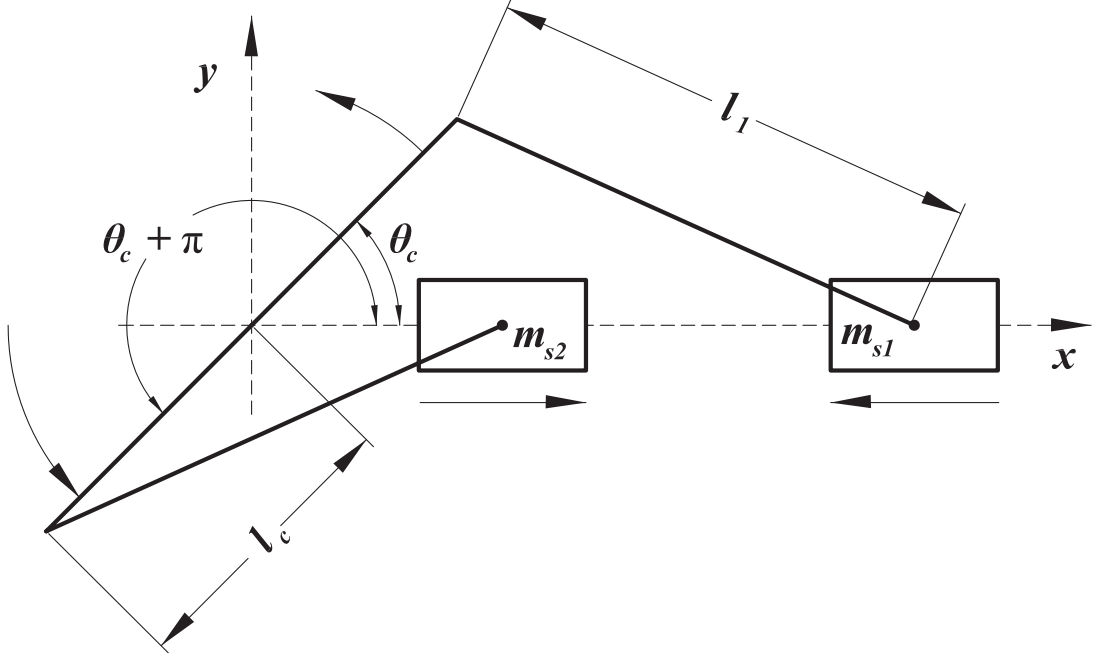


FIGURE 4.2: Geometric Illustration of Cylinder Offset

$$\phi_{12} = l_c \sin(\theta_c + \pi) + l_3 \sin(\theta_3) \quad (4.9d)$$

Crank offset of cylinder four, however, lies in the same orientation as the reference cylinder. Thus, constraints for fourth cylinder are of the form of Equation 4.9, as follows:

$$\phi_{13} = x_4 - (l_c \cos(\theta_c) + \frac{l_4}{2} \cos(\theta_4)) \quad (4.10a)$$

$$\phi_{14} = y_4 - (l_c \sin(\theta_c) + \frac{l_4}{2} \sin(\theta_4)) \quad (4.10b)$$

$$\phi_{15} = l_c \cos(\theta_c) + l_4 \cos(\theta_4) - x_{s4} \quad (4.10c)$$

$$\phi_{16} = l_c \sin(\theta_c) + l_4 \sin(\theta_4) \quad (4.10d)$$

Thus the following are obtained: i) Seventeen generalized coordinates (enlisted in Table 4.1) ii) Formulation of kinetic energy (Equation 4.3) iii) Constraints involved in motion of individual rigid bodies (Equations 4.7 to 4.10). Lagrangian EOM stated by Equations 4.1 and (4.2) can be applied to the mechanism. Application

to the crankshaft yields the following:

$$\begin{aligned}
J_c \ddot{\theta}_c = & \\
& - \lambda_1 l_c \sin(\theta_c) + \lambda_2 l_c \cos(\theta_c) + \lambda_3 l_c \sin(\theta_c) - \lambda_4 l_c \cos(\theta_c) \\
& + \lambda_5 l_c \sin(\theta_c) - \lambda_6 l_c \cos(\theta_c) - \lambda_3 l_c \sin(\theta_c) + \lambda_8 l_c \cos(\theta_c) \\
& + \lambda_9 l_c \sin(\theta_c) - \lambda_{10} l_c \cos(\theta_c) - \lambda_{11} l_c \sin(\theta_c) + \lambda_{12} l_c \cos(\theta_c) \\
& - \lambda_{13} l_c \sin(\theta_c) + \lambda_{14} l_c \cos(\theta_c) + \lambda_{15} l_c \sin(\theta_c) - \lambda_{16} l_c \cos(\theta_c)
\end{aligned} \tag{4.11}$$

TABLE 4.2: External Effort along Generalized Coordinates

Generalized Coordinate	Generalized Effort	Generalized Coordinate	Generalized Effort
θ_c	τ_N	θ_3	0
x_1	0	x_4	0
y_1	0	y_4	0
θ_1	0	θ_4	0
x_2	0	x_{s1}	f_{in1}
y_2	0	x_{s2}	f_{in2}
θ_2	0	x_{s3}	f_{in3}
x_3	0	x_{s4}	f_{in4}
y_3	0		

As there are three generalized coordinates for motion of each connecting rod, constrained EOM when applied to each connecting rod, results in three 2^{nd} order ODEs. When applied to the connecting rod of first cylinder, following equations are obtained:

$$m_1 \ddot{x}_1 + \lambda_1 = 0 \tag{4.12a}$$

$$m_1 \ddot{y}_1 + \lambda_2 = 0 \tag{4.12b}$$

$$J_1 \ddot{\theta}_1 = -\lambda_1 \frac{l_1}{2} \sin(\theta_1) + \lambda_2 \frac{l_1}{2} \cos(\theta_1) + \lambda_3 l_1 \sin(\theta_1) - \lambda_4 l_1 \cos(\theta_1) \tag{4.12c}$$

likewise, for second connecting rod:

$$m_2\ddot{x}_2 + \lambda_5 = 0 \quad (4.13a)$$

$$m_2\ddot{y}_2 + \lambda_6 = 0 \quad (4.13b)$$

$$J_2\ddot{\theta}_2 = -\lambda_5\frac{l_2}{2}\sin(\theta_2) + \lambda_6\frac{l_2}{2}\cos(\theta_2) + \lambda_7l_2\sin(\theta_2) - \lambda_8l_2\cos(\theta_2) \quad (4.13c)$$

when applied to 3rd connecting rod, it yields the following:

$$m_3\ddot{x}_3 + \lambda_9 = 0 \quad (4.14a)$$

$$m_3\ddot{y}_3 + \lambda_{10} = 0 \quad (4.14b)$$

$$J_3\ddot{\theta}_3 = -\lambda_9\frac{l_3}{2}\sin(\theta_3) + \lambda_{10}\frac{l_3}{2}\cos(\theta_3) + \lambda_{11}l_3\sin(\theta_3) - \lambda_{12}l_3\cos(\theta_3) \quad (4.14c)$$

for 4th connecting rod, following equations are obtained:

$$m_4\ddot{x}_4 + \lambda_{13} = 0 \quad (4.15a)$$

$$m_4\ddot{y}_4 + \lambda_{14} = 0 \quad (4.15b)$$

$$J_4\ddot{\theta}_4 = -\lambda_{13}\frac{l_4}{2}\sin(\theta_4) + \lambda_{14}\frac{l_4}{2}\cos(\theta_4) + \lambda_{15}l_4\sin(\theta_4) - \lambda_{16}l_4\cos(\theta_4) \quad (4.15c)$$

and finally for the four sliders following four equations are obtained:

$$m_{s1}\ddot{x}_{s1} - \lambda_3 = f_{in1}(\theta_c) \quad (4.16a)$$

$$m_{s2}\ddot{x}_{s2} - \lambda_7 = f_{in2}(\theta_c) \quad (4.16b)$$

$$m_{s3}\ddot{x}_{s3} - \lambda_{11} = f_{in3}(\theta_c) \quad (4.16c)$$

$$m_{s4}\ddot{x}_{s4} - \lambda_{15} = f_{in4}(\theta_c) \quad (4.16d)$$

Model is described by ODEs (Equations 4.11 to 4.16) and constraints (stated by Equations 4.7 to 4.10). It should be noted that seventeen 2nd order ODEs together with sixteen constraints bestow the model one degree of freedom. The conclusion is well in agreement with physical intuition from the nature of the mechanism. Model simplification and strategy of the solution is discussed next.

4.1.2 Model Simplification

As described earlier in Chapter 3, there are different strategies for solution of DAEs formed by the constrained EOM in Lagrangian Mechanics, such as Kane's Method [75]. However, since efforts in this study are made to develop a multi-cylinder control oriented model. Developing the matrices for system of DAEs under study would rather be problematic in integrating with model of other subsystems. Moreover, resultant model would not be of the form, as that of accustomed in the control community. For a control oriented model, finally model of the form shown by the following equation would be required:

$$\dot{\theta}_c = \omega_c \quad (4.17a)$$

$$\dot{\omega}_c = f(\theta_c, \omega_c, \Gamma) + \mathbf{g}_1(\theta_c, \omega_c, \Gamma)\tau_N + \mathbf{g}_2(\theta_c, \omega_c, \Gamma)F \quad (4.17b)$$

$$= f(\theta_c, \omega_c, \Gamma) + \mathbf{g}_1(\theta_c, \omega_c, \Gamma)\tau_N + \sum_{b=1}^4 g_b(\theta_c, \omega_c, \Gamma)f_{inb} \quad (4.17c)$$

However, a significant difference here as compared with those dealt in Chapter 3, that F represents a vector here containing four elements. Each element of the vector corresponds to the force acting on each piston, $F = [f_{in1} \ f_{in2} \ f_{in3} \ f_{in4}]'$. Solution strategy, used in Chapter 3 explained in [77] is again utilized. Procedure for cylinder one and two is explained, while the same procedure is followed for cylinder three and four.

1. Simplification procedure for first cylinder

- (a) Equation 4.7d is used to express θ_1 , $\dot{\theta}_1$ and $\ddot{\theta}_1$ as function of θ_c , $\dot{\theta}_c$ and $\ddot{\theta}_c$, the same equation is also used to express $\sin(\theta_1)$ and $\cos(\theta_1)$ as function of θ_c .
- (b) Equation 4.7a is used to express x_1 and its higher time derivatives as function of θ_c ¹
- (c) Equation 4.12a is then used to express λ_1 as function of θ_c

¹ x_1 and its higher time derivatives are also expressed as function of θ_c , $\dot{\theta}_c$ and $\ddot{\theta}_c$. Written in short, here and in subsequent steps, for simplicity

-
- (d) Equation 4.7b is used to express y_1 and its higher time derivatives as function of θ_c
 - (e) Equation 4.12b is then used to express λ_2 as function of θ_c
 - (f) Equation 4.7c is used to express x_{s1} and its higher time derivatives as function of θ_c
 - (g) Equation 4.16a is used to express λ_3 as function of θ_c
 - (h) Results from Step 1a ($\ddot{\theta}_1$) as function of θ_c , Step 1c (λ_1), Step 1e (λ_2) and Step 1g (λ_3) all as function of θ_c , $\dot{\theta}_c$ and $\ddot{\theta}_c$ are used to express λ_4 as function of θ_c , $\dot{\theta}_c$ and $\ddot{\theta}_c$ using Equation 4.12c
2. By virtue of Step 1a to 1h, λ_1 through λ_4 are expressed as function of θ_c , $\dot{\theta}_c$ and $\ddot{\theta}_c$
3. Derivation procedure for second cylinder
- (a) Equation 4.8d is used to express θ_2 , $\dot{\theta}_2$ and $\ddot{\theta}_2$ as function of θ_c , $\dot{\theta}_c$ and $\ddot{\theta}_c$, the same equation is also used to express $\sin(\theta_2)$ and $\cos(\theta_2)$ as function of θ_c .
 - (b) Equation 4.8a is used to express x_2 and its higher time derivatives as function of θ_c^2
 - (c) Equation 4.13a is then used to express λ_5 as function of θ_c
 - (d) Equation 4.8b is used to express y_2 and its higher time derivatives as function of θ_c
 - (e) Equation 4.13b is then used to express λ_6 as function of θ_c
 - (f) Equation 4.8c is used to express x_{s2} and its higher time derivatives as function of θ_c
 - (g) Equation 4.16b is used to express λ_7 as function of θ_c
 - (h) Results from Step 3a ($\ddot{\theta}_2$) as function of θ_c , Step 3c (λ_1), Step 3e (λ_2) and Step 3g (λ_3) all as function of θ_c , $\dot{\theta}_c$ and $\ddot{\theta}_c$ are used to express λ_8 as function of θ_c , $\dot{\theta}_c$ and $\ddot{\theta}_c$ using Equation 4.12c

² x_2 and its higher time derivatives are also expressed as function of θ_c , $\dot{\theta}_c$ and $\ddot{\theta}_c$. Written in short, here and in subsequent steps, for simplicity

4. By virtue of Step 3a to 3h, λ_5 through λ_8 are expressed as function of θ_c , $\dot{\theta}_c$ and $\ddot{\theta}_c$
5. Following the same procedure for third cylinder, λ_9 through λ_{12} are obtained as function of θ_c , $\dot{\theta}_c$ and $\ddot{\theta}_c$
6. Following the same procedure for 4th cylinder, λ_{13} through λ_{16} are obtained as function of θ_c , $\dot{\theta}_c$ and $\ddot{\theta}_c$
7. Steps 2, 4, 5 and 6 present λ_1 through λ_{16} as function of θ_c , $\dot{\theta}_c$ and $\ddot{\theta}_c$
8. Results from Step 7 are used to replace λ_1 through λ_{16} in Equation 4.11, equation is then solved for $\ddot{\theta}_c$. Finally a 2nd order ODE, of the form of Equation 4.17, for θ_c is obtained.

All of the steps described above are carried out in Mathematica[®]. Results of the form shown in Equation 4.17 are obtained after simplification. Detailed mathematical expressions are presented in Appendix C.

Model of the mechanism is solved in Mathematica, results of the simulation for two revolution are presented in Figure 4.3. System is solved with no force acting on any piston, and a constant torque applied at crankshaft. It should be noted that there are four angular speed fluctuations in 4π angular distance, that is two revolutions or one complete four stroke cycle. The fluctuation patterns further verifies the correctness of derivation and simplification procedure, [85].

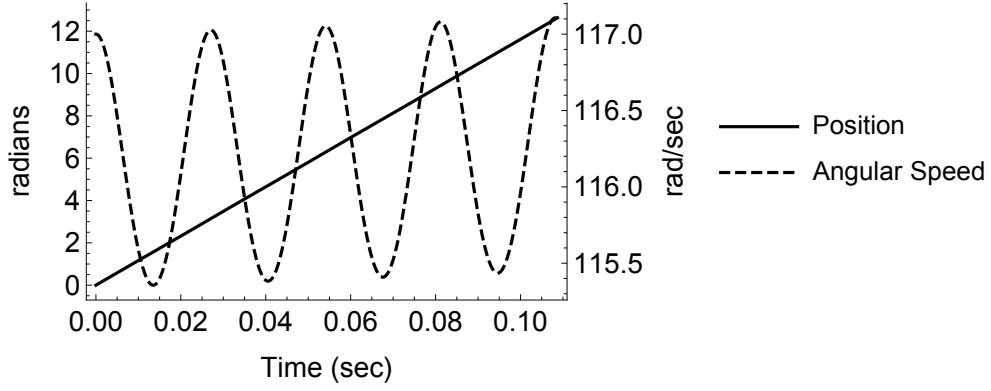


FIGURE 4.3: Solution of the Model of Torque Producing Mechanism (shown in Figure 4.1). Initial Conditions for the Simulation are $\theta_c = 0\text{rad}$ and $\dot{\theta}_c = 117\text{rad/sec}$

4.2 Cylinder Pressure Model

As described earlier, *Cylinder Pressure Model* is required to evaluate force acting on the piston in all four phases of strokes and whole operational range of the engine. On the other side, along-with state variables and operational parameters, cylinder pressure in a four stroke engine also depend on different phases of four stroke cycle. Since motion of the piston follow some constraints put by the mechanism, direction of motion of the piston and *net external force* acting on it decides whether work is performed on the system or work is performed by the system.

A free body diagram of piston is shown in Figure 4.4. Other than the force exerted on piston by connecting rod (which is not a generalized effort, since its not external), there are two forces acting on piston. The force acting on piston due to a particular pressure in crankcase, the component is shown as (F_{ck}) . The other force is due to a particular pressure in respective cylinder, the component shown as (F_{ci}) where i correspond to the i^{th} cylinder. The net force acting on the i^{th} piston thus becomes the difference of (F_{ck}) and (F_{ci}) , as follows:

$$f_{ci} = P_{cyl i} A_p \quad (4.18a)$$

$$f_{ck} = P_{ck} A_p \quad (4.18b)$$

$$f_{ini} = f_{ci} - f_{ck} \quad (4.18c)$$

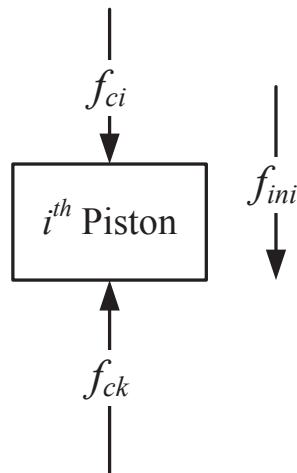


FIGURE 4.4: Free Body Diagram of i^{th} Piston

where, P_{cyl_i} is the pressure in i^{th} cylinder, P_{ck} is crank-case pressure and f_{ini} is force acting on i^{th} piston.

Rest of this section deals with the development of an appropriate cylinder pressure model for four-stroke four cylinder gasoline engine. Subsequent model is then used to evaluate force acting in each piston. As a first step, a short summary of an analytical gasoline cylinder pressure model is presented, the model is explained in details in [78] and [84]. The model is extended for four cylinders. Positive Crankcase Ventilation System is assumed to be working fine and pressure in crankcase is taken as constant.

4.2.1 Single Cylinder Pressure Model

An analytical parametric model for cylinder pressure in a four stroke gasoline engine is presented in [78]. The model is parametric and simple. Cylinder pressure model is developed by joining the asymptotes of intake, compression, power and exhaust stroke.

Each phase of four stroke is realized by its own physical principle. For intake stroke, intake manifold pressure and volumetric efficiency are utilized to estimate the in-cylinder pressure. Doing so, mass of air and that of the fuel are also estimated

inducted by the cylinder for a given air-to-fuel ratio. Likewise the exhaust stroke. Rest of the phases are modeled as follows:

Compression: Compression asymptote is modeled by a polytropic process, with polytropic compression exponent γ_c . Initial conditions for polytropic compressions process are taken by the end of intake stroke. Following such a strategy, asymptotes of intake and compression strokes are automatically joined. Mathematical description of pressure and temperature during compression are as follows:

$$P_c(\theta_c) = P_{ivc} \left(\frac{V_{ivc}}{V(\theta_c)} \right)^{\gamma_c} \quad (4.19a)$$

$$T_c(\theta_c) = T_{ivc} \left(\frac{V_{ivc}}{V(\theta_c)} \right)^{\gamma_c - 1} \quad (4.19b)$$

Combustion Phase: The combustion phase, starts with SOC event physically triggered by a spark plug and remains until the EOC. Duration between SOC and EOC is called Combustion Phasing [78]. Combustion phasing is realized by Mass Fraction Burn (MFB). The MFB has been modeled using Wiebe Functions, as explained in [78] and [80]. More details in combustion phasing and MFB is presented after this discussion.

Expansion Phase: The expansion asymptote is well described by a polytropic process, with polytropic exponent γ_e . Mathematically it is described as:

$$P_e(\theta_c) = P_3 \left(\frac{V_3}{V(\theta_c)} \right)^{\gamma_e} \quad (4.20a)$$

$$T_e(\theta_c) = T_3 \left(\frac{V_3}{V(\theta_c)} \right)^{\gamma_e - 1} \quad (4.20b)$$

The Wiebe Function is most widely used technique to model the combustion phasing and mass fraction burn, for instance [79] and [80]. It is expressed as:

$$m_{fb} = 1 - \exp \left[-a \left(\frac{\theta_c - \theta_o}{\delta\theta_c} \right)^{m+1} \right] \quad (4.21)$$

where, $\delta\theta$ is burn duration, θ_o is SOC and a, m are Wiebe shape factor. Approximation of shape factor a, m are described in [78]. An average value of $\delta\theta$ for

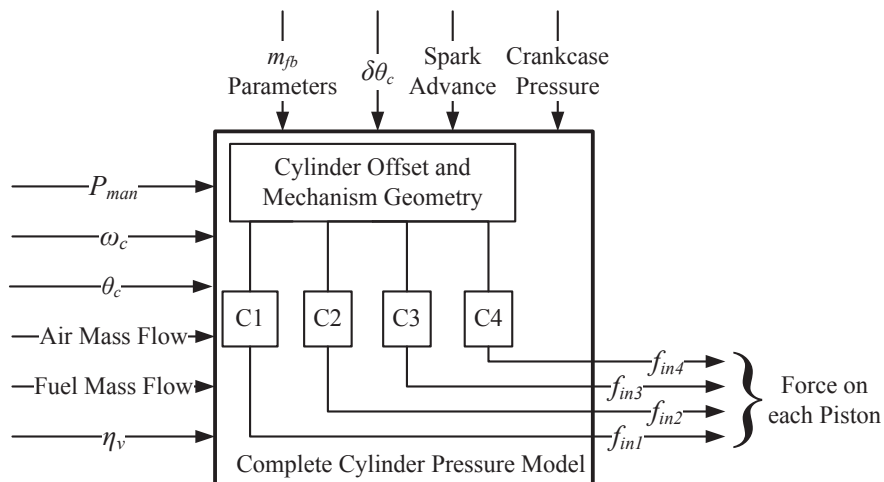


FIGURE 4.5: A Multi-Cylinder Pressure Model (C_i in the Figure shows i^{th} Cylinder)

gasoline is used, evaluated in [79]. SOC is assumed to be the spark timing, which has been acquired from engine as explained in Section Appendix A.

In addition values of the combustion parameters (a, m) and nominal values for $\Delta\theta$ for pure gasoline are presented in [79].

4.2.2 Structure of a Multi-Cylinder Pressure Model

Analytical cylinder pressure model described in Section 4.2.1 is extended to four cylinder by adding the valve timing and spark information corresponding to four cylinders. The architecture of resulting combustion model is shown in Figure 4.5. Individual cylinder pressure together with crankcase pressure is used to evaluate net force acting on each piston. Doing so, this part of the model provides four variables, which serve input to the model of torque producing mechanism described in Section 4.1.2.

Overall structure, inputs and outputs of the combustion model for a four stroke four cylinder arrangement are shown in Figure 4.5.

Moreover, it is explained in [78], that since compression and expansion asymptote are modeled with polytropic constant. The heat rejected during the processes can mathematically be formulated. In such a condition, it becomes possible to

integrate the engine thermo-management with control oriented engine model. It could possibly be done by dividing the heat rejected into components, rejected through engine exhaust and the other part being rejected to cooling system. This feature is discussed in detail in Section Section 4.4.4.

4.3 Model Realization

To begin with the realization of whole engine model, model of torque producing mechanism developed above and models of subsystems those taken from the literature are to be integrated. Model of subsystems taken from literature are explained in Chapter 2 and Chapter 3. This section aims at describing the integration procedure and presenting the overall picture.

4.3.1 Model Integration

For subsystems integration, there are air intake, intake manifold, fuel, torque producing mechanism and cylinder pressure model to be integrated. Interconnect of intake air and intake manifold subsystem has already been presented in Chapter 3. The flows \dot{m}_{ao} and \dot{m}_{fo} eventually reach to the cylinder.

The model of torque producing mechanism (derived in Section 4.1) and analytic gasoline engine cylinder pressure model (discussed in Section 4.2) are put together as shown in Figure 4.6.

The air intake, intake manifold, fuel and torque production subsystem are joined together to form the full picture of the engine system. Mathematically the state equation are stated as follows:

$$\dot{P}_{man} = \frac{T_{amb}R\gamma}{V_{man}} \times (\dot{m}_{ai}(\alpha, P_{man}) - \dot{m}_{ao}(P_{man}, \omega_c)) \quad (4.22a)$$

$$\dot{\theta}_c = \omega_c \quad (4.22b)$$

$$\dot{\omega}_c = f(\theta_c, \omega_c, \Gamma) + g_1(\theta_c, \omega_c, \Gamma)\tau + g_2(\theta_c, \omega_c, \Gamma)F \quad (4.22c)$$

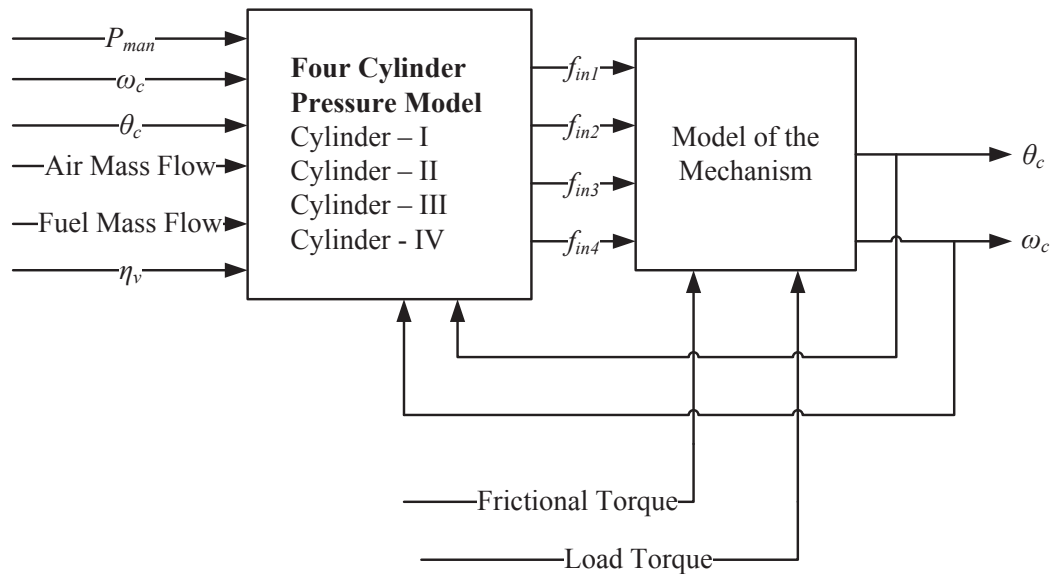


FIGURE 4.6: Integrated Model of the Mechanism and Combustion Model

Together with first order model of fuel system. Tuning variables in overall model are identified and model is tuned as according to the procedure described in Appendix A.

4.3.2 Tuning of the Model Parameters

Tuning of the model is carried out in accordance with the procedure described in Appendix A. Table 4.3 summarize the tuning variables in the model along-with their tuned values.

Other than force acting on each piston, torque acting on the crankshaft is another input to the torque producing mechanism. Forces generated by combustion and those generated by suction in and pump out (from cylinder, intake and exhaust stroke respectively) are taken into account by cylinder pressure model. As a result, load torque and frictional torque are only two torques acting on the crankshaft, as explained in Section 3.3.3. The frictional torque is evaluated using the frictional

mean effective pressure, the formulation is as follows:

$$f_{mep} = a_o + a_1\omega_c + a_2\omega_c^2 + a_3\omega_c^3 + a_4\omega_c^4 \quad (4.23a)$$

$$\tau_{fr} = \frac{V_d}{4\pi} \times f_{mep} \quad (4.23b)$$

$$\tau_N = -\tau_{fr} - \tau_L \quad (4.23c)$$

TABLE 4.3: Model Tuning Variables and Their Values

Parameter	Value
η_v	Curve Fit Appendix A
C_D	0.32
\dot{m}_{aio}	0.1g/sec
a_o	5.5×10^4
a_1	350.41×10^{-5}
a_2	520×10^{-3}
a_3	6.6×10^{-6}
a_4	4.3×10^{-9}

4.4 Results and Discussion

Model of the gasoline engine developed and tuned above is validated against data acquired from the engine. The validation data is acquired with a square wave type input throttle to engine. After validation, model performance is shown against two different inputs. First one, the staircase input. This data set aims at showing performance of the model against multiple operating points. Second one, the larger throttle changes than the validation data. This data set aims at showing model performance against large throttle changes.

Input throttle position for validation data-set is shown in Figure 4.7(a). Output of the model is shown in Figures 4.7(b) and 4.7(c), showing P_{man} and ω respectively.

Simulation results of staircase type input are shown in Figures 4.8(a) and 4.8(b). In addition to showing the states, different model capabilities explained later are

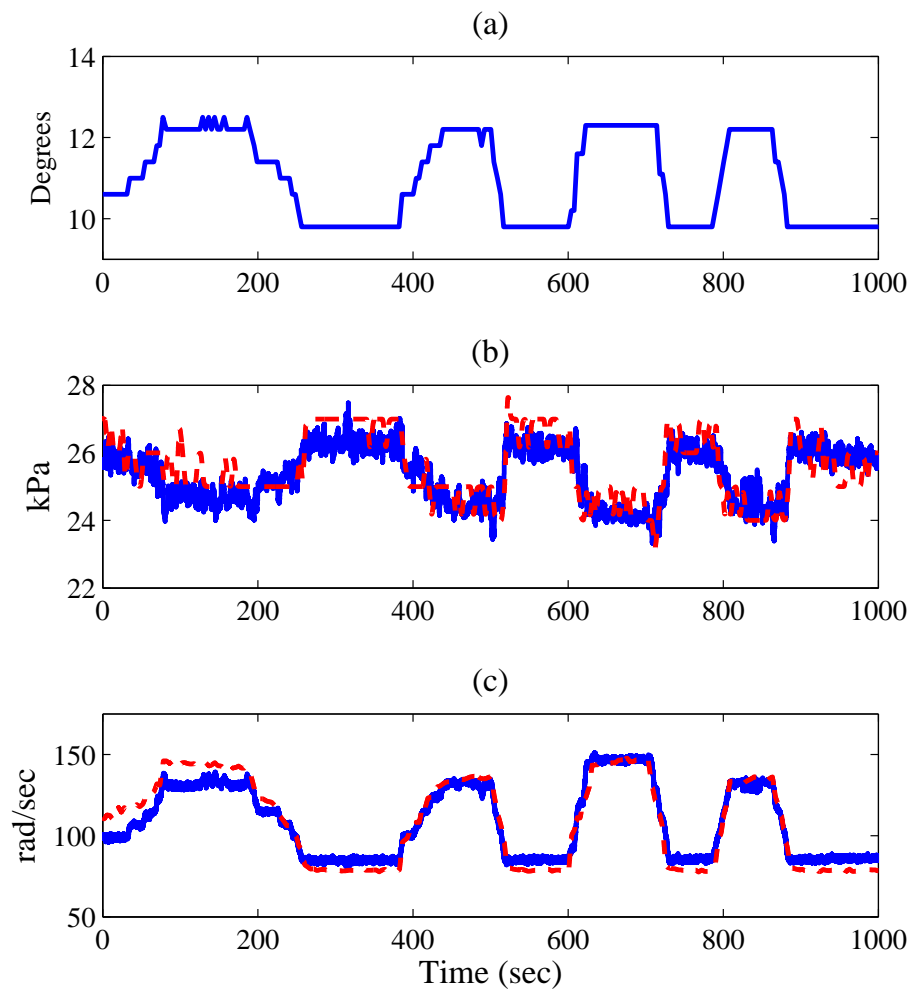


FIGURE 4.7: Model Validation Results (a) Throttle Position (b) Intake Manifold Pressure (P_{man}) (c) Crankshaft Angular Speed (ω_c) (continuous line is actual engine response acquired experimentally, dashed line is output of the FPDM)

also shown. Magnified view of crankshaft angular speed fluctuations is shown in Figure 4.9. Whereas, Figure 4.10 shows different parameters solved with model.

Response of the model against relatively larger input throttle input is shown in Figure 4.11(a) Figure 4.11(b), input throttle and crankshaft angular speed respectively.

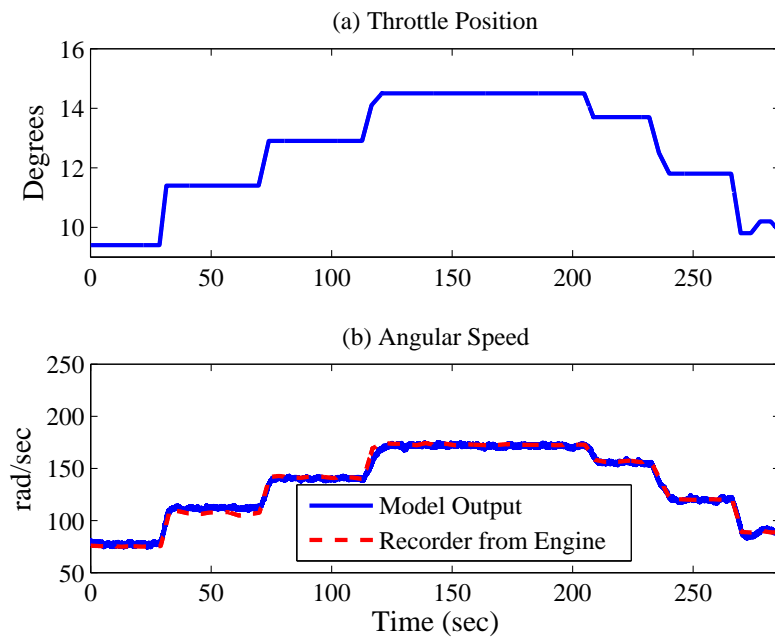


FIGURE 4.8: Simulation Results for Staircase Input

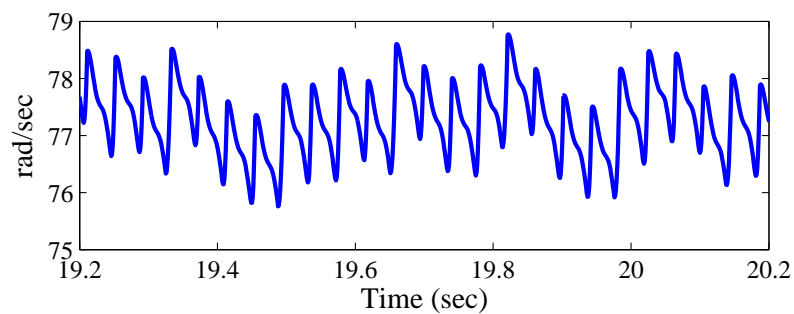


FIGURE 4.9: Crankshaft Angular Speed Fluctuations (Magnified View of Figure 4.8(b))

4.4.1 Features of FPEM

Complete engine has been developed by integrating the existing models of air intake, intake manifold and fuel subsystems to a novel torque production subsystem. Torque production subsystems further consist of two parts: 1) Model of the multi-cylinder torque producing mechanism 2) Analytical gasoline combustion model.

Following such a modeling approach, the model is bestowed with additional capabilities. Model based description of fluctuations or oscillations in the angular speed

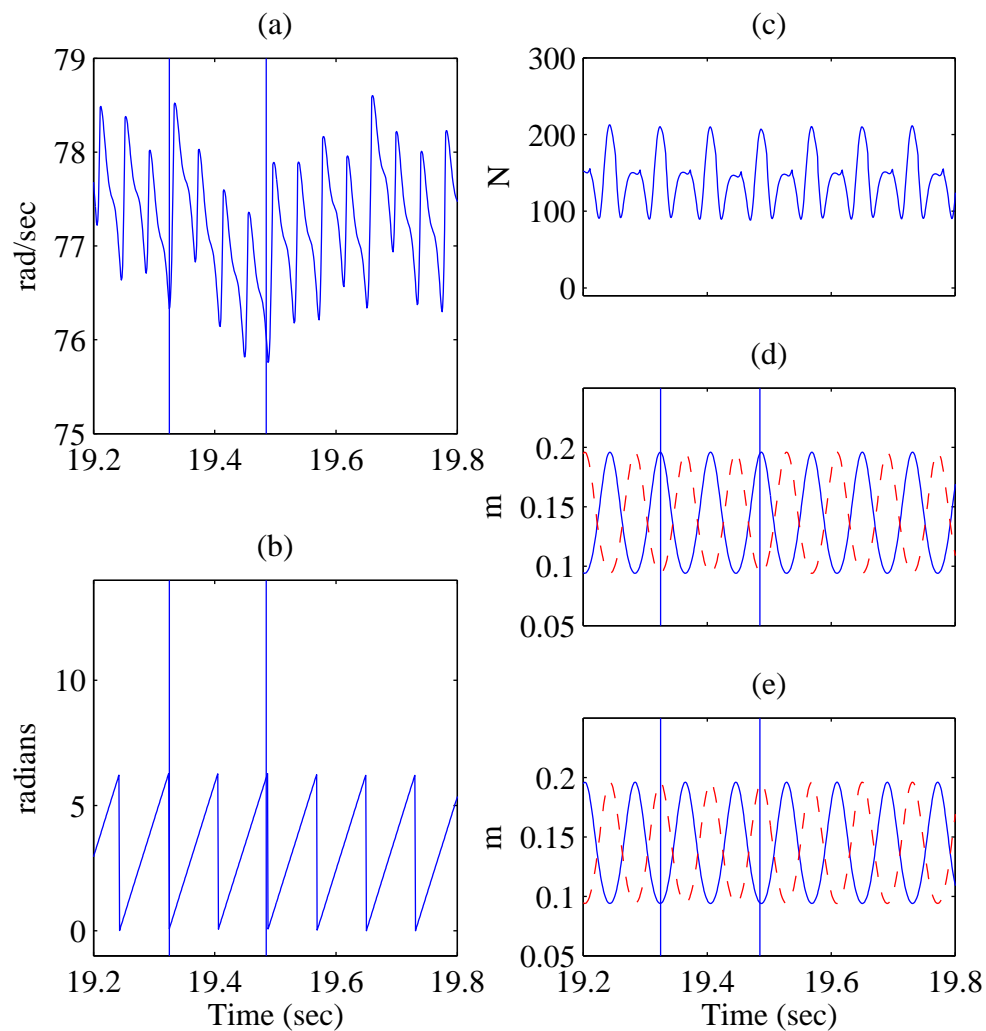


FIGURE 4.10: Additional FPDM Features, showing one four stroke cycle indicated between two vertical lines a) Crankshaft Angular Speed Fluctuations b) Crankshaft Angular Position c) Translational Tension in First Connecting Rod d) Piston 1 and 2 Position e) Piston 3 and 4 Position

of the crankshaft is very first and prominent feature. As described earlier, these oscillations exist due to two major factors. First one is dynamics of torque producing mechanism itself. The second one is rapidly changing in-cylinder thermodynamic conditions. The proposed model attains the capability, firstly by incorporating the mathematical model of the torque producing mechanism and afterward the other part contributed by rapidly changing in-cylinder conditions is incorporated by cylinder pressure model. Despite of many other possible utilization, crankshaft angular speed fluctuations directly correspond to in-cylinder conditions, [62]. As a result, application of model based diagnostic and prognostic techniques can be

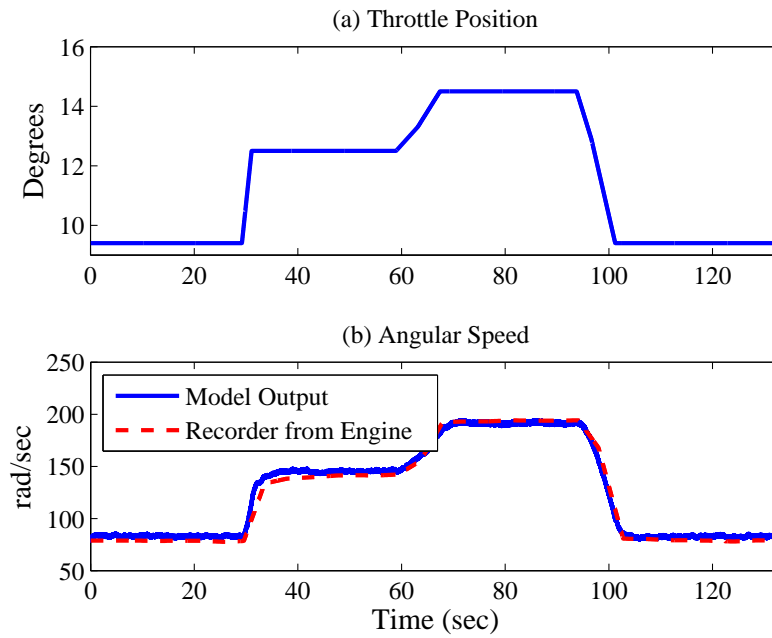


FIGURE 4.11: Simulation Results for Large Throttle Changes

applied to engine torque producing mechanism.

Model of the mechanism and solution strategy provide means for analyzing the tension in the individual bodies of the mechanism. For a vibrant insight, equation of the following form could be considered:

$$m\ddot{x} + \lambda = 0 \quad (4.24)$$

The term $-\lambda$ in above equation correspond to a force/ tension term. It should be noted that, equations for translational motion of connecting rods are of the same form, for example for first cylinder Equations 4.12a and 4.12b. As a result following could be concluded:

$$T_{trans1} = \sqrt{\lambda_1 + \lambda_2} \quad (4.25a)$$

$$T_{trans2} = \sqrt{\lambda_5 + \lambda_6} \quad (4.25b)$$

$$T_{trans3} = \sqrt{\lambda_9 + \lambda_{10}} \quad (4.25c)$$

$$T_{trans4} = \sqrt{\lambda_{13} + \lambda_{14}} \quad (4.25d)$$

where T_{transi} is translational tensions in i^{th} connecting rod. Such capability when

linked with inputs to the derived model, lead to new model based considerations. For example, valve timing and spark advance are inputs to cylinder pressure model. Thus, model based study of variation in translational tension in connecting rods against different valve timing pattern and ignition timing can be carried out.

In addition, with increase in number of engine cylinders complexity of the model in CCEM approaches increases significantly while order of the system also increases. However, in comparison to FPEM based single cylinder study ([86]), complexity has slight increase while order does not increase with increase in number of engine cylinders.

Comparison of capabilities and attributes of FPEM and most commonly and widely applied control oriented model (MVEM) is shown in Table 3.5.

4.4.2 FPEM Diagnostic Capabilities

Crankshaft angular speed fluctuations are constructed by the model. As described in Section Appendix A, these fluctuations are captured using standard crankshaft position sensing arrangement. As a result, capturing the fluctuations do not require high resolution sensor arrangement. Model based techniques similar to one presented in [62] can be formulated for diagnostic purpose.

A distinguishing feature of the proposed model is its unique and wide range of system description. That is, the proposed model describes the engine under normal or healthy conditions as well as engine dynamics under faulty conditions misfire for example. The proposed model carry the structure of a control oriented model, in addition it also describes the system response in conditions under faults. For the purpose, a misfire conditions has been created by replacing the cylinder pressure model of one cylinder by a model performing intake, polytropic compression, polytropic expansion and exhaust, in the same order as enlisted. Results of the simulation are shown in Figure 4.12(a).

Figure 4.12(a) and 4.12(b) shows crankshaft fluctuation profile for misfire generated by model and that acquired from the engine respectively. Figure 4.12 presents

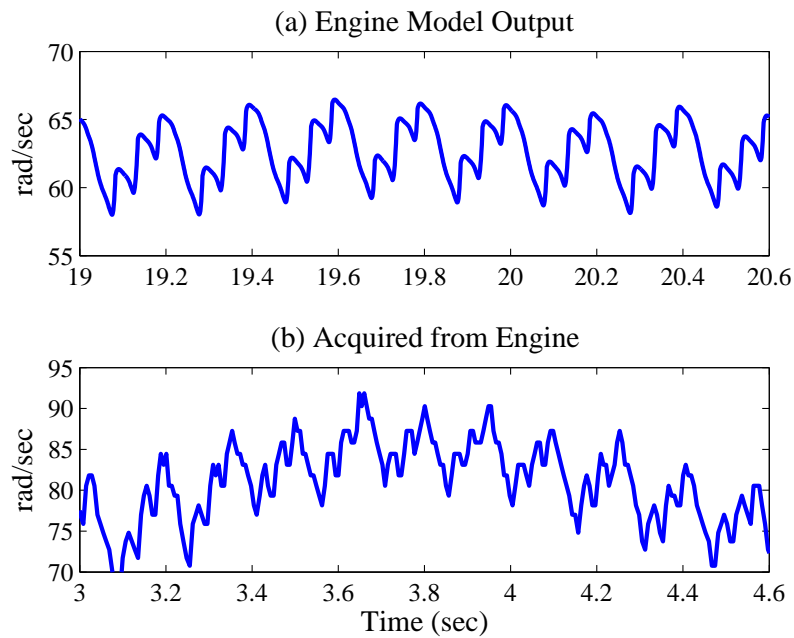


FIGURE 4.12: Pattern of the Crankshaft Angular Speed Fluctuations (a) Output of the Model for Misfire in One Cylinder (b) Acquired from Engine for One Cylinder Misfire

the angular speed fluctuation pattern, however both outputs, Figure 4.12(a) and 4.12(b), belong to different experiment of same setup (at existing setup, it was not possible to acquire high resolution angular speed and other engine parameters simultaneously and synchronized). Agreement of the results in fluctuation profile with experimental data and from the existing literature,[11], clearly shows the model capacity to describe the plant under faulty conditions. To extend the case study and further explore the proposed FPEM, a simulated intermittent misfire condition is generated. Pattern of crankshaft angular speed fluctuation for a single and two consecutive intermittent misfire events in one cylinder are shown in Figure 4.13.

Thus model offers its capability for development of model based FTC framework, as it describes the system dynamics under fault conditions.

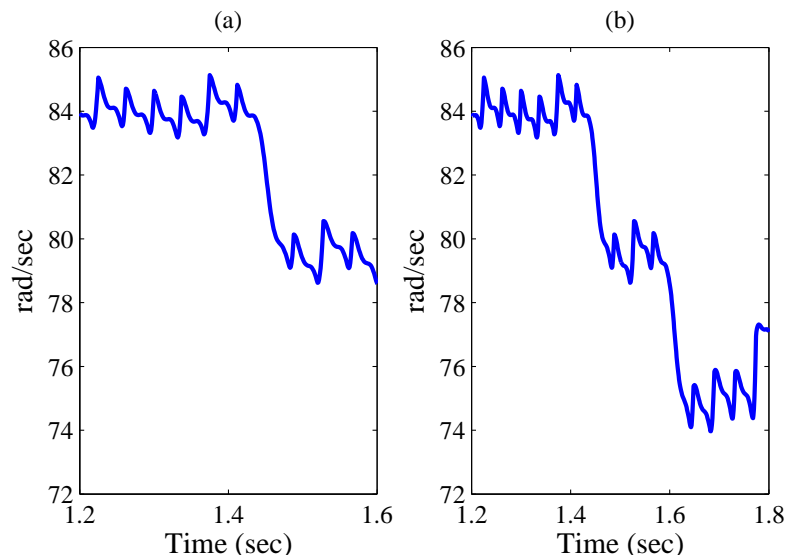


FIGURE 4.13: Pattern of Crankshaft Angular Speed Fluctuation for an Intermittent Misfire Condition (a) Single Intermittent Misfire (b) Two Consecutive Intermittent Misfires in one Cylinder

4.4.3 FPEM Control Capabilities

Cylinder pressure model for multi-cylinders together with other inputs can serve in many ways. One could be the tuning and defining the control laws or variation in tension in rigid bodies against variation in spark or valve timing.

As explained earlier, the proposed model not only describes the healthy system under normal operating conditions. The control oriented model also describes the faulty system as well. As the model attains this features it become more suitable for application of conventional model based fault tolerant control (FTC) schemes. As, application of conventional FTC techniques require that model of the plant should be capable of describing the healthy as well as the faulty system, as explained in [69]. In this manner, model could be utilized for application of conventional FTC techniques and novel gasoline Engine FTC Framework could be developed. Gasoline engine FTC framework can help in better limp home modes with reduced emission levels to cater for stringent limp home mode requirements, such as [72] and [71].

Additionally, as seen in Section 4.3.1, there are five inputs to the model of mechanism corresponding to a four cylinder engine. Namely, torque on crankshaft and

force acting on each piston. With this degree of freedom and controllability, model based cylinder-to-cylinder (CTC) fuel management can be performed. Moreover, problem could be the run-time cylinder power balance. Cylinder power balance is still an active research area, for example [87, 88]. CTC is considered to be part of the engine control in near future, [89]. Individual inputs defined for each cylinder and visibility individual cylinder in the output make the proposed FPEM suitable for development of model based algorithms, for skipping the cylinder firing and enhancing the NVH.

4.4.4 Model Integrability with Other Systems

There is still another prominent model feature. Since expansion and compression are modeled as polytropic processes. Which can lead to model based estimation of heat rejected by the system. Rejected heat either goes to environment via engine exhaust or is transferred to the engine coolant. Thus, modification in combustion model can lead to integration of engine control and diagnosis framework with engine thermo-management.

It is also worthy to note that torque production subsystem has capability to run the engine under wide range of valve timing. Thus same engine model with slight modifications in the model of intake manifold can be used to model the Atkinson Cycle based engines. Especially in the application where it is desirable to run Otto and Atkinson Cycles interchangeably. Different attributes of the proposed multi-cylinder based FPEM are compared with those of a conventional control oriented engine model in Table 4.4, whereas lumped cylinder and multi-cylinder approaches are compared in Table 4.5.

TABLE 4.4: Comparison of MVEMs and Proposed FPEM

Attribute	Existing MVEMs	Proposed FPEM
Speed Equation	$\dot{\omega}_c = \frac{1}{J_e} \tau_b$ J_e is Engine moment of Inertia τ_b is brake torque	$\dot{\omega}_c = f(\theta_c, \omega_c, \Gamma)$ $+g_a(\theta_c, \omega_c, \Gamma)F(t)$ $+g_b(\theta_c, \omega_c, \Gamma)\tau_N$
Rotational Dynamics	Modeled	Modeled
Crankshaft Speed Fluctuations	Since Mechanism, is replaced, fluctuations are not modeled	Fluctuations are modeled
Source of Fluctuation	No Fluctuation present	Mechanism and Combustion are both modeled
Tension in Individual Bodies of Mechanism (Connecting Rod, Crankshaft)	Not Capable	Evaluated along with rotational Dynamics
Torque Generation Mechanism related Ageing and Diagnostic	Not capable, as mechanism is replaced in the model	Model has the capability
Spark Advance (SA) and Variable Valve Timing (VVT)	Modeled indirectly or empirically	Can directly be modeled with $F(t)$
Multi Cylinder Dynamics	Model cannot show multi- cylinder dynamics	Model shows the multi- cylinder dynamics
Cylinder to Cylinder Control (CTC)	Not capable	Model is capable
Model Complexity	Low Complexity	Complexity higher than MVEMs

4.5 Conclusions

A novel FPEM of a multi-cylinder gasoline engine is proposed. Model of the mechanism for a four cylinder arrangement is derived using Constrained Lagrangian EOM, while multi-cylinder gasoline engine cylinder pressure model is derived through a single cylinder pressure model. It is shown that the model reconstructs the whole crankshaft angular speed profile. Salient features of the proposed FPEM for example extended diagnostic capabilities; enhanced control features (cylinder to cylinder control) are discussed. The model defines the inputs to the mechanism such as spark advance; valve timing and those giving basis for model based

TABLE 4.5: Comparison of Lumped Cylinder and Multi-Cylinder Approaches

Attribute	Lumped Cylinder Dynamics	Multi-Cylinder Dynamics
Number of engine cylinders	Cylinders are lumped into one bigger cylinder	Approach considers multi-cylinder explicitly
Crankshaft angular speed fluctuations	Correspond to lumped cylinder equivalent	True Multi-cylinder fluctuations
Cylinder-to-Cylinder control	Not capable	Capable

cylinder to cylinder control in more transparent manner. Indicated inputs are defined based on first principle, thus bestowing the model with global validity. A case study is presented, showing close resemblance between the following two 1) Pattern of crankshaft angular fluctuation acquired from engine with one misfiring cylinder 2) Pattern of crankshaft angular fluctuation generated by the FPEM for one cylinder misfire. Besides, model with slightly modified intake manifold model can be used for modeling the Atkinson cycle based engines. The proposed FPEM is validated successfully against actual engine. Model validation errors are within nominal range.

Comparison of Appendix A and Appendix B lead to an interesting fact that following the same approach the model complexity has not grown with increased number of cylinders. By virtue of the modeling approach the model now describes the multi-cylinder dynamics, contribution of each cylinder and components of response added by four strokes, without significant increase in model complexity as compared with that developed in Chapter 3.

Chapter 5

CONCLUSIONS AND FUTURE WORK

Every true love and friendship is a story of unexpected transformation. If we are the same person before and after we loved, that means we haven't loved enough.

Elif Shafak

On the pedestal laid by Chapter 3 and Chapter 4, this chapter presents a summary on work presented in this thesis and possible future directions. Possible extensions to the work presented in this thesis are categorized in two major categories, those are utilization of the FPEM for development of control and diagnostic techniques and possible expansion work to the model itself.

5.1 Featured Aspects

Internal combustion engines run in a space shared by many engineering areas. Multi-disciplinary nature, non-linear processes, presence of strict legislation and ever increasing efficiency requirements make the control oriented modeling of gasoline engines a worthwhile venture. Other reasons for taking special considerations

for development of control oriented models of gasoline engines are elaborated in the thesis. In existing literature, an analogical replacement is performed while developing the control oriented models. That is, whole mechanism formed by the engine cylinder(s), piston(s), connecting rod(s) and crankshaft is assumed to be replaced by a volumetric pump. Such a pump operates continuously, it pumps air from intake manifold to the exhaust manifold and generated torque in proportion to mean value of air and fuel flow.

Such a modeling approach hides dynamics introduced by the mechanism (piston, connecting rod and crankshaft), number and orientation of the engine cylinders. It has further been shown that model development on the conventional avenue let the model capture the approximate output dynamics and a few components of response are suppressed by the model. Such a round-about creates hindrance in development of unified frameworks and give rise to application specific modeling domains. A step-wise approach is adopted to bridge the indicated gap. The efforts to carry out the inception are presented in Chapter 3, while efforts for the subsequent step are presented in Chapter 4.

In the first step, model of the mechanism is derived by application of constrained Lagrangian EOM and a suitable model simplification strategy. Whereas, the whole work is carried out with an assumption of lumped cylinder dynamics. With the said assumption, though the model still remains incapable of describing the multi-cylinder dynamics, but the components of the response imparted by the mechanism no longer remain invisible in the model output.

In the second step, model of a mechanism corresponding to a four cylinder engine is derived, using the same methodology. The said model of the mechanism together with an analytical gasoline engine cylinder pressure model completes the picture of a *First Principle based Engine Model (FP-EM)*, initiated by preceding chapter. Profile of the output contains the harmonics imparted by the multi-cylinder mechanism and those added by the process of four strokes. It is worthy to note that due to application of Lagrangian Mechanics and selection of suitable simplification

strategy, the model complexity do not increases with number of engine cylinders, as evident from comparison of Appendix B and Appendix C.

Through discussions presented along-with simulation results, it is shown that how the FPEM is capable of developing an integrated advanced and unified engine control and diagnostic framework presented in Chapter 2. Each possible utilization of FPEM presented in Section 5.2.1 is based on already discussed attributes of the proposed model.

5.2 Future Direction

As described earlier, there are two major directions for the research to extend the work presented in the thesis. They are as follows:

1. Utilization of the FPEM
2. Extending the proposed FPEM

Each of the possible direction is discussed separately in subsequent sections.

5.2.1 Utilization of the Model

In nexus to the unified control and diagnostic framework presented in Section 2.5, each of the following step constitute a phase in developing the said framework.

As seen in the discussions included in Chapter 3 and Chapter 4, FPEM solves other mechanism related physical variables along-with rotational dynamics. Among others, highlighting variables are the translational and rotational tension in connecting rods. The attribute can be used for development of spark or the valve timing optimization against tension in connecting rods, especially for controlling or manipulating the system under fault conditions.

From aspect of modeling and control model based description of the fluctuations in crankshaft angular speed is another prominent attribute, [90]. These represent the in-cylinder conditions and other information regarding the mechanism. Application of this feature can enhance the misfire detection at high engine angular speeds. These can also be used for development of spark health estimation.

As already discussed in detail, the model describes the system dynamics in healthy as well as faulty conditions, comprehensively. The fact is elaborated by validating the crankshaft oscillation pattern in case of misfire in one cylinder (for both cases, persistent and intermittent misfire conditions). As a result, model becomes suitable for application of fault tolerant control techniques to the gasoline engines.

At later stages, it is seen that model eventually attains the capability to describe the multi-cylinder dynamics. That is, number and orientation of the cylinders is not invisible in the control oriented model. Indicated feature of the model could be utilized for development of model based cylinder power balance algorithms. This could also prove itself helpful in enhancing the NVH. Moreover, visibility of individual cylinders make the model attractive for technologies, such as VCM and DSF.

The model incorporates an analytical cylinder pressure model, developed on the base of physical principles. In current research work, cylinder pressure model is used to evaluate the force acting on each piston. Since the heat rejected by the system can now be expressed based on analytical formulation, model can therefore be helpful in developing an integrated control and thermo-management framework. Model based description of combustion, in the cylinder pressure mode, and heat rejected by the system can be used for integration of exhaust and emission models with the engine control framework.

Model based description of combustion bestows the FPEM with sufficient flexibility for application in flex-fuel engines. Explicit, model based definitions of valve and spark timing make the FPEM capable of developing control and diagnostic frameworks for Otto-Atkinson engines, [74].

5.2.2 Extension to Model

Intake manifold dynamics are taken from the literature, which describe the process with a mean value philosophy. Integration of more detailed model of intake manifold dynamics (such as [91]) together with FPEM can result in more powerful and descriptive model. Moreover, PDE based description of torque production subsystem could be another endeavor, this could provide a wider arena for advanced and unified engine controls.

On the other hand, system of an engine considered while development of an FPEM is a basic engine. There are auxiliaries, which are considered as part of an engine system now a days. These auxiliaries include:

1. An arrangement of internal/ external EGR ([92])
2. Turbine and turbocharging compressor

FPEM presented in this thesis requires extension to include the said engine auxiliaries, such that novel model based diagnostic and control capabilities could be explored.

Appendix A

EXPERIMENTAL SETUP AND PARAMETER TUNING

This appendix aims at explaining the experimental setup, engine under study and mechanism of data acquisition. Furthermore, Optimization procedure used to tune the tuning parameters of the model is also explained. Precise listing of the parameters and optimization results are discussed in each respective section of this thesis.

A.1 Experimental Setup

The description on experimental setup, engine and the auxiliary equipment used to acquire data-sets for model tuning and subsequent validation is described here in this section. Experimental arrangement is shown in Fig. [A.1](#), whereas major engine specifications are included in Table [A.1](#)

A.1.1 Onboard Diagnostic Interface

Experimental setup consist of a commercial 1300cc spark ignition engine, detailed specifications of the engine under study are enlisted in Table [A.1](#). The engine

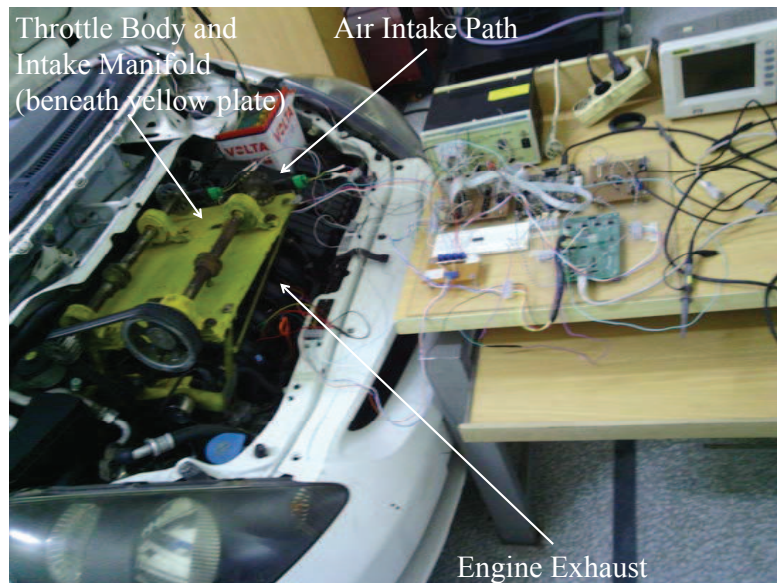


FIGURE A.1: Engine Setup

TABLE A.1: Specifications of Engine Under Study

Parameter	Value
V_{man}	1127cc
V_d	1294cc
Compression Ratio	10.5
Crank offset	5.1cm
Mass of Crankshaft	11kg
Length of Connecting Rod	14.5cm
Mass of Connecting Rod	0.6kg
Mass of one Piston	0.5kg

is equipped with an OBD-II compliant ECU. The interface supports acquisition of engine parameters. Engine operational data is acquired through the OBD-II interface, using standard OBD-II data logging device. The interface provides information on load torque based on the static modeling techniques.

Since sampling instant of a specific sample of parameter is an important factor, when model tuning and validation are subject of study. The indicated data acquisition interface provides each sample with its own time stamp. Parameter values and their respective time stamps are thus acquired at the host computer. Linear interpolation is used between two consecutive data samples. Following engine variables were acquired for each data-set:

1. Throttle Position

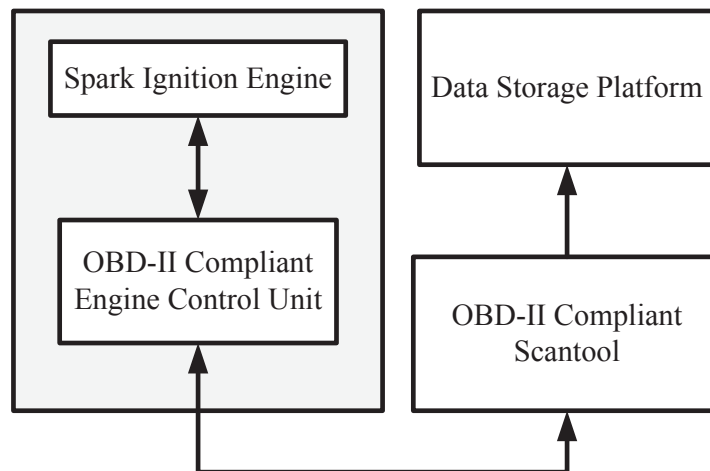


FIGURE A.2: OBD-II based Data Acquisition Scheme

2. Intake Manifold Pressure
3. Crankshaft Angular Speed
4. Engine Load
5. Spark Advance

Two data sets are acquired from the engine, to accomplish the model tuning and validation of different data sets. Both data sets are acquired with throttle position having a square like pattern, for the purpose of capturing the rich dynamics of the engine. The engine operational data for parameter estimation/model tuning is acquired having square wave shape throttle input is applied to the engine. A mechanism with an adjustable screw is used to apply the throttle input to the engine. Input is applied such that crankshaft angular speed ranges between idle speed of $75\text{rad}/\text{sec}$ to speed around $150\text{rad}/\text{sec}$.

Other than mentioned data sets more data sets are acquired, which cover more rich dynamics and wider operating range.

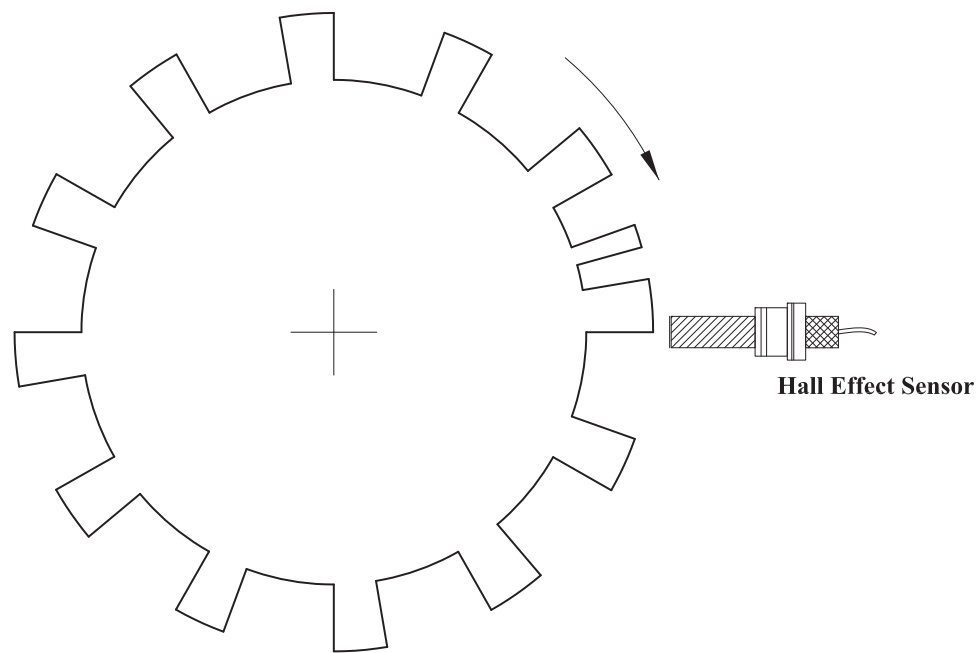


FIGURE A.3: Arrangement of Crankshaft Position Sensor

A.1.2 High Speed DAQ Interface

High speed DAQ interface is used to acquire data for further validation of crankshaft angular speed fluctuations. The engine under study is equipped with contactless hall effect based rotational encoder. The sensor uses a configuration of 12-1, that is twelve teeth with an extra teeth to reference position. The sensor configuration is shown in Fig. A.3. This kind of sensor is commonly found in engine, along-with other kind of commonly found configurations like 36-2 and 60-2. A data acquisition card NI-DAQ-9001 is used to acquire the sensor data.

Two kinds of data are acquired using this configuration, stated as follows:

1. Crankshaft angular speed pattern for healthy engine.
2. Crankshaft angular speed pattern for one cylinder mis-fire.

The first data-set is acquired to validate the fluctuation pattern of crankshaft angular speed under healthy conditions, while second data-set is acquired to validate

the theme of the model that system also describes the system dynamics under fault conditions.

A.2 Parameter Tuning

For the sake of parameter estimation Nelder-Mead algorithm [93] is utilized. The Nelder-Mead algorithm is easy to apply, fast in estimation and works good when initial conditions are not completely unknown. The algorithm, proposed in 1965, is simplex based derivative free direct search method. Mathematically, the algorithm can be described as follows:

$$\min e(x)$$

where $e : \mathbb{R}^n \rightarrow \mathbb{R}$, is called objective function, n is dimensional order of the problem. A Simplex is essentially a polytope of $n + 1$ vertices in n dimensions. Each iteration of the algorithm consist of sort, reflection, expansion, outside contraction, inside contraction and shrink operations on vertices defined by the problem. The problem of parameter estimation is posed as nonlinear optimization problem, which is solved using the algorithm described above. The initial guess for the parameters of intake manifold are based on [7] and [67]. Whereas, the initial guess for torque production subsystem are tuned manually by running the optimization problem repeatedly for different initial values based on the system insight.

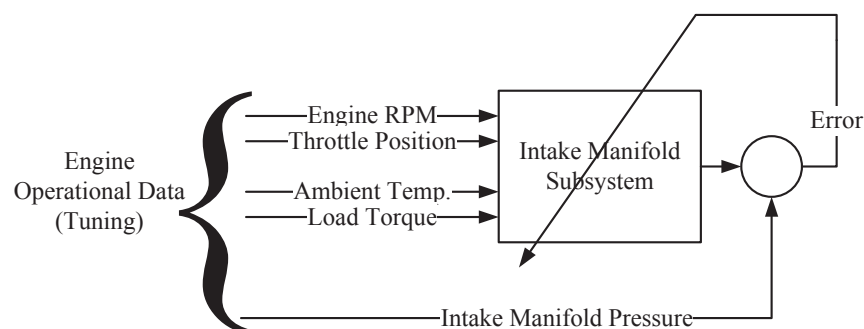


FIGURE A.4: Structure of the Optimization Problem for Parameters Estimation of Intake Manifold Subsystem

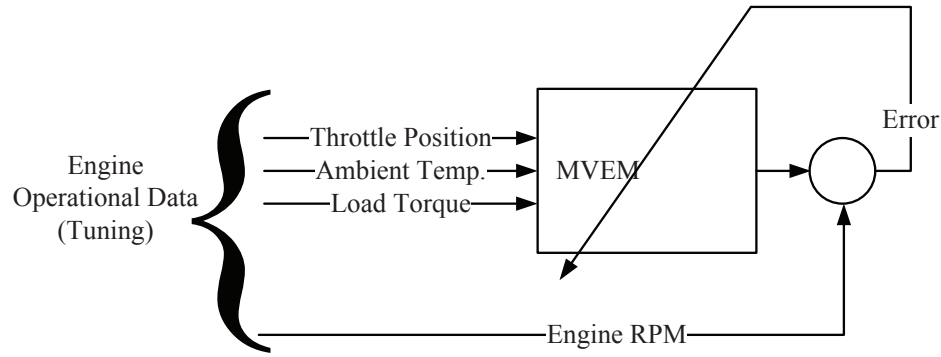


FIGURE A.5: Structure of the Optimization Problem for Parameters Estimation of Torque Production Subsystem

The process of parameter estimation is carried out stepwise. Details of each step are as follows:

1. *Step 1*: Tuning of the parameters of the intake manifold. Structure of the problem formulated for the said purpose is shown in Figure A.4
2. *Step 2*: In this step, parameters belonging to the torque production subsystem are tuned. Structure of the problem formulated for this step is shown in Figure A.5

Solving the problem in step 1 requires crankshaft angular speed, as shown in Figure A.4. Crankshaft angular speed for this step is provided to the problem from the data acquired from the engine.

Formulation of net torque acting on the crankshaft shaft is included in each respective chapter of the thesis.

For volumetric efficiency, thermodynamic conditions of intake manifold and port mass flow rate of air are used to evaluate the volumetric efficiency at different crankshaft angular speeds. The structure of cubic polynomial for η_v is shown in Eq. A.1. The values of the coefficients determined by experimental data are shown in Table A.2.

$$\eta_v = b_3\omega^3 + b_2\omega^2 + b_1\omega + b_o \quad (\text{A.1})$$

TABLE A.2: Parameters of Volumetric Efficiency

Parameter	Value
b_o	0.6718
b_1	0.00162
b_2	-3.19×10^{-6}
b_3	7.623×10^{-10}

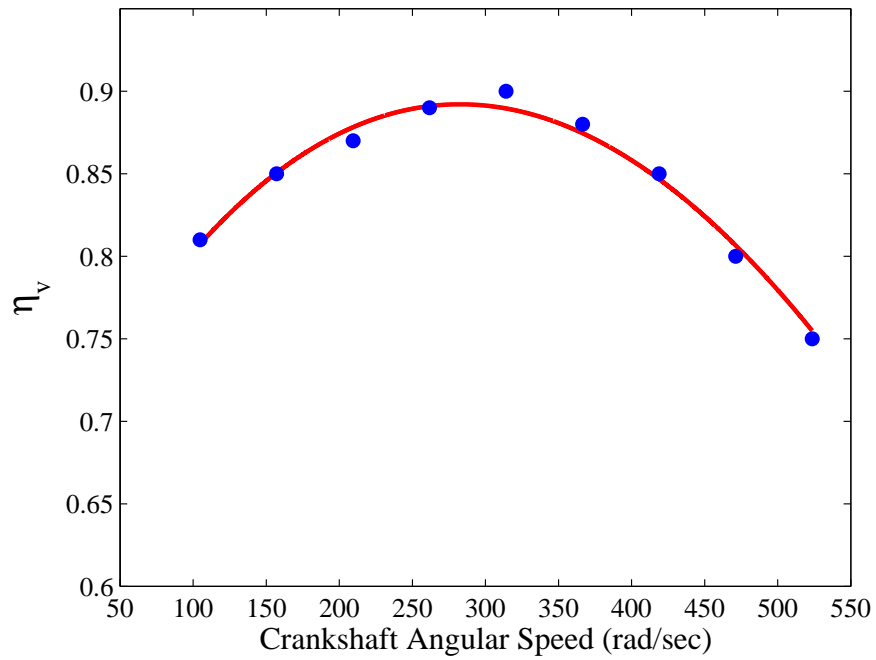


FIGURE A.6: Volumetric Efficiency η_v and data points. Root Mean Square evaluated by Matlab curve fitting toolbox is 0.0081

The plot of cubic polynomial and data points for η_v are shown in Fig. A.6.

Appendix B

DETAILED MATHEMATICAL EXPRESSIONS IN LUMPED CYLINDER DYNAMICS

Details of the mathematical expressions mentioned in Chapter 3 is presented here. All f , g_i , n_i and d_i are functions θ_1 , ω_1 and Γ . Included here in the appendix simply to avoid repetition.

$$\begin{aligned}\dot{\theta}_1 &= \omega_1 \\ \dot{\omega}_1 &= f + g_1 f_{in} + g_2 \tau \\ &= \frac{-4n_3 l_1^2 \dot{\theta}_1^2}{d_o (d_2 l_1^2 + d_1)} - \frac{n_2 f_{in}}{d_o (d_2 l_1^2 + d_1)} - \frac{n_1 \tau}{d_o (d_2 l_1^2 + d_1)}\end{aligned}$$

where,

$$\begin{aligned}n_1 &= 8k_1 (l_2^2 - l_1^2 \sin^2(\theta_1(t)))^{5/2} \\ n_2 &= 8l_1 \sin(\theta_1(t)) (l_2^2 - l_1^2 \sin^2(\theta_1(t)))^2 \left(\sqrt{l_2^2 - l_1^2 \sin^2(\theta_1(t))} + l_1 \cos(\theta_1(t)) \right)\end{aligned}$$

$$\begin{aligned}
n_3 = & l_2^4 (4m_3 - 3m_2) \sin(2\theta_1(t)) \sqrt{l_2^2 - l_1^2 \sin^2(\theta_1(t))} + \\
& l_1 l_2^4 (m_2 - 2m_3) (\sin(\theta_1(t)) - 3 \sin(3\theta_1(t))) - 4l_1^5 (m_2 - 2m_3) \\
& \sin^5(\theta_1(t)) \cos(2\theta_1(t)) + 2l_1^3 l_2^2 (m_2 - 2m_3) \sin^3(\theta_1(t)) \\
& (5 \cos(2\theta_1(t)) + 1) - l_1^2 l_2^2 \sin(2\theta_1(t)) \sqrt{l_2^2 - l_1^2 \sin^2(\theta_1(t))} \\
& (m_2 (4 \cos(2\theta_1(t)) - 3) + 4m_3 (1 - 2 \cos(2\theta_1(t)))) - 8l_1^4 (m_2 - 2m_3) \\
& \sin^5(\theta_1(t)) \cos(\theta_1(t)) \sqrt{l_2^2 - l_1^2 \sin^2(\theta_1(t))}
\end{aligned}$$

$$d_o = 2l_2^2 - 2l_1^2 \sin^2(\theta_1(t))$$

$$d_1 = -16k_1 (l_2^2 - l_1^2 \sin^2(\theta_1(t)))^{3/2}$$

$$\begin{aligned}
d_2 = & -8l_1 l_2^2 (m_2 - 2m_3) \sin(2\theta_1(t)) \sin(\theta_1(t)) + 16l_1^3 (m_2 - 2m_3) \\
& \sin^4(\theta_1(t)) \cos(\theta_1(t)) + 4l_1^2 \sin^2(\theta_1(t)) \sqrt{l_2^2 - l_1^2 \sin^2(\theta_1(t))} \\
& (4m_2 \sin^2(\theta_1(t)) + 4m_3 \cos(2\theta_1(t)) + m_1) - 2l_2^2 \\
& \sqrt{l_2^2 - l_1^2 \sin^2(\theta_1(t))} (-8m_3 \sin^2(\theta_1(t)) + m_2 (5 - 3 \cos(2\theta_1(t))) + 2m_1)
\end{aligned}$$

Appendix C

DETAILED MATHEMATICAL EXPRESSIONS IN MULTI-CYLINDER DYNAMICS

Details of the mathematical expressions mentioned in Chapter 4 is presented here. It is to be noted that f , \mathbf{g}_i , g_i and k all are function of θ , $\dot{\theta}$ and Γ . Shown in the subsequent equations in simple form for simplicity.

$$\ddot{\theta}_c = \frac{1}{k} [f + \mathbf{g}_1 \tau_b + \mathbf{g}_2 F(\theta_c)]$$

where,

$$F(\theta_c) = \begin{bmatrix} f_{in1}(\theta_c) \\ f_{in2}(\theta_c) \\ f_{in3}(\theta_c) \\ f_{in4}(\theta_c) \end{bmatrix}$$

$$\mathbf{g}_1 = -1$$

and

$$\mathbf{g}_2 = \begin{bmatrix} g_2 + g_1 & g_2 - g_1 & g_2 - g_1 & g_2 + g_1 \end{bmatrix}$$

and,

$$g_1 = \frac{l_c \sin(\theta_c)}{J_c}$$

$$g_2 = \frac{l_c^2 \sin(\theta_c) \cos(\theta_c)}{J_c \sqrt{l_1^2 - l_c^2 \sin^2(\theta_c)}}$$

$$f = + \frac{2m_1 l_c^6 \theta_c'^2 \sin^5(\theta_c) \cos(\theta_c)}{J_c (l_1^2 - l_c^2 \sin^2(\theta_c))^2} + \frac{l_1^4 m_1 l_c^2 \theta_c'^2 \sin(\theta_c) \cos(\theta_c)}{J_c (l_1^2 - l_c^2 \sin^2(\theta_c))^2}$$

$$+ \frac{2l_1^2 m_1 l_c^4 \theta_c'^2 \sin(\theta_c) \cos(\theta_c) \cos(2\theta_c)}{J_c (l_1^2 - l_c^2 \sin^2(\theta_c))^2} - \frac{l_1^2 m_1 l_c^4 \theta_c'^2 \sin(\theta_c) \cos(\theta_c)}{J_c (l_1^2 - l_c^2 \sin^2(\theta_c))^2}$$

$$+ \frac{2m_1 l_c^2 \theta_c'^2 \sin(\theta_c) \cos(\theta_c)}{J_c} + \frac{4l_1^2 l_c^4 m_{s1} \theta_c'^2 \sin(\theta_c) \cos(\theta_c) \cos(2\theta_c)}{J_c (l_1^2 - l_c^2 \sin^2(\theta_c))^2}$$

$$+ \frac{4l_c^6 m_{s1} \theta_c'^2 \sin^5(\theta_c) \cos(\theta_c)}{J_c (l_1^2 - l_c^2 \sin^2(\theta_c))^2} + \frac{4l_c^2 m_{s1} \theta_c'^2 \sin(\theta_c) \cos(\theta_c)}{J_c}$$

$$k = - \frac{4l_c^2 m_{s1} \sin^2(\theta_c)}{J_c} - \frac{2l_1^2 l_c^4 m_{s1} \sin(\theta_c) \sin(2\theta_c) \cos(\theta_c)}{J_c (l_1^2 - l_c^2 \sin^2(\theta_c))^2}$$

$$+ \frac{2l_c^6 m_{s1} \sin^3(\theta_c) \sin(2\theta_c) \cos(\theta_c)}{J_c (l_1^2 - l_c^2 \sin^2(\theta_c))^2} + \frac{m_1 l_c^6 \sin^3(\theta_c) \sin(2\theta_c) \cos(\theta_c)}{J_c (l_1^2 - l_c^2 \sin^2(\theta_c))^2}$$

$$- \frac{2m_1 l_c^2 \cos^2(\theta_c)}{J_c} - \frac{4m_1 l_c^2 \sin^2(\theta_c)}{J_c} + \frac{l_1^4 m_1 l_c^2 \cos^2(\theta_c)}{J_c (l_1^2 - l_c^2 \sin^2(\theta_c))^2}$$

$$- \frac{3l_1^2 m_1 l_c^4 \sin(\theta_c) \sin(2\theta_c) \cos(\theta_c)}{2J_c (l_1^2 - l_c^2 \sin^2(\theta_c))^2}$$

Bibliography

- [1] L. Guzzella and C. H. Onder, *Introduction to Modeling and Control of Internal Combustion Engine Systems*. Verlag Berlin Heidelberg: Springer-Verlag Berlin Heidelberg, 2010.
- [2] D. J. Dobner, “A mathematical engine model for development of dynamic engine control,” SAE Technical Paper, Tech. Rep., 1980.
- [3] N. Otto, “Improvement in gas-motor engines,” Aug. 14 1877, uS Patent 194,047.
- [4] M. Athans, “The role of modern control theory for automotive engine control,” SAE Technical Paper, Tech. Rep., 1978.
- [5] M. Wilcutts, J. Switkes, M. Shost, and A. Tripathi, “Design and benefits of dynamic skip fire strategies for cylinder deactivated engines,” *SAE Int. J. Engines*, vol. 6, pp. 278–288, 04 2013.
- [6] W. W. Pulkrabek, *Engineering Fundamentals of the Internal Combustion Engine*. Prentice Hall, 2003.
- [7] J. Heywood, *Internal Combustion Engine Fundamentals*, ser. Automotive technology series. McGraw-Hill, 1988.
- [8] A. K. Oppenheim, *Combustion in Piston Engines: Technology, Evolution, Diagnosis and Control*. Springer, 2004.
- [9] E. Hendricks and S. C. Sorenson, “Mean value modelling of spark ignition engines,” SAE Technical paper, Tech. Rep., 1990.
- [10] J. Karlsson and J. Fredriksson, “Cylinder-by-cylinder engine models vs mean value engine models for use in powertrain control applications,” *SAE Technical Paper 1999-01-0906*, 1999.

-
- [11] M. Rizvi, A. Bhatti, and Q. Butt, "Hybrid model of the gasoline engine for misfire detection," *Industrial Electronics, IEEE Transactions on*, vol. 58, no. 8, pp. 3680–3692, Aug 2011.
- [12] I. Rasmussen, "Emission fra biler emissions from cars," Ph.D. dissertation, Ph. D. thesis, Laboratory for Energetic, Technical University of Denmark, Lyngby, Denmark, 1971.
- [13] B. Powell, "A dynamic model for automotive engine control analysis," in *Decision and Control including the Symposium on Adaptive Processes, 1979 18th IEEE Conference on*, vol. 2. IEEE, 1979, pp. 120–126.
- [14] D. J. Dobner, "Dynamic engine models for control development-part i: Nonlinear and linear model formulation," *Int. J. of Vehicle Design. Special Publication SP4*, pp. 54–74, 1983.
- [15] D. J. Dobner and R. D. Fruechte, "An engine model for dynamic engine control development," in *1983 American Control Conference*, 1983, pp. 73–78.
- [16] C. F. Aquino, "Transient a/f control characteristics of the 5 liter central fuel injection engine," SAE Technical Paper, Tech. Rep., 1981.
- [17] J. J. Moskwa and J. K. Hedrick, "Automotive engine modeling for real time control application," in *1987 American Control Conference*, June 1987, pp. 341–346.
- [18] J. J. Moskwa, "Automotive engine modeling for real time control," Ph.D. dissertation, Massachusetts Institute of Technology, 1988.
- [19] J. J. Moskwa and J. Hedrick, "Modeling and validation of automotive engines for control algorithm development," *Journal of dynamic systems, measurement, and control*, vol. 114, no. 2, pp. 278–285, 1992.
- [20] R. W. Weeks and J. J. Moskwa, "Automotive engine modeling for real-time control using matlab/simulink," *SAE Technical Paper 950417*, 1995.
- [21] E. Hendricks and S. C. Sorenson, "Si engine controls and mean value engine modelling," SAE Technical paper, Tech. Rep., 1991.
- [22] E. Hendricks and T. Vesterholm, "The analysis of mean value si engine models," SAE Technical Paper, Tech. Rep., 1992.

- [23] P. Crossley and J. Cook, "A nonlinear engine model for drivetrain system development," in *Control 1991. Control'91., International Conference on.* IET, 1991, pp. 921–925.
- [24] F. T. Connolly and G. Rizzoni, "Real time estimation of engine torque for the detection of engine misfires," *Journal of dynamic systems, measurement, and control*, vol. 116, no. 4, pp. 675–686, 1994.
- [25] D. Cho and J. K. Hedrick, "Automotive powertrain modeling for control," *Journal of dynamic systems, measurement, and control*, vol. 111, no. 4, pp. 568–576, 1989.
- [26] V. Chaumerliac, P. Bidan, and S. Boverie, "Control-oriented spark engine model," *Control Engineering Practice*, vol. 2, no. 3, pp. 381–387, 1994.
- [27] J. Powell, "A review of ic engine models for control system design," in *Proc. of the 10th IFAC World Congress, San Francisco, 1987*, 1987.
- [28] E. Hendricks, "Engine modelling for control applications: a critical survey," *Mechanica*, vol. 32, no. 5, pp. 387–396, 1997.
- [29] J. A. Cook, J. Sun, J. H. Buckland, I. V. Kolmanovsky, H. Peng, and J. W. Grizzle, "Automotive powertrain control survey," *Asian Journal of Control*, vol. 8, no. 3, pp. 237–260, 2006.
- [30] P. Falcone, M. C. De Gennaro, G. Fiengo, L. Glielmo, S. Santini, and P. Lanthaler, "Torque generation model for diesel engine," in *Decision and Control, 2003. Proceedings. 42nd IEEE Conference on*, vol. 2. IEEE, 2003, pp. 1771–1776.
- [31] A. Shamekhi and S. A.H., "A new approach in improvement of mean value models for spark ignition engines using neural networks," *Journal of Expert Systems with Applications*, 2015.
- [32] K. Nikzadfar and A. H. Shamekhi, "An extended mean value model (emvm) for control-oriented modeling of diesel engines transient performance and emissions," *Fuel*, vol. 154, pp. 275 – 292, 2015.
- [33] A. H. Winkler and R. W. Sutton, "Electrojectorbendix electronic fuel injection system," in *SAE Technical Paper*. SAE International, 01 1957.

-
- [34] H. Eisele, F. Rabus, and W. Rimatzki, "Fuel injection system for internal combustion engines," Patent, Oct, 1969, uS Patent 3,470,854.
- [35] P. Romann and E. Nagele, "Fuel injection system for internal combustion engines with combined fuel pump control switch," Patent, Jan. 27, 1976, uS Patent 3,934,561.
- [36] H. Knapp, R. Sauer, R. Krauss, and U. Hafner, "Fuel injection system," Nov. 22 1983, uS Patent 4,416,238.
- [37] U. Hafner, H. Knapp, and R. Sauer, "Fuel injection system," May 31 1988, uS Patent 4,747,384.
- [38] M. Entenmann and S. Meyer, "Fuel injection apparatus," Jan. 25 1994, uS Patent 5,280,774.
- [39] N. Nakada, "Fuel injection control system for in-cylinder direct injection spark-ignition internal combustion engines," Patent, March, 1999, uS Patent 5,881,694.
- [40] Y. Kawashima, "Drive apparatus for hybrid vehicle," Patent, june, 1994, uS Patent 5,323,868.
- [41] D. Csandy and E. Woydt, "Valve-operating means," Patent, Feb, 1925, uS Patent 1,527,456.
- [42] G. Garcea, "Timing variator for the timing system of a reciprocating internal combustion engine," Patent, Nov, 1980, uS Patent 4,231,330.
- [43] N. Fujii, K. Nakamura, K. Yoshida, H. Sakai, T. Shoji, and M. Maruyama, "Variable valve actuating device," Patent, Nov, 2005, uS Patent 6,968,819.
- [44] E. Forstner, "Valve control arrangement for internal combustion engines," Sep. 27 1960, uS Patent 2,954,017.
- [45] Y. Zhao and B. Zhou, "Dynamic cylinder deactivation with residual heat recovery," August 2009, uS Patent App. 12/550,056.
- [46] "European union directive," 1970, 70/220/EEC.
- [47] "European union directive," July 1992, 91/441/EEC.

-
- [48] “European union directive,” January 1996, 94/12/EC.
- [49] “European union directive,” January 2000, 98/69/EC.
- [50] “European union directive,” January 2005, 2003/76/EC.
- [51] “European union directive,” September 2009, regulation 715/2007.
- [52] “European union directive,” September 2014, eCE-R-83/06.
- [53] “General provisions for emission regulations,” 1994, 40CFR Part 86.
- [54] “Control of air pollution from new motor vehicles: Tier 2 motor vehicle emissions standards and gasoline sulfur control requirements,” 2000, 40CFR Part 86.
- [55] “Control of air pollution from new motor vehicles: Tier 3 motor vehicle emission and fuel standards,” 2014, 40CFR Part 86.
- [56] H. Wu, C. Aquino, and G. Chou, “A 1.6 liter engine and intake manifold dynamic-model,” in *Mechanical Engineering*, vol. 106, no. 2. ASME-AMER SOC Mechanical Eng 345 E 47TH St, NY 10017, 1984, pp. 92–92.
- [57] G. Rizzoni, “Dynamic model for the internal combustion engine,” Ph.D. dissertation, 1986.
- [58] K. Follen, M. Canova, S. Midlam-Mohler, Y. Guezennec, G. Rizzoni, B. Lee, and G. Matthews, “A high fidelity lumped-parameter engine model for powertrain control design and validation,” in *ASME 2010 Dynamic Systems and Control Conference*. American Society of Mechanical Engineers, 2010, pp. 695–702.
- [59] L. Eriksson, “Spark advance modeling and control,” Ph.D. dissertation, Division of Vehicular Systems, Department of Electrical Engineering, Linköping University, Linköping University, SE581 83 Linköping, Sweden, 1999.
- [60] P. Andersson, L. Eriksson, and L. Nielsen, “Modeling and architecture examples of model based engine control,” *Vehicular Systems, ISY, Linköping University, Sweden*, 1999.
- [61] A. Greene and G. Lucas, *The testing of internal combustion engines*. The English University Press, 1969.

-
- [62] T. S. Brown and W. S. Neil, "Determination of engine cylinder pressures from crankshaft speed fluctuations," *SAE Technical Paper 920463*, 1992.
- [63] G. Rizzoni, "Estimate of indicated torque from crankshaft speed fluctuations: a model for the dynamics of the ic engine," *Vehicular Technology, IEEE Transactions on*, vol. 38, no. 3, pp. 168–179, Aug 1989.
- [64] Y. W. Kim, G. Rizzoni, and Y.-Y. Wang, "Design of an ic engine torque estimator using unknown input observer," *Journal of Dynamic Systems, Measurement, and Control*, vol. 121, no. 3, pp. 487–495, 09 1999.
- [65] D. Brand, C. H. Onder, and L. Guzzella, "Estimation of the instantaneous in-cylinder pressure for control purposes using crankshaft angular velocity," *SAE Technical Paper*, Tech. Rep., 2005.
- [66] Y.-K. Chin and F. E. Coats, "Engine dynamics: Time-based versus crank-angle based," in *SAE Technical Paper*. SAE International, 03 1986.
- [67] Q. Ahmed and A. I. Bhatti, "Estimating si engine efficiencies and parameters in second-order sliding modes," *IEEE Transactions on Industrial Electronics*, vol. 58, no. 10, pp. 4837–4846, Oct 2011.
- [68] —, "Second order sliding mode observer for estimation of si engine volumetric efficiency amp; throttle discharge coefficient," in *11th International Workshop on Variable Structure Systems (VSS)*, 2010.
- [69] M. Blanke, M. Kinnaert, J. Lunze, and M. Staroswiecki, *Diagnosis and Fault-Tolerant Control*. Springer-Verlag Berlin Heidelberg, 2016.
- [70] Y.-W. Kim, G. Rizzoni, and V. I. Utkin, "Developing a fault tolerant power-train control system by integrating design of control and diagnostics," *International Journal of Robust and Nonlinear Control*, vol. 11, no. 11, pp. 1095–1114, 2001.
- [71] "Road vehicles – functional safety," International Organization for Standardization, Geneva, CH, Standard, 2011.
- [72] "The california low-emission vehicle regulations," California Air Resource Board, California, US, Standard, 2016.

- [73] J. Serrano, G. Routledge, N. Lo, M. Shost, V. Srinivasan, and B. Ghosh, “Methods of evaluating and mitigating nvh when operating an engine in dynamic skip fire,” *SAE Int. J. Engines*, vol. 7, pp. 1489–1501, 04 2014.
- [74] D. Boggs, H. Hilbert, and M. Schechter, “The otto-atkinson cycle engine-fuel economy and emissions results and hardware design,” SAE Technical Paper, Tech. Rep., 02 1995.
- [75] R. F. Gans, *Engineering dynamics: From the Lagrangian to Simulation*. Springer-Verlag New York, 2013.
- [76] J. Storch and S. Gates, “Motivating kane’s method for obtaining equations of motion for dynamic systems,” *Journal of Guidance, Control, and Dynamics*, vol. 12, no. 4, pp. 593–595, Jul. 1989.
- [77] R. Fitzpatrick, *Newtonian Dynamics*. Lulu, 2011.
- [78] L. Eriksson and I. Andersson, “An analytic model for cylinder pressure in a four stroke si engine,” SAE Technical Paper, Tech. Rep., 2002.
- [79] C. Cooney, J. Worm, D. Michalek, J. Naber *et al.*, “Wiebe function parameter determination for mass fraction burn calculation in an ethanol-gasoline fuelled si engine,” *Journal of KONES*, vol. 15, pp. 567–574, 2008.
- [80] K. Z. Mendera, A. Spyra, and M. Smereka, “Mass fraction burned analysis,” *Journal of KONES Internal Combustion Engines*, no. 3-4, pp. p193–201, 2002.
- [81] Y. A. Cengel and M. A. Boles, *Thermodynamics: An Engineering Approach*, 6th ed. McGraw-Hill Science, 2008.
- [82] R. Isermann, *Engine Modeling and Control: Modeling and Electronic Management of Internal Combustion Engines*. Springer-Verlag Berlin Heidelberg, 2014.
- [83] D. Jung, L. Eriksson, E. Frisk, and M. Krysander, “Development of misfire detection algorithm using quantitative fdi performance analysis,” *Control Engineering Practice*, vol. 34, pp. 49–60, 2015.
- [84] L. Eriksson and L. Nielsen, *Modeling and control of engines and drivelines*. John Wiley & Sons, 2014.

-
- [85] C. E. Wilson and J. P. Sadler, *Kinematics and Dynamics of Machinery*, 3rd ed. Pearson, 2003.
- [86] A. Yar, A. Bhatti, and Q. Ahmed, “First principle-based control oriented model of a gasoline engine,” *Journal of Dynamic Systems, Measurement, and Control*, vol. 139, no. 5, pp. 051 002–12, 2017.
- [87] H. Li, Y. Huang, G. Li, and Y. Yang, “Research on the cylinder-by-cylinder variations detection and control algorithm of diesel engine,” SAE Technical Paper, Tech. Rep., 2015.
- [88] F. Ostman and H. T. Toivonen, “Adaptive cylinder balancing of internal combustion engines,” *IEEE Transactions on Control Systems Technology*, vol. 19, no. 4, pp. 782–791, 2011.
- [89] M. Kassa, C. Hall, A. Ickes, and T. Wallner, “Cylinder-to-cylinder variations in power production in a dual fuel internal combustion engine leveraging late intake valve closings,” *SAE Technical Paper 2016-01-0776*, 2016.
- [90] S. Schagerberg and T. McKelvey, “Instantaneous crankshaft torque measurements - modeling and validation,” in *SAE Technical Paper*. SAE International, 03 2003.
- [91] K. Follen, M. Canova, S. Midlam-Mohler, Y. Guezennec, G. Rizzoni, B. Lee, and G. Matthews, “A high fidelity lumped-parameter engine model for powertrain control design and validation,” in *ASME 2010 Dynamic Systems and Control Conference*. American Society of Mechanical Engineers, 2010, pp. 695–702.
- [92] F. Millo, M. G. Bernardi, and D. Delneri, “Computational analysis of internal and external egr strategies combined with miller cycle concept for a two stage turbocharged medium speed marine diesel engine,” *SAE Int. J. Engines*, vol. 4, pp. 1319–1330, 04 2011.
- [93] J. C. Lagarias, J. A. Reeds, M. H. Wright, and P. E. Wright, “Convergence properties of the nelder–mead simplex method in low dimensions,” *SIAM Journal on Optimization*, vol. 9, no. 1, pp. 112–147, 1998.